# On the Relationship between Precipitation and Spatial Organisation in the Trades



## Jule Radtke

Hamburg 2023

# On the Relationship between Precipitation and Spatial Organisation in the Trades

Jule Radtke

Hamburg 2023

# Jule Radtke

aus Hamburg, Deutschland

Max-Planck-Institut für Meteorologie
The International Max Planck Research School on Earth System Modelling
(IMPRS-ESM)
Bundesstrasse 53
20146 Hamburg

Universität Hamburg
Erdsystemwissenschaften
Bundesstr. 55
20146 Hamburg

Tag der Disputation: 29. März 2023

Folgende Gutachter empfehlen die Annahme der Dissertation:
Dr. Ann Kristin Naumann
Prof. Dr. Felix Ament

Vorsitzender des Promotionsausschusses:
Prof. Dr. Hermann Held

Dekan der MIN-Fakultät:
Prof. Dr.-Ing. Norbert Ritter

Titelgrafik: Jule Radtke

# PREFACE

In this cumulative thesis, I explore the relationship between precipitation and spatial organisation in trade-wind convection. Two studies form the basis of this thesis and I present their essence in a unifying essay. The essay introduces the scientific background, motivation and gap that the two studies try to fill and summarises and interprets their findings in a broader scientific context. In this regard, it also touches upon further studies I contributed to during my PhD. The publications related to this dissertation are explicitly listed on page . The two studies are included as appendices.

This document was typeset using classicthesis developed by André Miede and Ivo Pletikosić available at https://bitbucket.org/amiede/classicthesis/.

ABSTRACT

The trade-wind region and its clouds cool our earth. Understanding controls on trade-wind clouds and their sensitivity to perturbations such as a warming climate is therefore crucial for projecting our future climate. However, this understanding remains incomplete. Over the past decade, it was shown that trade-wind convection, unlike previously thought, organises into a variety of spatial structures and commonly precipitates. In this thesis, I investigate whether and how these two processes are related. For my analyses, I draw on observations and high resolution large-eddy simulations (LES) of trade-wind convection near the island of Barbados in the North Atlantic trades which were conducted in the context of the ElUcidating the RolE of Cloud-Circulation Coupling in ClimAte (EUREC$^4$A) field campaign.

In a first study, I investigate how the occurrence, amount and intensity of rain are related to clustering. To this end, I analyse the spatial behaviour in trade-wind precipitation scenes scanned by a rain radar upstream of Barbados during EUREC$^4$A. I show that the occurrence of precipitation is associated with clustering. During EUREC$^4$A, rain cells almost always occurred in a clustered spatial distribution, i.e. they were spaced closer together than in a random distribution. However, the rain amount, i.e. the scene mean rain rate, does not scale with the cells' degree of clustering. Instead, rain amount varies largely independently from it. My analyses suggest that hypothesised mechanisms, such as an increase of precipitation with clustering through cell interaction or protection, play overall a subordinate role for a scene's rain amount. They do play a role for high rainfall intensities, and may be important to maintain rain amounts in dry environments. This raises the question of an influence of organisation on the precipitation process.

In a second study, I investigate whether and how spatial organisation affects the pathway to precipitation. Here, I analyse large-domain realistic LES of trade-wind convection during EUREC$^4$A. I decompose the formation of surface precipitation into (i) a production phase, where cloud condensate is converted to rain, and (ii) a sedimentation phase, where the produced rain falls towards the ground while part of it evaporates. Organisation affects how these two phases contribute to surface rain formation, by modulating the local moisture environment, cloud vertical motion and the microphysical conversion processes that determine the raindrops' properties. As organisation strengthens, cloud condensate is less efficiently converted to rain, but rain sediments more efficiently. Thus, while in less organised scenes rain formation is predominantly driven by an efficient production of rain, in more organised scenes, reduced evaporation increasingly contributes to rain formation. I conclude that the pathway to precipitation differs with organisation and propose that organisation might be a form of buffering in response to perturbations. These findings may contribute to the growing perception, supported by EUREC$^4$A, of the robustness of trade-wind clouds to perturbations such as a warming climate.

## ZUSAMMENFASSUNG

Die Passatwindregion und ihre Wolken kühlen unsere Erde. Ein Verständnis der Mechanismen von Passatwolken und ihrer Empfindlichkeit gegenüber Störungen wie einer Erwärmung des Klimas ist daher von entscheidender Bedeutung für die Vorhersage unseres zukünftigen Klimas. Dieses Verständnis bleibt jedoch unvollständig. In den letzten zehn Jahren hat sich gezeigt, dass sich die Passatkonvektion, anders als bisher angenommen, in einer Vielzahl von räumlichen Strukturen organisiert und häufig Niederschläge verursacht. In dieser Arbeit untersuche ich, ob und wie diese beiden Prozesse zusammenhängen. Für meine Analysen stütze ich mich auf Beobachtungen und hochauflösende Large-Eddy-Simulationen (LES) der Passatkonvektion in der Nähe der Insel Barbados im Nordatlantik, die im Rahmen der Feldkampagne ElUcidating the RolE of Cloud-Circulation Coupling in ClimAte (EUREC$^4$A) durchgeführt wurden.

In einer ersten Studie untersuche ich, wie das Auftreten, die Menge und die Intensität von Regen mit Clusterbildung zusammenhängen. Zu diesem Zweck analysiere ich das räumliche Verhalten in Passatwind-Niederschlagsszenen, die während EUREC$^4$A von einem Regenradar stromaufwärts von Barbados erfasst wurden. Ich zeige, dass das Auftreten von Niederschlägen mit Clusterbildung verbunden ist. Während EUREC$^4$A traten die Regenzellen fast immer in einer geclusterten räumlichen Verteilung auf, das heißt sie lagen näher beieinander als bei einer Zufallsverteilung. Die Regenmenge, d. h. die mittlere Regenrate der Szene, skaliert jedoch nicht mit dem Grad der Clusterung der Zellen. Sie variiert weitgehend unabhängig von dieser. Meine Analysen deuten darauf hin, dass angenommene Mechanismen, wie z. B. eine Zunahme der Niederschlagsmenge mit Clusterung durch Zellinteraktion oder -schutz, insgesamt eine untergeordnete Rolle für die Regenmenge einer Szene spielen. Sie spielen jedoch eine Rolle für hohe Niederschlagsintensitäten und könnten für die Aufrechterhaltung von Regenmengen in trockenen Umgebungen wichtig sein. Dies lässt die Frage nach einem Einfluss der Organisation auf den Niederschlagsprozess aufkommen.

In einer zweiten Studie untersuche ich, ob und wie räumliche Organisation den Entstehungsweg von Niederschlägen beeinflusst. Dazu analysiere ich realistische LES-Simulationen der Passatkonvektion während EUREC$^4$A. Ich zerlege die Bildung von Niederschlag am Boden in (i) eine Produktionsphase, in der Wolkenkondensat in Regen umgewandelt wird, und (ii) eine Sedimentationsphase, in der der produzierte Regen zu Boden fällt, während ein Teil dabei wieder verdunstet. Die Organisation wirkt sich darauf aus, wie diese beiden Phasen zur Regenbildung am Boden beitragen, indem sie das lokale Feuchtigkeitsmilieu, die vertikale Bewegung der Wolken, und die mikrophysikalischen Umwandlungsprozesse, die die Eigenschaften der Regentropfen bestimmen, moduliert. Mit zunehmender Organisation wird das Wolkenkondensat weniger effizient in Regen umgewandelt, der Regen setzt sich jedoch effizienter ab. Während also in weniger gut organisierten Szenen die Regenbildung überwiegend durch eine effiziente Regenproduktion angetrieben wird, trägt in stärker organisierten Szenen zunehmend zur Regenbildung bei, dass weniger Regen verdunstet. Ich schließe

daraus, dass der Weg zum Niederschlag je nach Organisation unterschiedlich ist, und stelle die Hypothese auf, dass Organisation eine Form von Pufferung als Reaktion auf Störungen sein könnte. Diese Erkenntnisse könnten zu der von EUREC$^4$A unterstützten zunehmenden Einschätzung der Robustheit von Passatwolken gegenüber Störungen wie einer Klimaerwärmung beitragen.

## PUBLICATIONS

The following two first-author publications are part of this dissertation and included in the appendix:

APPENDIX A

**Radtke, J.**, A. K. Naumann, M. Hagen, and F. Ament (2022). "The Relationship between Precipitation and Its Spatial Pattern in the Trades Observed during EUREC⁴A." In: *Quarterly Journal of the Royal Meteorological Society*, qj.4284. ISSN: 0035-9009, 1477-870X. DOI: 10.1002/qj.4284

APPENDIX B

**Radtke, J.**, R. Vogel, F. Ament, and A. K. Naumann (2023). "Spatial Organisation Affects the Pathway to Precipitation in Simulated Trade-Wind Convection." In: *preparation*

During my PhD I contributed to five further publications. The first one is a first-author paper that is based on results of my master thesis, to the other four I contributed as co-author:

**Radtke, J.**, T. Mauritsen, and C. Hohenegger (2021). "Shallow Cumulus Cloud Feedback in Large Eddy Simulations – Bridging the Gap to Storm-Resolving Models." In: *Atmospheric Chemistry and Physics* 21.5, pp. 3275–3288. ISSN: 1680-7316. DOI: 10.5194/acp-21-3275-2021

B. Stevens, S. Bony, D. Farrell, and 290 co-authors (incl. **Radtke, J.**) (2021). "EUREC⁴A." In: *Earth System Science Data* 13.8, pp. 4067–4119. ISSN: 1866-3508. DOI: 10.5194/essd-13-4067-2021

H. Konow, F. Ewald, G. George, and 35 co-authors (incl. **Radtke, J.**) (2021). "EUREC⁴A's *HALO*." In: *Earth System Science Data* 13.12, pp. 5545–5563. ISSN: 1866-3508. DOI: 10.5194/essd-13-5545-2021

G. George, B. Stevens, S. Bony, and 10 co-authors (incl. **Radtke, J.**) (2021). "JOANNE: Joint Dropsonde Observations of the Atmosphere in Tropical North atlaNtic Meso-Scale Environments." In: *Earth System Science Data* 13.11, pp. 5253–5272. ISSN: 1866-3508. DOI: 10.5194/essd-13-5253-2021

A. Schmitt, F. Burgemeister, H. Dorff, and 7 co-authors (incl. **Radtke, J.**) (in review). "Assessing the Weather Conditions for Urban Cyclists by Spatially Dense Measurements with an Agent-Based Approach." In: *Meteorological Applications*

# ACKNOWLEDGMENTS

*A cloud does not know why it moves in just such*
*a direction and at such a speed, it feels an*
*impulsion... this is the place to go now.*
— Richard Bach (1981)

"*This is the place to go now*" - wouldn't have been possible with many people supporting me along the way.

First of all, I would like to thank my supervisors, Ann Kristin, Felix and Raphaela. Thank you for your advice, feedback and discussions which oriented my thoughts but also allowed and motivated me to develop them freely. I am grateful for the support of Ann Kristin and Felix since the beginning of this journey and would like to thank Raphaela for stepping in along the way. I have enjoyed working with you all a lot. Your support made me go through this journey with trust that I am on the right track. I would also like to thank Dirk for guiding our panel meetings and reminding me not to forget what I have already achieved.

My thanks also go to all people that gave me the opportunity to participate in the EUREC$^4$A campaign and its measurements and made this experience such a unique and great experience. It will always be in my memory. Tobi and Theresa, it was such a privilege and joy to work with you on *How to EUREC$^4$A*.

In Hamburg, I am incredibly grateful to my colleagues in both the University and MPI working groups and departments. It is especially because of you that this journey was - besides pondering about trade-wind clouds - so enriching, and joyful. I will treasure the memories of shared office hours, lunches, yoga exercises and park beers with Theresa, Marc and Lukas. Thanks to Amelie, Bastian, Finn, Heike, Henning and Tobi for standing up at nine - I think that was during Corona times my light of day. Daniel, Finn, Henning, Julia, Kai, Kathi, Lara, Moritz, Tobi - thanks for days of refuelling to Denmark, your proofreading eyes and much more.

Further, I would like to thank Bastian, Clara, Hernan and Theresa for their constructive feedback on parts of this dissertation.

And last, but not least I would like to thank my family, and Lukas - for your trust in me and your patient listening to my cloud explanations.

# CONTENTS

## ACRONYMS

| | |
|---|---|
| BCO | Barbados Cloud Observatory |
| EUREC$^4$A | ElUcidating the RolE of Cloud-Circulation Coupling in ClimAte |
| GNSS | Global Navigation Satellite System |
| HALO | High Altitude and LOng range research aircraft |
| ICON | ICOsahedral Nonhydrostatic model |
| LES | Large-Eddy Simulation |
| NTAS | Northwest Tropical Atlantic Station |
| Poldirad | POLarization DIversity RADar |
| RICO | Rain In Cumulus over the Ocean field campaign |
| SRM | Storm-Resolving Model |

Part I

UNIFYING ESSAY

# INTRODUCTION

*A collection of vortices with an eddying nature . . . full of water, being necessarily precipitated when full of rain, then they fall heavily upon each other, and burst, and clap.*

— Socrates in Aristophanes' play The Clouds (417 BC)

Clouds shape our weather and climate, and fascinate. Their infinite variety of shapes, constantly in transformation, beautifully depict atmospheric motions and energy transfers. Clouds are among the most intriguing manifestations of our weather and our vital source of rainfall. Clouds have always fascinated humans, but the need to understand them has never been more important. In the context of humans changing the composition of our atmosphere and perturbing the Earth's radiation balance, clouds are the key uncertainty in projecting our future climate (Boucher et al., 2013).

At the heart of this uncertainty are clouds in the trade-wind region (Bony and Dufresne, 2005). Here, the advent of spatial overviews with satellite imagery and aircraft field campaigns have shown that clouds may not only exert a variety of shapes, but that cloud fields also show a rich collection of cloud patterns. Sometimes cloud patches are rather small and clouds distribute randomly. At other times, clouds align along arc-like structures or cluster together into large cloud structures. This behaviour is often termed as spatial organisation. Observations also showed that trade-wind clouds regularly cast rain showers. Both processes, spatial organisation and rain development, lack a thorough understanding of their mechanisms which impedes discerning controls on trade-wind clouds and anticipating their behaviour in a warming climate. Stevens et al. (2020) suggest that to understand either spatial organisation or precipitation formation, they may need to be understood jointly. In this thesis, I explore the relationship between spatial organisation in trade-wind convection and the development of precipitation.

To this end, I provide some background on trade-wind clouds and their importance for our climate. I discuss the current knowledge about precipitation and organisation in the trades and motivate why their relationship should be investigated. Finally, I present the specific research questions I investigate in this thesis.

## 1.1 ROLE OF TRADE-WIND CLOUDS IN CLIMATE

The trade-wind region is characterised by steadily blowing winds. These are prevalent between 10 and 30 °N and °S of the equator, as e.g. depicted in early maps of Halley (1686). The reliable winds were used by sailing ships and fostered global trade, which gave the trade-wind region its name. The first recorded recognition of the trade winds
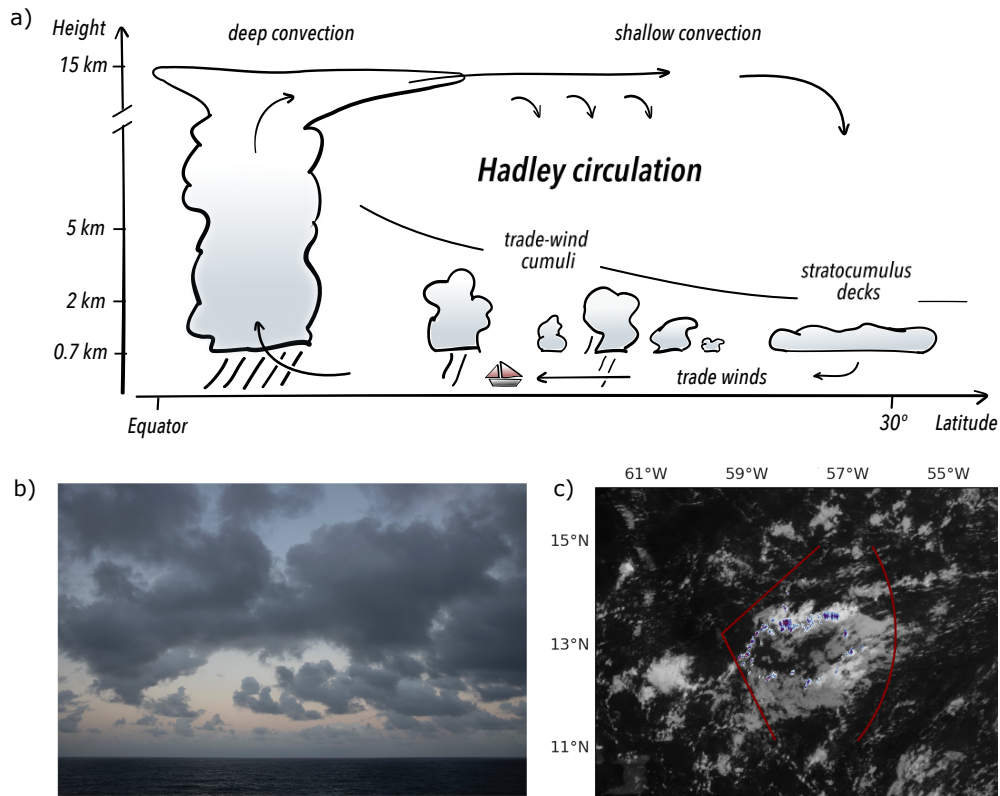
Figure 1.1: a) Sketch of Hadley circulation inspired by Mieslinger (2021) b) Picture of trade-wind clouds during the EUREC⁴A field campaign (courtesy: F. Batier) and c) satellite image upstream of Barbados in the North Atlantic trades overlaid with reflectivity of a scanning C-band radar.

dates back more than 2000 years, referring to winds blowing between Yemen and the mouth of Red Sea and Kerala in South India following the spice road. The recognition of the trade winds as a global wind system, giving rise to what later became known as the general circulation, followed much later. The first person to describe the theory behind the trade winds was George Hadley with his article on the cause of the trade winds (Hadley, 1735). The Hadley circulation identifies the trade-wind region as part of an overturning circulation with rising air at the equator that moves towards the poles, subsides and returns back to the equator in form of the easterly trade winds. Fig. 1.1a illustrates the trade-wind region in the context of the Hadley circulation.

As the trade winds blow over the ocean surface, moisture from the ocean reservoir evaporates into the atmosphere. While areas of large-scale subsidence over continents produce the largest deserts on Earth, the trade-wind regions over ocean are nourished by the unlimited reservoir of moisture. Therefore, they are abundantly populated by clouds – clouds that are confined to the lower troposphere due to the subsiding motions (Fig. 1.1b). Pioneering aircraft observations by Joanne Malkus (Malkus, 1954; Malkus, 1956; Malkus, 1958; Fleming, 2020) showed that in the vertical, trade-wind air is characterised by its layered structure. A moist and turbulent boundary layer is topped by the dry and subsiding free troposphere. The interface of

the two competing air masses marks the so called trade-wind inversion. As a layer of stably stratified air it caps cloud development. While some clouds only grow a few hundred meters deep, others reach higher up to the inversion, where they detrain and evaporate moisture, which helps to maintain the trade-wind inversion (e.g. Nitta and Esbensen, 1974). The moisture and heat stored by the clouds under the trade-wind inversion is transported by the trade winds to the equator, where they fuel deep convective towers. In this sense, trade-wind clouds are attributed an important role in driving the Hadley circulation (e.g. Riehl et al., 1951; Malkus, 1958; Tiedtke et al., 1988).

Besides their role in atmospheric motion and energy transport, trade-wind clouds are important for the Earth's radiation balance. Clouds cover more than 70% of the Earth at any time and interact with both the longwave thermal and shortwave solar radiation (Siebesma et al., 2020). In the shortwave range, clouds reflect sunlight, which cools our planet. In the longwave range, they absorb thermal radiation and, depending on their cloud top temperature, emit less radiation into space, thereby warming our planet. Whether clouds cool or warm our planet depends on their altitude, thickness, composition and latitude of occurrence. Trade-wind clouds exert a negligible effect in the longwave due to their generally low altitude and thus similar temperature to the Earth's surface, but they sharply increase the reflection of solar radiation (the albedo) compared to the underlying less reflective ocean (Hartmann and Short, 1980). Although trade-wind clouds are small in size, their abundance over tropical oceans makes them contribute largely to the mean cooling effect of clouds in our current climate (Loeb et al., 2018).

To date it is uncertain how the trade-wind clouds' cooling effect changes in a warming climate. This has important implications for climate projections. An altered cooling effect as the climate warms due to increased $CO_2$ concentrations can feed back on the warming, influencing the climate's sensitivity to the radiative perturbation. It was shown that the current climate models' inability to arrive at a robust estimation of the trade-wind cloud feedback is the major reason for climate models diverging in their projected future climate (Bony and Dufresne, 2005; Vial et al., 2013; Vial et al., 2016, further discussed in Sec. 2.1). The spread in estimates of the climate's sensitivity - often measured as the global temperature response to a doubling of $CO_2$ - has been stagnating for decades (Meehl et al., 2020). Current climate models exploit too coarse grids to explicitly simulate convective motions. Instead, they have to rely on simplified representations of clouds, so called parameterisations, which are highly uncertain. More lines of evidence, e.g. observational studies as well as process understanding, are needed to constrain the response of trade-wind clouds to warming and ultimately narrow the range of possible climate futures (Sherwood et al., 2020). Recent observational and process-based studies suggest a weak trade-wind cloud feedback (Vogel et al., 2016; Radtke et al., 2021; Cesana and Del Genio, 2021; Myers et al., 2021; Vogel et al., 2022). However, new uncertainty now arises regarding a cloud feedback organisation component (Bony et al., 2020).

In my thesis, I refer to (spatial) organisation as the different spatial structures that

convection adopts on the mesoscale (20-200 km). This scale roughly represents the grid size of current, so called conventional climate models. The question arises as to the importance of accounting for mesoscale spatial variability and of better resolving the mesoscale and its organisation - now that a new generation of global climate simulations is approaching storm-resolving (Stevens et al., 2019b) and likely finer convection-resolving resolution in the near future. Possibly, neglecting mesoscale interaction is one reason why conventional climate models poorly simulate the distribution of precipitation and formation of extreme precipitation (Fiedler et al., 2020). In the context of deep convection, studies are beginning to shed light on how the development of rain is influenced by and to what extent statistics of convection depend on mesoscale organisation (e.g. Tompkins, 2001; Muller and Held, 2012; Tobin et al., 2012; Tan et al., 2015; Tompkins and Semie, 2017; Semie and Bony, 2020). In the context of trade-wind convection, these questions have only recently started to get posed.

## 1.2    PRECIPITATION AND ORGANISATION IN THE TRADES

Both precipitation and spatial organisation have been ignored in many studies of the trades. Although it was noticed early on that trade-wind clouds also precipitate (e.g. Byers and Hall, 1955), precipitation was given minimal attention in reviews of trade-wind convection (Siebesma et al., 2003; Stevens, 2005) and trade-wind clouds were idealised as non-precipitating in modelling studies that investigated the response of trade-wind clouds to warming (e.g. Rieck et al., 2012). Studies also lacked a larger spatial view. High-resolution simulations that could simulate the motions of cloud formation, called large-eddy simulations (LES), used small domains (~20km, e.g. Rieck et al., 2012). These were too small for mesoscale organisation to emerge (Vogel et al., 2016). The assumption that trade-wind clouds are mostly randomly distributed shallow cumulus not associated with precipitation, along with their small size, was one reason why these clouds were studied relatively infrequently compared to other forms of convection (Stevens, 2005; Fleming, 2020) - before they were shown to dominate the spread in climate sensitivity estimates.

An important field campaign to help nuance the picture of trade-wind convection was the Rain In Cumulus over the Ocean field campaign (RICO, Rauber et al., 2007). RICO took place around the island of Barbuda in the western North Atlantic trades. Exploiting a scanning radar, this campaign substantiated that precipitation is not an exception but ubiquitous in the trades, with about one in ten clouds raining (Nuijens et al., 2009; Snodgrass et al., 2009). RICO thereby complemented estimates from satellite measurements that shallow or warm rain, which refers to rain produced by clouds below the freezing level, contributes 20-30% to the total precipitation amount and 70% to the total precipitation area over tropical oceans (Short and Nakamura, 2000; Lau and Wu, 2003). While studying precipitation through a spatial lens, the RICO campaign recognised and highlighted that clouds organised into a variety of spatial structures. Precipitation often seemed to be associated with clouds clustering along arc-like structures (Snodgrass et al., 2009, Fig.1.1c). The advent of detailed spatial overviews through high-resolution satellite imagery and high-flying aircrafts, as well

as advances in computing power allowing high-resolution simulations to span larger domains (e.g Seifert and Heus, 2013) made the prevalence of spatial organisation and precipitation in the trades visible.

The recognition of spatial organisation being ubiquitous in the trades attracts attention because studies on deep convection suggest that different forms of organisation affect the radiation balance (Tobin et al., 2012). The question arises as to how far this also applies to shallow convection in the trades. Have studies about the trade-wind cloud feedback neglected a cloud feedback component by ignoring spatial organisation? To answer this question, it needs to be understood which processes regulate spatial organisation and if these might change in a warming climate. Several approaches to characterise forms of organisations have been developed (Stevens et al., 2020; Denby, 2020; Janssens et al., 2021). Most studies to date have focused on four different re-occurring cloud patterns in the trades, which were named according to their visual appearance as sugar, gravel, fish, and flower (Stevens et al., 2020). Bony et al. (2020) and Schulz et al. (2021) showed that these patterns differ in their cloud radiative effect and correlate with differences in large-scale factors like wind speed or stability. This suggests that cloud patterns could change in a warming climate which would affect the trade-wind cloud feedback. A thorough understanding of the mechanisms of organisation and the implications for the trade-wind cloud feedback is thus needed (Nuijens and Siebesma, 2019).

Besides a relationship to large-scale controls, Stevens et al. (2020) and Schulz et al. (2021) found the cloud patterns, when inspecting radar imagery, to relate also to precipitation. It suggests that precipitation plays a role in the patterning process. Precipitation could influence the patterning process as it redistributes moisture and induces local circulations. The horizontal structure of three of the four cloud patterns displays mesoscale arcs, which also struck in the RICO observations. These mesoscale arcs depict cold pool outflows. As rain evaporates, the air gets cooled and moistened, causing it to sink to the surface and to spread horizontally away as a cold dense body of air, referred to as a cold pool. At the edge of a cold pool lighter air may get lifted, triggering the birth of new and often deeper convective clouds (Schlemmer and Hohenegger, 2014). Thus, precipitation may control patterns in the cloud field through cold pool interactions (Zuidema et al., 2012; Seifert and Heus, 2013; Vogel et al., 2016; Vogel et al., 2021). However, spontaneous clustering also occurs without precipitation (Vogel et al., 2016; Bretherton and Blossey, 2017; Narenpitak et al., 2021; Janssens et al., 2022). Possibly, precipitation is more decisive for maintaining than for initiating organisation.

Conversely, spatial organisation could be important for rain formation. Precipitation formation depends on subtle interactions of dynamic, thermodynamic, and microphysical processes on different spatial and temporal scales. This makes the understanding of rain formation challenging, even for warm shallow cumulus clouds. Early observational studies roughly related cloud depth to surface precipitation, but differences between clouds remained (Byers and Hall, 1955). Organisation is thought to enable

the interaction of updrafts and reduce the dilution of clouds (López, 1978; Houze Jr. and Betts, 1981; Tompkins and Semie, 2017; Becker et al., 2018), both of which may contribute to a deepening of clouds or the development of rain in shallower clouds. Nuijens et al. (2009) found that variability in precipitation relates most strongly to variability in humidity and zonal wind speed. Organisation may create such variability. Much rain in the trades also re-evaporates before reaching the ground (Naumann and Seifert, 2016; Sarkar et al., 2022), which could be influenced by organisation. Local circulations associated with organised convection (e.g. induced by cold pools) can also alter the vigor and microphysical properties of clouds such as their mixing characteristics, which thus influences the formation of rain (Stevens et al., 2021) - a process that Seifert and Heus (2013) suggested may be self-reinforcing. Although precipitation may be key to understanding the trades' vertical thermodynamic structure, cloudiness, and spatial patterns (e.g. Vogel et al., 2016), the representation of precipitation in LES of the trades differs largely (van Zanten et al., 2011). An understanding of how spatial organisation influences precipitation might help interpret and reduce these differences.

All in all, precipitation and spatial organisation seem associated, but their relationship remains unclear. However, understanding the relationship between precipitation and spatial organisation identifies to be crucial to understand the mechanisms of either of them - and ultimately understand and anticipate the behaviour of trade-wind clouds and their cooling effect in our current and future climate.

## 1.3  RESEARCH QUESTIONS

In this thesis, I investigate how precipitation and spatial organisation in the trades depend on and influence each other by exploring both observational data and high-resolution simulations to answer two main questions:

1. How are the occurrence, amount and intensity of rain in observations of the trades related to clustering (study A)?

2. Does spatial organisation affect the pathway to precipitation in simulated trade-wind convection (study B)?

To investigate these questions, I take advantage of the recent ElUcidating the RolE of Cloud-Circulation Coupling in ClimAte (EUREC$^4$A) field campaign (Stevens et al., 2021, Chapter 2). This campaign took place in January and February 2020 in the North Atlantic trades around the island of Barbados. The following chapter outlines the motivation for this campaign (Sect. 2.1), its measurements and the accompanying modelling activities (Sect. 2.2). I will introduce the observations and simulations used in the two subsequent studies and also touch upon further studies to which I contributed during my PhD, mostly in the context of this campaign.

Before outlining the two studies, I would like to shortly discuss the term and meaning of spatial organisation in this thesis as it might evoke different perceptions in different people. There has been no agreement on a unique definition of organisation and several approaches and metrics exist. Common ingredients in these metrics are the

number (Tobin et al., 2012), size (Retsch et al., 2020) and spacing (Tompkins and Semie, 2017; White et al., 2018) of convective elements. These are discussed in study A, targeting the spacing, that is spatial distribution or arrangement of convective elements. Instead of focusing on individual convective properties, metrics also use the spatial variability in the closely connected moisture structure (Bretherton and Blossey, 2017; Narenpitak et al., 2021), which is applied in study B. Different metrics and wordings reflect different focus on theses features of organisation, combining some or focusing on one. I use spatial organisation as term in a broad sense and attribute a high degree of organisation to scenes with high variability in the spatial moisture structure, where convective elements are closely spaced or form large convective structures. This configuration is often associated with the term clustering, which I use to refer to the close spacing, i.e. the spatial distribution of convection following Tompkins and Semie (2017, see Sect. 3.1). Lastly, spatial organisation can only be assessed in reference to a certain spatial domain. Throughout this thesis, I will refer to this as a scene.

In study A (Chapter 3), I analyse the spatial organisation of trade-wind precipitation fields scanned by a rain radar upstream of Barbados. Recalling the RICO campaign, I use the perspective of precipitation to investigate the importance of spatial organisation in the context of how these fields and their rain amount and intensity relate to clustering. In doing so, I go beyond the mostly visual inspections of Snodgrass et al. (2009) and Stevens et al. (2020) to systematically investigate and quantify for the first time how precipitation and clustering relate in observations. I thereby also complement the research focusing mostly on clustering from the cloud field perspective. I show that the occurrence of precipitation is related to a clustered spatial distribution (Sect. 3.1), but that the rain amount, i.e. mean rain rate, varies mainly independently from the cells' degree of clustering. The degree of clustering may only be important to maintain precipitation in dry environments, and for high rain intensities (Sect. 3.2).

In study B (Chapter 4), motivated by the results of study A, I turn to investigate how the process of precipitation might vary with organisation. Yamaguchi et al. (2019) found that in idealised LES, precipitation also varies little, but cloud sizes and spatial distributions differ in response to large changes in the aerosol environment. Could spatial organisation be a process to maintain precipitation in different environments, enabling or creating a different pathway to precipitation? Exploiting the process-based view of realistic large-domain LES, I decompose the pathway to surface precipitation into two phases: (i) a production phase where cloud condensate is converted to rain, and (ii) a sedimentation phase where the produced rain water falls towards the ground while part of it re-evaporates. I show that organisation affects how these two phases contribute to precipitation (Sect. 4.1) by modulating the local moisture environment, cloud vertical motion, and the dominant conversion mechanism (Sect. 4.2). I conclude that the pathway to precipitation differs with organisation.

In chapter 5, I conclude on both questions (Sect. 5.1) and on what they, in light

of the recent body of literature, infer about the relationship between precipitation and spatial organisation in the trades and the robustness of trade-wind clouds (Sect. 5.2).

# EUREC⁴A - A COMMUNITY EFFORT TO BETTER UNDERSTAND TRADE-WIND CLOUDS

*An experiment is a question which science poses to Nature,
and a measurement is the recording of Nature's answer.*

— Max Planck (1949)

EUREC$^4$A[1] took place in January and February 2020 around the island of Barbados in the North Atlantic trades (see Fig. 2.1). Here, shallow cumuli are found to be ubiquitous and representative across the trades (Medeiros and Nuijens, 2016; Stevens et al., 2016). EUREC$^4$A was initially designed to test a hypothesised trade-cumulus feedback mechanism and constrain uncertainty in climate sensitivity estimates (Bony et al., 2017). However, the envisioned measurements motivated many more groups and ideas to join and EUREC$^4$A ultimately became a multi-faceted collaboration. It was one of the most ambitious efforts to quantify how clouds, circulation and the atmospheric and oceanic environment covary over a vast range of scales (Stevens et al., 2021). I was fortunate to not only draw on the rich measurements and modelling activities for my studies, but also to participate in the EUREC$^4$A campaign and contribute to a better understanding of trade-wind cumuli in a broader context.

In this chapter, I present the motivation of the EUREC$^4$A campaign, which ties in with recent efforts and developments to constrain the trade-wind cloud feedback (Sect. 2.1), and describe its measurements and simulations (Sect. 2.2). I highlight the measurements to which I contributed and introduce the measurements and simulations I use for study A and study B. I also outline other projects and studies, I contributed to during my PhD, mostly in the context of EUREC$^4$A. A thorough synopsis of EUREC$^4$A is provided in the overview paper that I co-author (Stevens et al., 2021, *"EUREC⁴A"*, ESSD).

## 2.1 CONSTRAINING THE TRADE-WIND CLOUD FEEDBACK

The original idea of EUREC$^4$A was to observationally constrain the trade-wind cloud feedback (Bony et al., 2017) that causes climate models to disagree in climate sensitivity estimates (Bony and Dufresne, 2005; Vial et al., 2013; Myers et al., 2021). In these climate models, the trade-wind cloud feedback could be traced to one hypothesised mechanism - that mixing desiccates clouds. But does this mechanism also occur in nature where the variety of clouds, cloud organisations and circulations is not neglected as in climate models but taken into account? EUREC$^4$A aimed to test whether the mixing-desiccation mechanism occurs in nature. Section 2.2 describes the

---

[1] is used as a name rather than an abbreviation and pronounced *heúrēka* - as Archimedes is said to have exclaimed when he discovered buoyancy while bathing (Stevens et al., 2021)
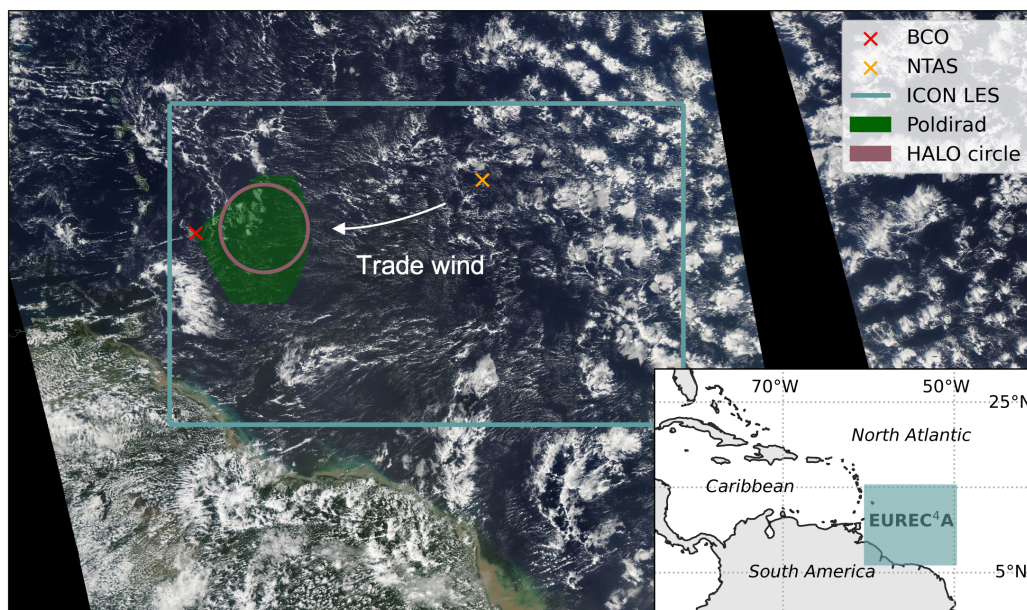
Figure 2.1: Overview of measurements and simulations used in this thesis conducted in the context of the EUREC⁴A campaign. The background shows a MODerate-resolution Imaging Spectroradiometer (MODIS) image from 8th January 2020 from Worldview (https://worldview.earthdata.nasa.gov).

measurements conducted to do so.

Apart from these observational efforts, hope to constrain cloud feedbacks soon emerges from the increase in computational power. Large-eddy simulations (LES), used in study B, explicitly simulate the convective motions to study trade-wind clouds. LES is a turbulence modelling technique, that resolves most of the energy-containing motions, on the scale of the larger boundary layer eddies. However, LES, which typically run with hectometer grid spacings, remain limited in their domain size and time period due to their computational expense (e.g. van Zanten et al., 2011; Bretherton et al., 2013; Heinze et al., 2017). Recently, the first multi-model ensemble of global simulations without convective parameterisations have been conducted, exploiting kilometre-scale gridspacings (Stevens et al., 2019b). Global storm-resolving models (SRMs), as theses models are called, provide the opportunity to study cloud feedbacks while interacting with the large-scale environment but without having to rely on an uncertain convective parameterisation. However, at a typical grid spacing of a few kilometres shallow convection is hardly resolved.

In my master thesis, I conducted a study to bridge the gap between findings based on limited-area LES and emerging global SRMs. I simulated a trade-wind cloud field with the LES version of the ICOsahedral Non-hydrostatic (ICON) Model in a setup based on the RICO campaign (Rauber et al., 2007; van Zanten et al., 2011), both in a control and a perturbed 4 K warmed climate while degrading horizontal resolution from those typically used in LES (100 m) to those typically used in global SRMs (5 km).

I find that in a warmer climate cloud cover reduces, constituting a positive shortwave cloud feedback. During my PhD, I discerned that another mechanism compensates for the decrease in cloud cover: clouds additionally thicken with warming. While the cloud cover reduction increases with coarser resolutions, the thickening is resolution independent. Taken together, these effects yield a positive feedback at coarse resolutions, but tend to cancel out at fine resolutions, suggesting SRMs to exaggerate the trade-wind cloud feedback and a convergence towards near-zero cloud feedback with increasing resolution. I wrote a manuscript about this finalised analysis and interpretation of the results during my PhD and published it with the help of all co-authors as Radtke et al. (2021, *"Shallow cumulus cloud feedback in large eddy simulations - bridging the gap to storm resolving models"*, ACP).

A weak trade-wind cloud feedback is now also supported by EUREC$^4$A data. EUREC$^4$A data shows that the mixing-desiccation mechanism is not active in nature (Vogel et al., 2022). Again, competing mechanisms are at play. Dynamical processes increase cloudiness, overwhelming the hypothesised decrease in cloudiness based on thermodynamic considerations, so that mixing does not desiccate cloudiness. These dynamical processes seem connected to local circulations associated with spatial organisation (Narenpitak et al., 2021; George et al., 2022). EUREC$^4$A thus identifies an understanding of the mechanisms of spatial organisation as key to anticipate trade-wind cloudiness and finally constrain the trade-cumulus feedback and climate sensitivity. Making progress in this understanding is now, with the EUREC$^4$A observations and the exploitation of LES over large domains, at the tips of our fingers.

## 2.2 CLOUD OBSERVATIONS AND SIMULATIONS

During EUREC$^4$A, measurements were predominantly conducted upwind of Barbados in a region called the "Tradewind Alley" stretching from the Barbados Cloud Observatory (BCO, Stevens et al., 2016) to the Northwest Tropical Atlantic Station (NTAS) - an advanced open-ocean mooring (see Fig. 2.1). The core of operations, aimed at addressing the initial objectives of EUREC$^4$A, formed the circling flights of the High Altitude and LOng range research aircraft (HALO, Stevens et al., 2019a), as marked by the black circle in Fig. 2.1. While HALO was circling above the clouds, a low-flying aircraft sampled cloudiness at cloud base height. The green shaded area in Fig 2.1 was additionally mapped out by scans of the C-band POLarization DIversity RADar (Poldirad, Schroth et al., 1988) installed on Barbados. Measurements at the BCO, on several ships, airplanes and autonomous vehicles complemented the array of observations. In study A, I analyse the low-level scans of the C-band rain radar Poldirad that scanned the spatial distribution of precipitating shallow convection upwind of Barbados, as sketched in Fig. 2.1 (Hagen et al., 2021). Additionally, I use measurements of integrated water vapour from Global Navigation Satellite System (GNSS) receivers at the BCO (Bock et al., 2021).

Besides the measurements, numerous modelling activities accompanied the campaign. Among others, a new ensemble of global SRMs (a follow up of Stevens et al.,

2019b) simulated the campaign period and different LES were conducted. In study B, I exploit large-domain realistic LES conducted with the ICON model (Schulz, 2021). To explore mesoscale convective variability, these simulations are performed with a relatively fine grid spacing of 625 m over a large domain of $\mathcal{O}(1000\text{km})$, covering the western tropical Atlantic from 60.2–45.0 °W and 7.5–17.0 °N, that is an extended "Tradewind Alley", as visualised in Fig. 2.1. The simulations run from 9 January to 19 February 2022 and exploit the two-moment mixed-phase bulk microphysics scheme of Seifert and Beheng (2006). They are initialised and nudged at the lateral boundaries to a limited-area storm-resolving simulation at 1.25 km grid spacing, which takes its initial and boundary data from the atmospheric analysis of the European Centre for Medium-Range Weather Forecasts (similar to Klocke et al., 2017).

During EUREC⁴A, I mainly contributed to the daily weather report and participated in the research flights of the high-flying aircraft HALO, monitoring the radar and radiometer measurements or carrying out dropsonde measurements. The latter allowed to measure the lower-tropospheric mixing and, together with measurements of cloudiness by the aircraft flying at cloud base height, to refute the mixing-desiccation mechanism. Due to taking responsibility for the dropsonde launch operations and real-time data quality control over different research flights, I co-author the paper George et al. (2021, *"JOANNE: Joint dropsonde Observations of the Atmosphere in tropical North atlaNtic meso-scale Environments"*, ESSD). It describes the dropsonde measurements and is named after Joanne Simpson in honour of her pioneering work on trade wind convection. The research flights and all measurements conducted with the HALO aircraft are described in the publication by Konow et al. (2021, *"EUREC⁴A's HALO"*, ESSD) that I co-author. Alongside the measurements, I contributed to the publication with a case study on how the different instruments on board of HALO view clouds (Fig. 2.2). The vertical cross sections in Fig.2.2 a and b show how some clouds remain shallow with their cloud tops near cloud base, while some clouds reach higher up to the inversion. These deeper clouds tend to rain, appearing in the view of the radar. Fig 2.2 c and d show corresponding horizontal views of the cloud scene. They indicate how different the spacing and size of trade-wind clouds can be and that clustering appears to be associated with rain.

What makes EUREC⁴A special, is the wealth of data collected through the many groups, institutions and nations that participated. At the same time, this quality holds the challenge to make this distributed wealth of data visible and usable. In this context, I contributed within a group of young researchers to the development of the openly accessible and executable book that we named *How to EUREC⁴A²*. *How to EUREC⁴A* consists of "how to" example scripts. Combining code and explanatory markdown files, these scripts show how to access the data, contain explanations about the instruments and provide quicklooks of the data or typical usage patterns - e.g. the cloud view case study[3] (Fig.2.2). In doing so, the book makes datasets visible and helps to get started with them while thriving on and stimulating collaboration, knowledge transfer

---

2 https://howto.eurec4a.eu
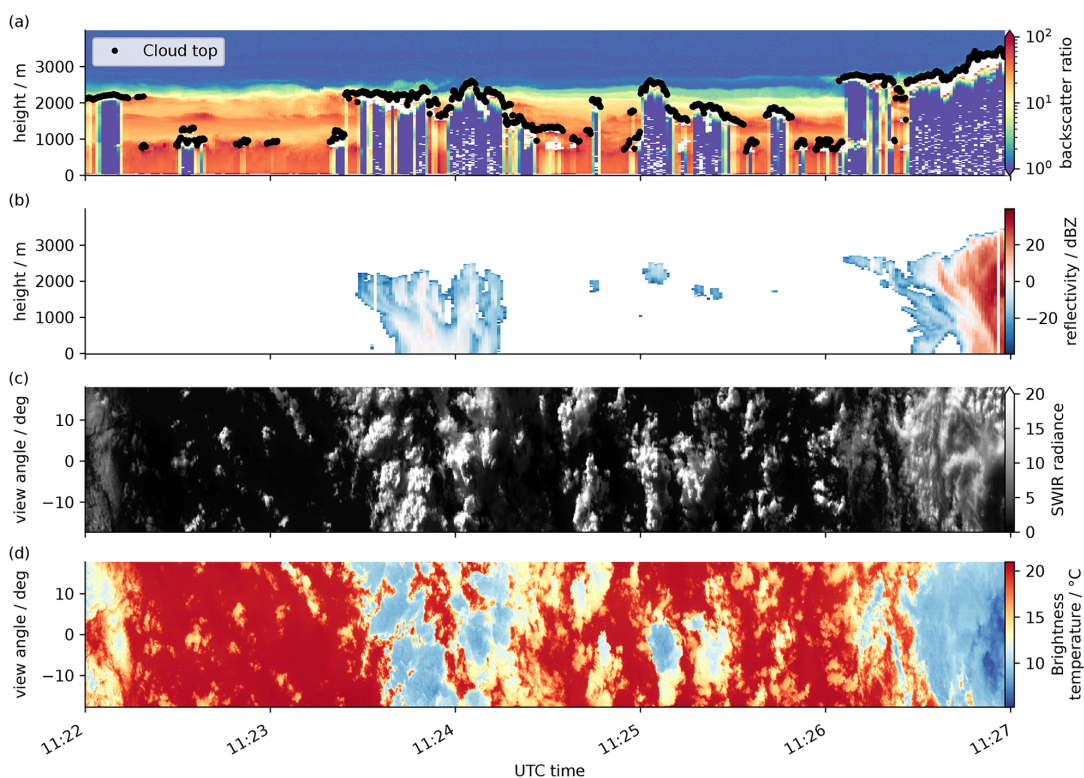3 https://howto.eurec4a.eu/cloudmasks.html

Figure 2.2: View on clouds from different instruments onboard HALO. Figure from Konow et al. (2021). Vertical profiles of (a) backscatter ratio at 1024 nm from the WALES lidar together with a cloud-top height estimate, (b) HAMP cloud radar reflectivity, and horizontal views on the cloud field from (c) the specMACS imager at 1.6 $\mu$m (SWIR, shortwave infrared), and (d) from the VELOX IR imager (7.7 and 12 $\mu$m). Please refer to (Konow et al., 2021) for an explanation of the acronyms and information about the instruments.

and the publication of accessible and analysis-friendly datasets. Data is accessed via (intake) catalogue structures, that contain links to the most recent versions of the publicly available EUREC$^4$A data and is continuously updated. As data user, no data has to be downloaded, no paths adjusted. Born in the context of the HALO datasets (Konow et al., 2021), *How to EUREC$^4$A* quickly matured through the contributions from the wider EUREC$^4$A community and also got adopted by other campaigns and projects. We hope it will contribute to a new way of handling, disseminating and collaborating on Earth system science data.

Although I concentrate in this thesis on the relationship between precipitation and spatial organisation in the trades, clustering and rain processes are important across the globe. As part of a local field campaign in Hamburg, I contributed to a study during my PhD focusing on the localised - temporally and spatially limited - nature of rain showers. We investigated the statistics of this locality from the perspective of how commuting cyclists are affected by rain and weather in Hamburg (Schmitt et al., in review, *"Assessing the weather conditions for urban cyclists by spatially dense measurements*

*with an agent-based approach"*). I mainly contributed to this work by conceptualising and interpreting the analyses and co-writing the manuscript. The study highlights the potential of guidance by weather observations and forecasts to anticipate the local rain showers and reduce the risk of experiencing bad weather during a ride. Let us turn back to the EUREC⁴A observations now, and see how clustering influences the risk of experiencing rain showers in the trades.

# THE RELATIONSHIP BETWEEN PRECIPITATION AND CLUSTERING OBSERVED DURING EUREC⁴A

*... experience suggests that the investigator who attempts to deduce ... without first observing it is placing himself at a considerable disadvantage...*

— Edward Lorenz (1967)

Inspecting radar and satellite imagery during the RICO campaign, Snodgrass et al. (2009) remarked that high precipitation rates are often observed with clouds clustered along arc-like structures. This raises the hypothesis that clustering increases precipitation, e.g. through cell interaction or protection. A systematic study of the relationship between precipitation and clustering in the trades beyond visual inspections, however, was lacking. Most studies also focused on clustering from the cloud field perspective. In spirit of the RICO campaign, study A uses the perspective of precipitation and analyses rain radar measurements upstream of Barbados conducted during the EUREC⁴A field campaign to investigate how clustering influences the occurrence, amount and intensity of rain. It addresses the following research questions:

1. How are trade-wind precipitation fields spatially organised? Are they clustered?

2. How does clustering affect rain amount and intensity? Do they increase with clustering?

In the following I outline the main methods I applied to answer these questions and summarise the key results.

## 3.1 SPATIAL ORGANISATION OF TRADE-WIND PRECIPITATION FIELDS

The research questions are addressed by analysing scenes of precipitating trade-wind convection scanned by the C-band radar Poldirad upstream of Barbados during the EUREC⁴A field campaign (see 2.2). An example scene is shown in Fig. 3.1a. In each scene, precipitating areas are segmented from the non-precipitating environment with a threshold value of $0.1 \, \mathrm{mm \, h^{-1}}$. From these areas, the individual rain cells that populate the scene are identified with a watershed segmentation, shown for example in Fig. 3.1a. After the segmentation, the spatial distribution of the cells is analysed with the $I_{\mathrm{ORG}}$ index (Tompkins and Semie, 2017), which ranges from 0 to 1. The $I_{\mathrm{ORG}}$ index compares the observed nearest-neighbour distances with those of a random distribution. When the observed distances are smaller than expected from a random distribution, the spatial distribution is classified as clustered, denoted by $I_{\mathrm{ORG}} > 0.5$. This is the case in the example scene. Values below 0.5 denote a regular distribution.
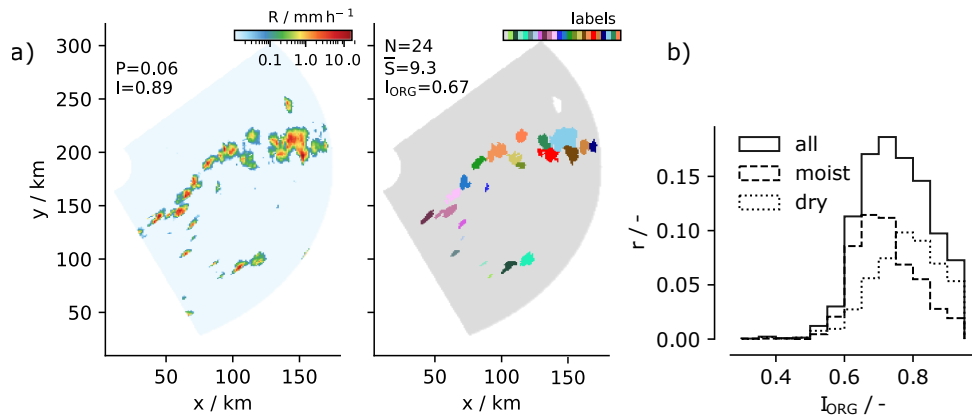
Figure 3.1: a) Example scene of rain rate and rain cell segmentation from February 11, 2020, 0050 h. For symbols, see text. b) Relative frequency of $I_{ORG}$ for all, dry ($W < \text{median}(W)$) and moist ($W < \text{median}(W)$) scenes with median$(W) = 36\,\text{kg}\,\text{m}^{-2}$.

A histogram of the trade-wind precipitation fields' spatial distributions as assessed with the $I_{ORG}$ index is shown in Fig. 3.1b. Values are mostly above 0.5, that is, in nearly all scenes scanned by the radar during EUREC[4]A, rain cells were spaced closer than in a random distribution, meaning they occurred in a clustered state. Thus, the occurrence of precipitation in the trades is indeed related to a clustered spatial distribution. Including measurements of integrated water vapour ($W$) in the analyses (see 2.2) shows that dry scenes (low $W$) typically exhibit a higher degree of clustering than moist scenes (high $W$). This is in line with idealised studies (Bretherton et al., 2005; Muller and Held, 2012) and satellite observations (e.g. Tobin et al., 2012) showing that clustered or aggregated states of deep convection are typically drier. Clustering may influence how clouds interact with their environment. More isolated rain cells - that is, cells with a low degree of clustering - may hardly exist in dry environments as they are strongly affected by entrainment. Clustering may prevent updrafts from losing buoyancy through entrainment, so that cells can develop in hostile, dry environments (Becker et al., 2018).

Besides their spatial distribution, I also analyse the number ($N$) and mean size ($\overline{S}$) of the rain cells. In the example scene, 24 cells with a mean cell size of about 9 km are present (Fig. 3.1). During EUREC[4]A up to 60 cells in one scene occurred and the most common mean rain cell size was about 5 km. Relating the cells' spatial distribution and integrated water vapour to the cell number and size, I find that the highest degree of clustering typically occurs in dry scenes that contain a few and on average large cells as shown in Fig. 3.2a. These are concordant findings to radar observations (Louf et al., 2019; Retsch et al., 2020) and simulations (Brueck et al., 2020) of deep convection suggesting similarities between the spatial organisation of shallow and deep precipitating convection. As the environment moistens, cells tend to be larger, more numerous and scattered (Fig. 3.2a). However, the mean area of the cells only varies weakly with $W$. Thus, my analyses suggest that precipitation increases

with water vapour path, as highlighted in Nuijens et al. (2009), because there are predominantly more numerous, scattered rain cells rather than larger cells.

## 3.2 HOW CLUSTERING RELATES TO RAIN AMOUNT AND INTENSITY

The amount of rain falling in a scene is important for the scene heating and drying through precipitation. Fig. 3.2b shows that the rain amount $P$ (mean rain rate), varies closely with cell number and size and hence with the precipitating area, as already suggested by previous studies (Nuijens et al., 2009). Highest rain amounts occur in scenes that contain many and on average large cells. Recalling the previous analyses, the degree of clustering, however, maximises towards scenes with rather large but few cells (Fig. 3.2b contour lines). Consequently, the rain amount does not scale with the cells' degree of clustering. Instead, the rain amount varies mainly independently of the degree of clustering, or if anything it shows a tendency towards a negative correlation. Scenes with small $N$ and large $\bar{S}$, which show on average a high degree of clustering, also contribute little to the total observed rain amount (not shown here, see Fig. A.8d). These findings suggest that the degree of clustering is of secondary importance for the rain amount in the trades. Hypothesised mechanisms, such as that clustering increases precipitation through cell interaction, seem to play overall no role or a subordinate one for the rain amount in a scene. Only when considering the moisture environment a positive effect of the degree of clustering on rain amounts may be seen. For scenes with similar precipitation, moving in the $N$-$\bar{S}$ phase space diagonally from moist scenes with many small cells to dry scenes with few large cells, the degree of clustering increases (Fig. 3.2a and b). In this sense the degree of clustering may be important to maintain precipitation in dry environments.
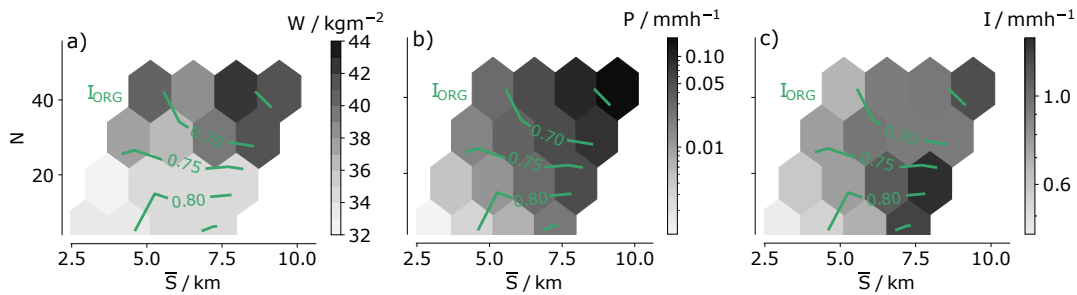


Figure 3.2: a) Integrated water vapour $W$, b) rain amount $P$ (mean rain rate) and c) rain intensity (mean conditional rain rate) $I$ as a function of mean cell size $\bar{S}$ and cell number $N$. Contour lines denote the cells' spatial distribution as measured by the $I_{\mathrm{ORG}}$.

Clustering may not be important for the rain amount, but possibly for the rain intensity. Rain intensity $I$ (mean rain rate conditioned on raining areas) is important e.g. for the triggering of cold pools (Snodgrass et al., 2009). Analysing rain intensity as a function of cell number and size, Fig.3.2c shows that rain intensity varies weakly with cell number but increases with the mean cell size. Thus while the convective

or precipitating area, often used in convective parameterisations, describes the rain amount well, distinguishing between cell number and size is imperative to capture variations in rain intensity. Rain intensity may increase with cell size because larger cells can sustain stronger updrafts since they are better protected from dilution by entrainment (e.g. Kirshbaum and Grant, 2012; Schlemmer and Hohenegger, 2014). Additionally, shallow circulations are found to accompany large clusters (Bretherton and Blossey, 2017), which could increase the liquid and rain water content. Figure 3.2c shows that the increase of rain intensity with cell size is stronger in scenes with fewer and more strongly clustered cells than in scenes with more and more weakly clustered cells. Rain intensity hence maximises in scenes that contain rather large, few, and strongly clustered cells. Clustering may enhance the effects described above. In weakly clustered scenes, many isolated cells may compete for moisture and heat, so that they can grow larger but not as intense as in strongly clustered scenes, where cells protect each other and shallow circulations draw in moisture and heat. Although the correlation between the degree of clustering and rain intensity is weak across the whole dataset, this suggests that the degree of clustering is important for high rain intensities.

Besides the snapshot view on precipitation adopted by the previous analyses, I also look at the relationship between precipitation and clustering in the diurnal cycle (not shown here, see Fig. A.13). The diurnal cycle is a prominent mode of variability recently revisited by Vial et al. (2019). In line with previous studies, precipitation maximises in the early morning before sunrise and minimises in the late afternoon before sunset (e.g. Nuijens et al., 2009; Snodgrass et al., 2009). The diurnal cycle of cell number and size roughly follows the diurnal cycle of precipitation, which matches my previous analysis, with a tendency of cell size to lag the cell number slightly. Roughly in anti-phase to cell number is the degree of clustering - being low at night and high during daytime. I use the diurnal cycle to relate my analyses to the cloud patterns gravel, fish and flower (Vial et al., 2021, see 1.2). Around midnight, where Vial et al. (2021) show that the gravel cloud pattern has its peak occurrence, rain cells are rather small, numerous, and weakly clustered. Before sunrise, flowers, which are large cloud clusters, occur most frequently. Here, rain cells also tend to be rather large. Around noon, the fish pattern occurs often associated with rain cells that still tend to be rather large but now also strongly clustered. This analysis suggests that precipitation and cloud patterns are closely linked.

In brief, study A yields the following key results:

- The occurrence of precipitation is related to a clustered spatial distribution.

- The mean rain rate does not scale with the cells' degree of clustering but varies largely independently from it.

- The degree of clustering may be important to maintain precipitation in dry environments and for high rain intensities.

# HOW SPATIAL ORGANISATION AFFECTS THE PATHWAY TO PRECIPITATION IN SIMULATED TRADE-WIND CONVECTION

*What do you say? Who rains, then?*
*For first of all explain this to me.*

— Strepsiades to Socrates in
Aristophanes' play The Clouds (417 BC)

What makes it rain? Study A showed that precipitation averaged over a scene varies independently of the degree of organisation. This could indicate that organisation also has no influence on the development of rain. However, in scenes with similar precipitation but different spatial organisation the moisture environment differs. Similarly, Yamaguchi et al. (2019) found that in idealised LES, precipitation varies little but cloud sizes and spatial distributions differ in response to large changes in the aerosol environment. Could spatial organisation be a mechanism to maintain precipitation in different environments, enabling different pathways to precipitation? To investigate this, study B exploits the process-based view of realistic large-domain LES of the trades during EUREC⁴A and decomposes the formation of surface precipitation into a production and a sedimentation phase following Langhans et al. (2015). It addresses the following research questions:

1. Does spatial organisation affect how the production or sedimentation phase contribute to the formation of precipitation? Does organisation alter how efficiently it precipitates in total?

2. If so, why does spatial organisation affect the production or sedimentation of rain? Which physical mechanisms are at play?

In the following, the main methods applied to answer these questions are introduced and the key results are summarised.

## 4.1 THE PATHWAY TO PRECIPITATION VARIES WITH ORGANISATION

The research questions are addressed by analysing realistic large-domain LES of the North Atlantic trades. These cover the period from January to February 2020 when the EUREC⁴A field campaign took place (see Chapt. 2). In scenes of $4 \times 4\,°$ (about $450 \times 450\,\mathrm{km}$), I assess spatial organisation by the spread in mesoscale coarse-grained total water path, $\mathcal{O}_{\mathrm{rga}}(\Delta W_{\mathrm{T_m}})$. Fig. 4.1 shows three example scenes with different degrees of organisation. On the left, the scene is weakly organised, showing a low $\mathcal{O}_{\mathrm{rga}}(\Delta W_{\mathrm{T_m}})$ and scattered convection. Towards the right, scenes are more strongly organised, showing a high $\mathcal{O}_{\mathrm{rga}}(\Delta W_{\mathrm{T_m}})$ and clustered convection. The simulations reproduce the EUREC⁴A observations according to which precipitation varies mainly

independently of the degree of organisation (Radtke et al., 2022, Study A). This is illustrated by the three example scenes. While the rain amount is similar in these scenes, the degree of organisation varies vastly. In total about 2000 scenes are used in the analysis and domain mean values are investigated if not mentioned otherwise.
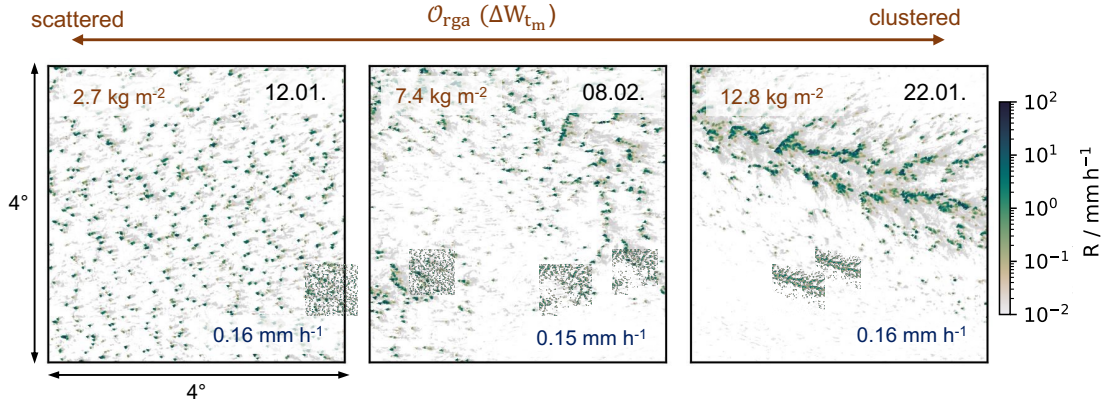


Figure 4.1: Three example scenes with similar rain amount (blue) but different degrees of organisation $\mathcal{O}_{\mathrm{rga}}(\Delta W_{\mathrm{T_m}})$ (orange). Colour shading denotes rain rate $R$. Grey shading denotes cloud albedo calculated from simulated cloud liquid water path.

To investigate the pathway to precipitation, I decompose the formation of surface precipitation into (i) a production and (ii) a sedimentation phase. Phase (i), the production of rain water from cloud water, is microphysically parameterised following Seifert and Beheng (2001) by the autoconversion rate ($C_{\mathrm{Auto}}$), which parameterises the merging of small cloud droplets to initially form rain, and the accretion rate ($C_{\mathrm{Acc}}$), which parameterises the collection of cloud droplets by falling raindrops. To quantify how efficient the production of rain is, I define a conversion efficiency $\epsilon_{\mathrm{conv}} = C_A/W_L$, where $C_A = C_{\mathrm{Auto}} + C_{\mathrm{Acc}}$ and $W_L$ denotes the cloud liquid water path. In phase (ii), the rain water produced by autoconversion and accretion sediments towards the ground. During this process, some rain evaporates while the rest reaches the ground as surface precipitation, $P$, so that I call $\epsilon_{\mathrm{sed}} = P/C_A$ the sedimentation efficiency. The product of the conversion and sedimentation efficiency describes how much cloud water precipitates (Langhans et al., 2015), in other words a precipitation efficiency $\epsilon_P$ defined as the ratio of precipitation to cloud liquid water path:

$$\underbrace{\frac{P}{W_L}}_{\epsilon_P} = \underbrace{\frac{C_A}{W_L}}_{\epsilon_{\mathrm{conv}}} \cdot \underbrace{\frac{P}{C_A}}_{\epsilon_{\mathrm{sed}}} . \tag{4.1}$$

How organisation varies as a function of conversion and sedimentation efficiency is shown in Fig. 4.2a. The contour lines denote the precipitation efficiency, showing that one to four times the cloud liquid water path precipitates per hour. This demonstrates the rapid turnover and rain formation in trade-wind clouds, which are reported to "usually rain within half an hour" when cloud tops reach higher than 2500 m (Squires,

1958). Sedimentation efficiency varies between 0.1 and 0.3, which reflects that additionally a great amount of rain re-evaporates, as reported by Naumann and Seifert (2016) and Sarkar et al. (2022). Organisation maximises towards the lower right of the phase space, at low conversion and high sedimentation efficiency. An increase in the degree of organisation is thus related to a decrease in how efficient cloud water is converted to rain and an increase in how efficient rain sediments, meaning a greater contribution of rain reaches the ground instead of evaporating. Precipitation maximises towards the upper right of the same phase space (Fig. 4.2b) and thus varies closely with the precipitation efficiency. Because conversion efficiency decreases but sedimentation efficiency increases with organisation, contours of organisation and precipitation efficiency lie perpendicular to each other in the phase space. This means that precipitation efficiency, like precipitation, varies mainly independently of organisation. Thus, organisation weakly affects how efficiently it precipitates compared to the available cloud water but it changes the pathway to precipitation in terms of how much the production versus the sedimentation phases contribute to the formation of surface precipitation.
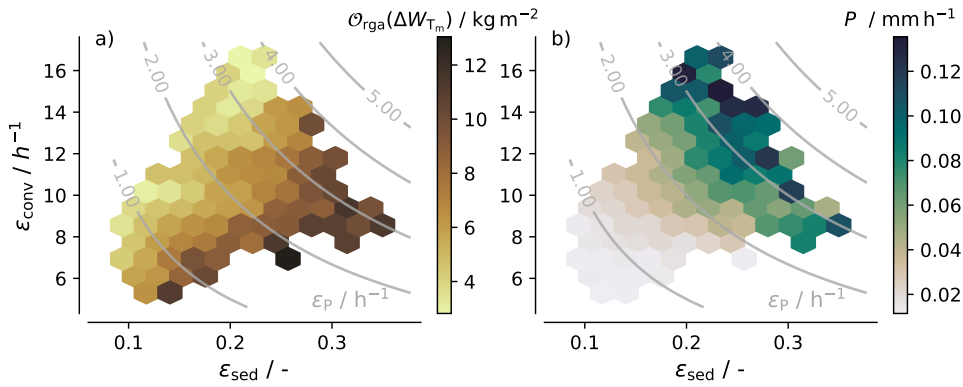


Figure 4.2: a) Degree of mesoscale organisation $\mathcal{O}_{\mathrm{rga}}(\Delta W_{T_m})$ and b) precipitation $P$, shading, as a function of conversion efficiency $\epsilon_{\mathrm{conv}}$ and sedimentation efficiency $\epsilon_{\mathrm{sed}}$. Contour lines denote precipitation efficiency $\epsilon_P = \epsilon_{\mathrm{conv}} \cdot \epsilon_{\mathrm{sed}}$.

## 4.2 WHY ORGANISATION ALTERS THE PATHWAY TO PRECIPITATION

The sedimentation efficiency describes how much rain reaches the ground instead of evaporating. It may be affected to first order by the moisture environment through which the rain falls and the time it takes the rain to fall, which depends on the fall velocity and height (Lutsko and Cronin, 2018). Organisation manifests itself in the (inhomogeneous) horizontal distribution of moisture, as also used in the metric of organisation, suggesting that organisation influences the raindrops' moisture environment. Fig. 4.3a shows that with strengthened organisation, the environment through which rain falls indeed typically has a higher relative humidity. This acts to reduce the evaporation of raindrops. With strengthened organisation, rain is also increasingly produced by accretion (Fig. 4.3b), indicating the growth of larger raindrops. Larger

raindrops fall faster, reducing the time it takes for rain to reach the ground and thus the time available for evaporation. The relative importance of autoconversion versus accretion to rain production explains 79% of the variations in sedimentation efficiency, increasing to 85% when including the rain-conditioned relative humidity as an additional predictor. Variations in the fall height cannot explain any additional variations in sedimentation efficiency. My analysis thus suggests that organisation reduces evaporation and increases the sedimentation efficiency because rain in more organised scenes is increasingly produced by accretion, so that raindrops are larger, and rain falls through a locally more humid environment.
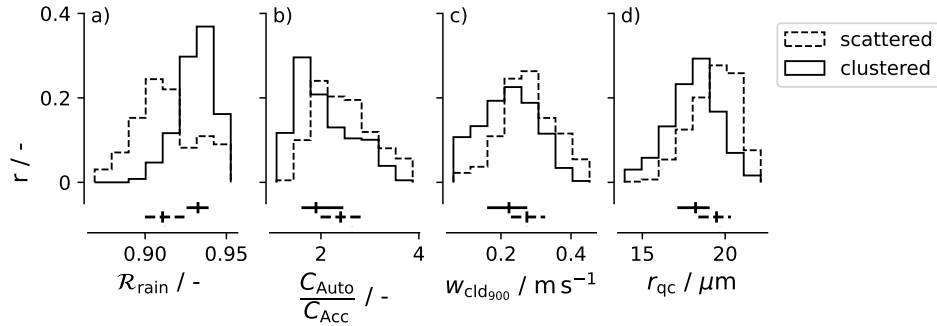


Figure 4.3: Relative frequency of a) rain-conditioned relative humidity $\mathcal{R}_{\text{rain}}$, b) ratio of auto-conversion rate $C_{\text{Auto}}$ to accretion rate $C_{\text{Acc}}$, c) cloud-conditioned vertical velocity at 900 hPa $w_{\text{cld}_{900}}$ and d) mean cloud droplet radius $r_{\text{qc}}$ for a scattered ($<$30th percentile) and clustered ($>$70th percentile) sample of scenes. Horizontal lines denote the interquartile range, vertical lines the median.

Cloud condensate is converted to rain when sufficient cloud water has been produced and cloud droplets have grown to precipitation size. To initiate and grow cloud particles the air's saturation is important and influenced by the thermodynamic conditions as well as vertical motions. I find that organisation in the simulations influences the clouds' vertical motion. With strengthened organisation, the mean vertical motion at cloud base decreases (Fig. 4.3c). As organisation creates more favourable thermodynamic conditions for cloud and rain formation (Fig. 4.3a), clouds might be able to develop in weaker dynamic conditions. The cloud base vertical motions explain 70% of the variations in conversion efficiency. Correlated with the cloud base vertical motion, the mean cloud droplet size also decreases as organisation increases (Fig. 4.3d). To the change in cloud droplet size may also contribute that organisation is thought to change the mixing characteristics of clouds. In conclusion, my analysis suggests that organisation reduces the efficiency with which cloud water is converted to rain water, because rain forms in weaker updrafts from smaller cloud droplets.

With increased organisation, the competing effects of increased sedimentation efficiency and decreased conversion efficiency compensate one another. Why? One explanation may be that organisation establishes more favourable thermodynamic conditions. This allows more rain to sediment to the ground instead of evaporating, but could also allow clouds to develop in less dynamic conditions, leading to a less

efficient production of rain. An alternative explanation is that (life)time effects could couple the production and sedimentation efficiency. As clouds grow more slowly due to weaker vertical motions that inefficiently produce rain, the lifetime of clouds may increase. This allows the rain production process to evolve, leading to an increased contribution of accretion to rain production and raindrops growing larger, so that rain falls out more efficiently. This is in line with the concept of buffering (Feingold et al., 2017), which states that if there are different paths leading to the same state, they buffer the system against disruptions to any particular path. I conclude that organisation is one form of buffering. While in less organised scenes rain development is predominantly driven by efficient conversion of cloud water to rain water, in more organised scenes more efficient sedimentation of rain increasingly contributes to rain formation. The pathway to precipitation differs with organisation.

## 4.3 OUTLOOK: TEMPORAL PATHWAY

Besides the snapshot view taken in the above analyses, I started to investigate how the formation of precipitation relates to organisation in a temporal manner. This may point to the chronology of events and whether feedbacks between the precipitation pathway and organisation exist. To this end, I adopt a lagrangian view, tracking scenes with the mean 950 hPa wind for 24 hours, and compose the temporal evolution of precipitation as a function of the time of maximum organisation (Fig. 4.4). Here, only scenes with a minimum rain rate >0.04 mm h and a minimum of variation in the degree of organisation $> 2\,\mathrm{kg\,m^{-2}}$ are included.



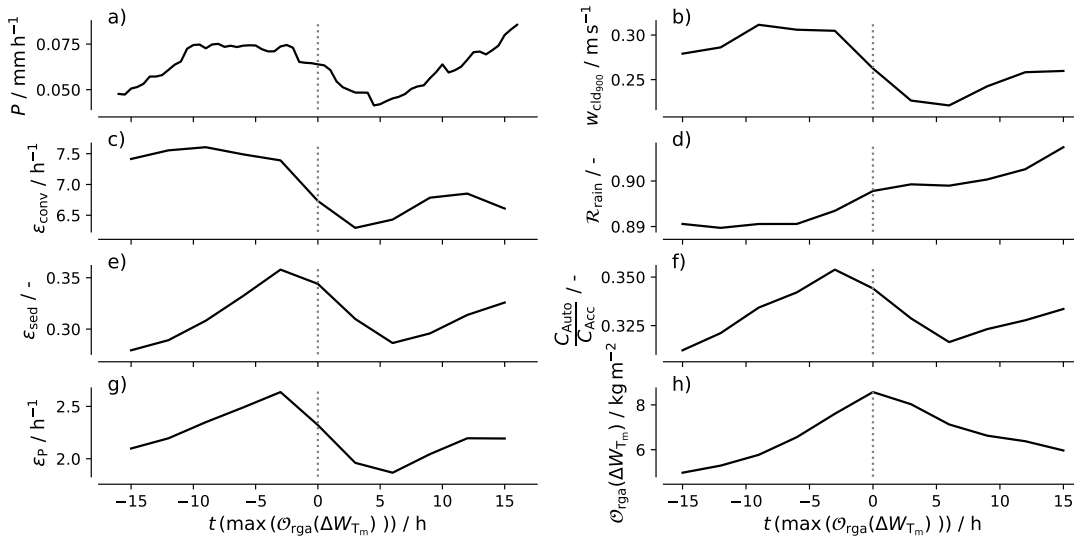Figure 4.4: a) Precipitation $P$, b) cloud-conditioned vertical velocity at 900 hPa $w_{\mathrm{cld}_{900}}$, c) conversion efficiency $\epsilon_{\mathrm{conv}}$, d) rain-conditioned relative humidity $\mathcal{R}_{\mathrm{rain}}$, e) sedimentation efficiency $\epsilon_{\mathrm{sed}}$, f) ratio of autoconversion rate $C_{\mathrm{Auto}}$ to accretion rate $C_{\mathrm{Acc}}$, g) precipitation efficiency $\epsilon_{\mathrm{P}}$ and h) degree of mesoscale organisation $\mathcal{O}_{\mathrm{rga}}(\Delta W_{\mathrm{T_m}})$ as a function of the time of maximum organisation $t(\max(\mathcal{O}_{\mathrm{rga}}(\Delta W_{\mathrm{T_m}}))).$

Precipitation peaks on average about ten to five hours before organisation as shown in Fig. 4.4a. This is in line with the different diurnal cycles of precipitation and organisation (Study A), which the simulations reproduce (not shown). Similarly to precipitation, conversion efficiency maximises around seven hours before the time of maximum organisation and then decreases towards it, evolving quite aligned with the cloud base vertical motion (Fig. 4.4b,c). In contrast, sedimentation efficiency maximises towards the time of maximum organisation (Fig. 4.4e). At this time, the rain-conditioned moisture increases, possibly because mesoscale circluations draw in moisture or because the evaporation of precipitation contributes to a moistening of the subcloud layer which could accelerate the process of organisation (Fig. 4.4d). The evolution of sedimentation efficiency is quite well aligned with the relative importance of accretion and autoconversion (Fig. 4.4f), which seems to indicate how progressed the rain production and how mature the cloud population is. Fig. 4.4g shows that precipitation efficiency is thus highest shortly before the time of maximum organisation where both conversion and sedimentation efficiency are rather high. This analysis suggests that the redistribution of moisture and an ageing of the cloud population are important factors in relating, as well as separating, the evolution of precipitation and organisation, and identifies them as possible candidates for feedbacks between precipitation and organisation.

In brief, study B yields the following key results:

- Organisation affects the pathway to precipitation altering how much the production versus sedimentation phases contribute to the formation of surface precipitation. It weakly affects how efficiently it precipitates in total.

- In more organised scenes, cloud water is less efficiently converted to rain because rain forms in weaker updrafts from smaller mean cloud droplet sizes.

- In more organised scenes, less rain evaporates and the sedimentation efficiency increases because rain falls in locally more humid environments and rain is increasingly produced by accretion, so that raindrops are larger.

# 5

## SUMMARY, CONCLUSIONS AND OUTLOOK

*... the sky knows the reasons and the patterns behind
all clouds, and you will know too, when you lift
yourself high enough to see beyond horizons.*

— Richard Bach (1981)

In this thesis, I investigate the relationship between precipitation and spatial organisation in trade-wind convection. In study A, I use rain radar observations from the EUREC⁴A field campaign to investigate how rain occurrence, amount and intensity relate to clustering. In study B, I exploit realistic large-domain LES of the trades during EUREC⁴A to analyse how spatial organisation affects the pathway to precipitation in simulated trade-wind convection. In contributing to EUREC⁴A measurements, I was fortunate to, in Bach's words, "*lift high enough*" to observe the intriguing formation of rain and cloud patterns myself. In addition, I could help to improve the understanding of trade-wind convection in a broader context. Section 5.1 answers the specific research questions posed at the beginning in Sect. 1.3. Sect. 5.2 concludes on the findings and discusses their implications.

### 5.1 RESULTS IN A NUTSHELL

1. How are the occurrence, amount and intensity of rain related to clustering in observations of the trades?

   During EUREC⁴A, scenes of precipitating trade-wind convection scanned by a rain radar almost always contained rain cells that were spaced closer than in a random distribution. Thus, the occurrence of precipitation in the trades is related to clustering. However, the rain amount, i.e. the scene's mean rain rate, does not scale with the cells' degree of clustering. Instead, rain amount varies largely independently from it. Whereas the rain amount maximises towards scenes with high water vapour path (a moist environment) containing many and large cells, the degree of clustering maximises towards scenes with low water vapour path (a dry environment) containing few and large cells and which rain intensively. My analyses thus suggest that hypothesised mechanisms, such as an increase of precipitation with clustering through cell protection or interaction, play overall a subordinate role for a scene's rain amount. They do influence the intensity of rain and, considering the moisture environment, may be important to maintain precipitation in dry environments.

2. Does spatial organisation affect the pathway to precipitation in simulated trade-wind convection?

   Organization affects the production and sedimentation efficiency of rain. As organisation strengthens, rain forms in weaker updrafts from smaller mean cloud droplet sizes. This reduces the efficiency with which cloud water is converted to rain. At the same time, accretion increasingly contributes to rain production, indicating that raindrops grow larger. Additionally, raindrops fall in locally moister environments. As a consequence the evaporation of rain is reduced which increases the sedimentation efficiency. Both effects mostly compensate so that organisation does not substantially affect how much cloud water is removed by precipitation, i.e. the efficiency of precipitation. The findings suggest that organisation might be one form of buffering - while in less organised scenes, rain development is predominantly driven by an efficient conversion of cloud condensate to rain, in more organised scenes a greater sedimentation efficiency, that is more of the rain reaching the ground instead of evaporating, increasingly contributes to rain formation. In this way, the pathway to precipitation differs with spatial organisation.

## 5.2 (NOT SO) CLOUDY PERSPECTIVES

My analyses substantiate that spatial organisation and precipitation in the trades are associated (Snodgrass et al., 2009; Stevens et al., 2020; Schulz et al., 2021), but show that their relationship is by no means trivial. They refute hypotheses such as that clustering increases precipitation in terms of a scene's rain amount. Rather, I show that organisation affects the intensity of rain, that is rain rates more locally. Simulations of trade-wind convection reproduce this behaviour, lending trust to the robustness of results derived from the EUREC⁴A observations, and provide a first explanation: enhanced rain production by accretion produces larger raindrops, which could explain the tendency of more organised convection to produce more intense rainfall. Since this is physically sound, it could suggest that a different model and different microphysics would produce similar results, but this remains to be tested. I suggest to proceed by understanding why accretion is enhanced with organisation. I hypothesise it could be related to organisation increasing the lifetime of clouds. Contrary to presumptions, I find that spatial organisation also has no substantial influence on precipitation efficiency in terms of how much cloud water is on average removed by precipitation. A temporal view in a future study might detail this relationship also further. My analyses suggest to direct it to the role of moisture redistributed by precipitation and spatial organisation (Narenpitak et al., 2021), and including the development of cold pools (Vogel et al., 2021; Narenpitak et al., 2022).

In addition to focusing on lifetime and moisture mechanisms, much may also be learned by bringing studies of deep and shallow precipitating convection together. According to my analyses, the spatial organisation of shallow and deep precipitating convection shows many similarities. Both observations (Study A; Pscheidt et al.,

2019; Retsch et al., 2020) and simulations (Study B;  Brueck et al., 2020) of deep and shallow convection show that scene precipitation varies mainly independently of the degree of organisation. Additionally, more organised shallow and deep convection are associated with few and large cells (Study A;  Brueck et al., 2020; Retsch et al., 2020), intense rain (Study A;  Louf et al., 2019; Retsch et al., 2020) and a different rain formation process (Study B;  Bao and Windmiller, 2021; Nuijens et al., 2017; Lutsko and Cronin, 2018). This yields that studies on the organisation of deep and shallow precipitating convection should be linked. The upcoming EarthCARE, Tropical Oceans and Organised Convection (EC-TOOC) field campaign planned for the year 2024 in the tropical Atlantic and new satellite missions such as the Earth Cloud Aerosol and Radiation Explorer (EarthCARE) mission (Illingworth et al., 2015) may prove valuable in doing so. Here, a focus could lie on how much the behaviour of precipitation in relationship to spatial organisation is energetically constrained in shallow versus deep convection. Additionally, it could be tested in how far the results of study B hold true in observations in deep convection. A prerequisite for linking different studies and field campaigns is that the data is readily accessible and usable. To this end, EC-TOOC could build on the idea of the *How to EUREC⁴A* book I co-developed.

Due to field campaigns like EUREC⁴A, the complexity of trade-wind clouds are seen and taken into account more and more. It emerges that due to subtle interactions of different processes they might be more robust to perturbations than thought. EUREC⁴A showed how the coupling of trade-wind clouds with dynamic processes overcomes a hypothesised positive feedback mechanism grounded on thermodynamic considerations. EUREC⁴A thus suggests a weak sensitivity of trade-wind clouds to perturbations such as warming (Vogel et al., 2022). My studies supplement this picture. There is not just one pathway to rain, nor only one trade cumulus structure, and buffering mechanisms seem to take place in response to perturbations. I do not find indications of a positive amplifying feedback between precipitation and clustering, such as suggested by Seifert and Heus (2013). Instead, I find rather the opposite. Narenpitak et al. (2022) also found that the development of precipitation and cold pools actually weaken the clustering process as they transport moisture to drier regions where new convection is formed. Another factor in reducing the trade-wind clouds' sensitivity to perturbations could be that organisation may make rain production less sensitive to aerosols. The simulations suggest that organisation is associated with rain increasingly being produced by accretion which is roughly independent of the cloud droplet number concentration and thus aerosols. However, to finally constrain the trade-wind clouds' sensitivity to perturbations, it needs to be brought together how large scale *external* forcings (Bony et al., 2020; Schulz et al., 2021) interact with the *internal* process of precipitation and pattern formation.

In this thesis, I have shown that understanding the relationship between precipitation and spatial organisation is a promising tool to better understand either of these processes and finally the sensitivity of trade-wind clouds to perturbations. Moving forward, my analyses suggest focusing on two key areas: firstly, how precipitation, cold pools and organisation redistribute moisture, and secondly, how organisation

affects the lifetime of clouds and precipitation. My analysis suggest that these two processes may explain why organisation as shown in this thesis influences the intensity of and the pathway to precipitation ... or, in the words of Socrates from the beginning, how clouds "*burst and clap*".

Part II

APPENDIX

# A

## THE RELATIONSHIP BETWEEN PRECIPITATION AND ITS SPATIAL PATTERN IN THE TRADES OBSERVED DURING EUREC⁴A

The work in this appendix has been published as:

### AUTHOR CONTRIBUTIONS

Together with A. K. Naumann and F. Ament I conceptualized the study. A. K. Naumann and F. Ament supervised the study. M. Hagen contributed to the data collection and interpretation. I conducted the analysis and prepared the manuscript with contributions from all co-authors. All authors contributed to the discussion of the results.

# THE RELATIONSHIP BETWEEN PRECIPITATION AND ITS SPATIAL PATTERN IN THE TRADES OBSERVED DURING EUREC⁴A

Jule Radtke[1,2], Ann Kristin Naumann[3,1], Martin Hagen[4], Felix Ament[1,3]

[1]*Meteorological Institute, Center for Earth System Research and Sustainability, Universität Hamburg, Hamburg, Germany*
[2]*International Max Planck Research School on Earth System Modelling, Max Planck Institute for Meteorology, Hamburg, Germany*
[3]*Max Planck Institute for Meteorology, Hamburg, Germany*
[4]*Deutsches Zentrum für Luft- und Raumfahrt, Institut für Physik der Atmosphäre, Oberpfaffenhofen, Germany*

ABSTRACT

Trade-wind convection organises into a rich spectrum of spatial patterns, often in conjunction with precipitation development. Which role spatial organisation plays for precipitation and vice versa is not well understood. We analyse scenes of trade-wind convection scanned by the C-band radar Poldirad during the EUREC⁴A field campaign to investigate how trade-wind precipitation fields are spatially organised, quantified by the cells' number, mean size and spatial arrangement, and how this matters for precipitation characteristics. We find that the mean rain rate (i.e. the amount of precipitation in a scene) and the intensity of precipitation (mean conditional rain rate) relate differently to the spatial pattern of precipitation. While the amount of precipitation increases with mean cell size or number, as it scales well with the precipitation fraction, the intensity increases predominantly with mean cell size. In dry scenes, the increase of precipitation intensity with mean cell size is stronger than in moist scenes. Dry scenes usually contain fewer cells with a higher degree of clustering than moist scenes. High precipitation intensities hence typically occur in dry scenes with rather large, few and strongly clustered cells, while high precipitation amounts typically occur in moist scenes with rather large, numerous and weakly clustered cells. As cell size influences both the intensity and amount of precipitation, its importance is highlighted. Our analyses suggest that the cells' spatial arrangement, correlating mainly weakly with precipitation characteristics, is of second order importance for precipitation across all regimes, but it could be important for high precipitation intensities and to maintain precipitation amounts in dry environments.

## A.1   INTRODUCTION

The trades are raining. This fact is, however, given minimal attention in many studies of the trades (e.g. Siebesma et al., 2003; Stevens, 2005; Rieck et al., 2012). Trade-wind

convection is typically described as non-precipitating and randomly distributed 'pop-corn' convection (e.g. Betts, 1997; Siebesma, 1998; Stevens, 2005). Since the trade-wind region and its clouds, important to cool our earth, emerged as central to the issue of climate change because they dominate the spread in climate sensitivity among climate models (e.g. Bony and Dufresne, 2005; Vial et al., 2013), new studies have proven this description to be wrong. Field studies and satellite imagery have emphasized how trade-wind convection organises into a rich spectrum of spatial patterns, often in conjunction with precipitation development (Snodgrass et al., 2009; Stevens et al., 2020; Schulz et al., 2021). This raises the question of the role of spatial organisation for precipitation and vice versa. To address this question, this study investigates the spatial behaviour of precipitating shallow convection and how it matters for precipitation characteristics in the trades.

A fair part of the motivation for our study dates back to the Rain In Cumulus over the Ocean field campaign (RICO, Rauber et al., 2007). RICO showed that shallow precipitation is common in the trades, with about one-tenth of the cloudy areas raining (Nuijens et al., 2009; Snodgrass et al., 2009). Other studies estimate that warm rain showers contribute 20-30% to the total precipitation amount over tropical oceans and 70% to the total precipitation area (Lau and Wu, 2003; Short and Nakamura, 2000). Precipitation might be key to understand the vertical thermodynamic structure, cloudiness, and spatial organisation of the trade regime (e.g. Vogel et al., 2016). Controls on precipitation in shallow convection, however, remain poorly constrained and the representation of precipitation in large eddy simulations differs largely (van Zanten et al., 2011). An understanding of how spatial organisation influences precipitation rates might help interpret and reduce these differences (Stevens et al., 2021).

Besides quantifying precipitation rates, the RICO campaign highlighted that precipitation was often observed with arc-shaped cloud patterns associated with cold pool outflows (Snodgrass et al., 2009; Zuidema et al., 2012). These cold pool signatures reflect how precipitation links processes acting on different scales. The evaporation of precipitation on the microscale can induce cold pools (Seifert and Heus, 2013; Touzé-Peiffer et al., 2022) and local circulations on the mesoscale, which can trigger the birth of new convective cells and pattern the convection. These local circulations may change the characteristics of clouds and therefore also precipitation formation. Precipitation, convection, and their spatial patterns or organisation are thus highly intertwined. Understanding their interplay could be crucial for a better understanding of the individual processes. In turn, to better understand their interplay, a view from the different individual perspectives might be needed.

However, recent studies have mainly focused on the perspective of clouds and their spatial patterns (e.g. Rasp et al., 2019; Denby, 2020; Bony et al., 2020). An investigation from the perspective of precipitation on its interaction with spatial organization and an analysis of precipitation patterns in the trades is lacking. Which role spatial organisation plays for precipitation and vice versa is poorly understood. Bony et al. (2020) show that cloud patterns differ in their cloudiness and net radiative effect. How do

precipitation characteristics relate to precipitation patterns in the trades? For the case of deep convection, Brueck et al. (2020) found, using a storm-resolving model, that mesoscale tropical precipitation varies independently from the spatial arrangement of its convective cells. Louf et al. (2019), investigating radar observations in the tropics, found that rainfall intensities are strongest for few large cells. How does shallow convection differ from deep convection or resemble it in these relationships?

To address our questions, we investigate scenes of trade-wind convection scanned by the C-band radar Poldirad (Polarization Diversity Radar, Hagen et al., 2021) during the EUREC$^4$A field campaign (Stevens et al., 2021), which took place in January and February 2020 in the western tropical North Atlantic near Barbados. In these scenes, we analyse how trade-wind precipitation fields are organised into spatial patterns and how this relates to the scenes' precipitation amount and intensity. While the amount of precipitation is related to the scene heating and drying (e.g Nuijens et al., 2009), the intensity of precipitation is important e.g. in a local sense for the triggering of cold pools (Snodgrass et al., 2009). Spatial organization is not straightforward to define, and different metrics weight different attributes. We jointly analyse three attributes to investigate the spatial pattern into which trade-wind precipitating convection is organised: the number, size, and spatial arrangement of cells. Given the relationship between water vapour, precipitation and organisation found in earlier studies (e.g Nuijens et al., 2009; Bretherton and Blossey, 2017), we further include vertically integrated water vapour as measured by Global Navigation Satellite System (GNSS) receivers (Bock et al., 2021) during EUREC$^4$A as a supplementary variable in our analysis.

The data and methods used in this study are described in Section A.2. First, we investigate the spatial organisation in trade-wind precipitation fields (Sect. A.3) by analysing the number, size, and spatial arrangement of rain cells and how they covary (Sect. A.3.1). Second, we show how the moisture environment of rain cells relates to their spatial behaviour and identify two moisture regimes (Sect. A.3.2). With this information, we then analyse and interpret the relationship between the cells' spatial organisation and the amount and intensity of precipitation in Section A.4. Finally, we show how the relationship between precipitation and its spatial pattern behaves in the diurnal cycle (Sect. A.5), before we conclude in Section A.6.

## A.2   DATA AND METHODOLOGY

### A.2.1   *EUREC$^4$A field campaign*

EUREC$^4$A was designed to elucidate the coupling between clouds, circulation, and convection (Bony et al., 2017). The field campaign took place in January and February 2020 in the western tropical Atlantic, with most operations based out of the island Barbados and targeting a comprehensive observation of clouds, precipitation, and their atmospheric and oceanic environment in the trades upwind of Barbados. A thorough overview of EUREC$^4$A is provided in Stevens et al. (2021). Here, we exploit observational data from the C-band radar Poldirad that was deployed on Barbados to

provide a detailed view of the upstream precipitating trade-wind convection (Hagen et al., 2021). Furthermore, we include observations of vertically integrated water vapour from GNSS receivers (Bock et al., 2021) at the Barbados Cloud Observatory (Stevens et al., 2016).

A.2.1.1 *C-band research radar Poldirad*

Poldirad is a polarimetric C-band research radar of the German Aerospace Center (DLR) (Schroth et al., 1988). During EUREC[4]A, Poldirad took long-range surveillance scans at a 5 minute schedule with a maximum range of 375 km in a sector of about 100 degree eastward and upwind of Barbados, thus mapping out the spatial distribution of rain cells in the trade-wind region. Here, we use the gridded data interpolated on a 1 by 1 km grid with a size of 400 x 400 km$^2$ from these long surveillance scan and covering the month of February (Fig. A.1). This dataset and Poldirads deployment in the EUREC[4]A field campaign are described in detail in Hagen et al. (2021). For our analyses we examine the scans between 25 km and 175 km range (see Fig. A.2) as the radar beam remains below about 3 kilometres height up to this range and the frequency of strong echoes is approximately constant, and to limit effects of sea clutter. To discriminate between meteorological echoes and non-meteorological echoes (like sea clutter, vessels, aircraft and other targets), a threshold in the copolar correlation coefficient $\rho$HV was applied (see Hagen et al., 2021).

The dataset by Hagen et al. (2021) provides a rain rate derived from the commonly used Z-R relationship $Z = 200R^{1.6}$ (Marshall et al., 1955). Here, we use another Z-R relationship $Z = 148R^{1.55}$ as in Nuijens et al. (2009), which is specifically derived for shallow precipitation. Differences in the Z-R relationship lead to uncertainties in the absolute estimation of rain rates, which, however, is not the aim of this study and a shortcoming we accept for this paper. Please also note that peaks in rainfall are smoothed by the radar beam and the gridding, resulting in lower absolute rain rates. Additionally, Poldirads' radar beam showed an elliptical shape that caused the cells to appear stretched in azimuthal direction, resulting in an overestimation of the size of the rain cells. For an estimation of this effect please see Appendix A in Hagen et al. (2021).

For each scene scanned by the radar, we calculate the precipitation amount $P$ (rain rate averaged across the entire scene, which includes non-precipitating and precipitating areas) and precipitation intensity $I$ (rain rate averaged across the precipitating area only), whereby $P = I \cdot F$ with $F$ the rain fraction. To give an overview of the dataset, Fig. A.1 shows the time series of both $P$ and $I$. Gaps in a continuous operation are caused by failures and limited personnel resources. In our subsequent analyses we exclude radar scans from the period 13-15 February because not only shallow cloud systems were present and captured by the radar at this time (Villiger et al., 2022). We also exclude all scans with less than five precipitating cells as a characterization of the spatial arrangement is difficult for scenes with few objects. The dataset captures maxima in $P$ up to roughly $0.2\,\mathrm{mm\,h^{-1}}$, which compares well to precipitation amounts observed in the RICO campaign (Nuijens et al., 2009), and values of $I$ up to

roughly $4\,\mathrm{mm\,h^{-1}}$. Please note that the dominant relationships between precipitation characteristics and spatial organization that we show in the following are qualitatively similar when we consider only independent scenes, i.e. only about every 6 hours.
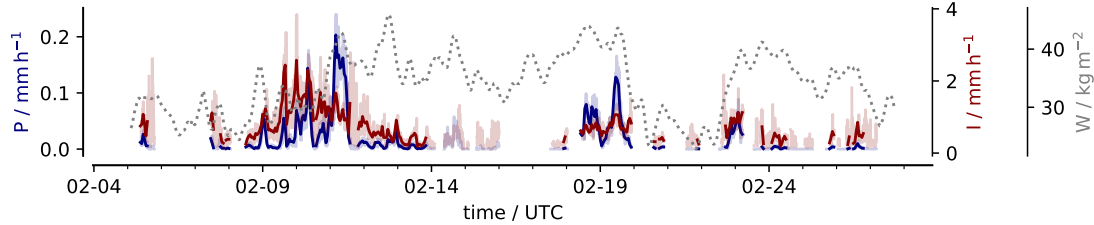


Figure A.1: Time series of precipitation amount $P$, precipitation intensity $I$ (thick lines display hourly means of the dataset used in the analysis, shading full dataset), and integrated water vapour $W$.

A.2.1.2  *Integrated water vapour observations*

To analyse the moisture environment of the rain cells, we use integrated water vapour $W$ observations from GNSS receivers (Bock et al., 2021) installed at the Barbados Cloud Observatory. This dataset provides high temporal resolution integrated water vapour measurements at a 5 minute time interval. To provide an estimate of $W$ for the scenes scanned by the radar to the east, we shift the time series of $W$ by 100 km (that is, to the scene center approximately) assuming a mean wind speed of $6\,\mathrm{m\,s^{-1}}$ and smooth the time series with a running mean of $100\,\mathrm{km}\,/\,6\,\mathrm{m\,s^{-1}}$ to account for a field mean. The integrated water vapour field is rather smooth so that changes in the interpolation details do not lead to substantial differences. According to Nuijens et al. (2009), most of the variability in moisture, when conditioned on precipitation, is in the lower free troposphere. The time series of $W$ is shown as well in Fig.A.1.

A.2.2  *Identification of rain cells and derivation of their spatial attributes*

To identify the rain cells that populate each scene we follow Brueck et al. (2020). We use a lower threshold of $0.1\,\mathrm{mm\,h^{-1}}$, that is $\sim 7\,\mathrm{dBZ}$, to define a rain mask that segments precipitating objects from their non-precipitating environment. The rain cells are derived by a 2D watershed segmentation technique based on the local precipitation maxima. To detect the local maxima the precipitation field is first smoothed with a multidimensional Gaussian filter with a standard deviation for the Gaussian kernel of 1. The filtering is not applied to, and does not affect the precipitating area and rate. The local maxima are detected by using a maximum filter. This dilates the image. If a pixel is unchanged following this dilation, i.e. the dilated image equals the original image, then that pixel is a local maximum. The local maxima serve as starting points for the watershed procedure. In this procedure, the precipitating neighbourhood surrounding a local maximum is filled until it gets into contact with another neighbourhood. Due to possible regridding artefacts we only consider rain cells of minimum two pixel size. Furthermore, we exclude rain cells that touch the scene boundary. Figure A.2 shows
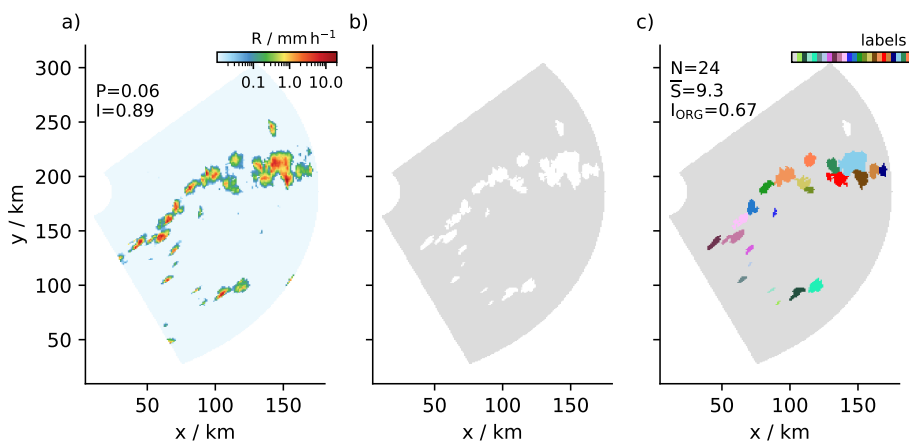
Figure A.2: Example scene of a) rain rate, b) rain mask, and c) rain cell segmentation from 2020-02-11 00:50. For symbols see text.

the segmentation for one exemplary scene.

After the segmentation procedure, we calculate for each scene the cells' geometrical properties size, number and distance between cells. From these, we derive the attributes that we will use to analyse the organisation of trade-wind precipitation fields into spatial patterns. Size, number, and distance are common ingredients in metrics of spatial organisation, e.g. in the Simple Convection Aggregation Index SCAI (Tobin et al., 2012), the Convective Organisation Potential COP (White et al., 2018), or the Radar Organisation Metric ROME (Retsch et al., 2020). Depending on the metric, certain spatial properties are weighted more heavily than others. Therefore, rather than focusing on just one metric, we choose to investigate three attributes of spatial organisation together, based on the number, size and spacing between cells.

For each scene, we derive the mean cell size $\overline{S}$, which we express in terms of the area equivalent diameter to provide a length scale similar to the distances between the cells. We will provide an overview of the individual cell sizes and show how the mean cell size scales with the distribution of cell sizes in a scene in Section A.3. The product of mean cell size expressed in terms of the area $\pi/4 \cdot \overline{S}^2$ and the number of cells $N$ equals the precipitating area $A = F \cdot A_{\mathrm{scene}}$ with $F$ the rain fraction and $A_{\mathrm{scene}}$ the scene area. The first two measures, $\overline{S}$ and $N$, hence, inform about the spatial composition of the precipitation area. We will use this relationship in our analyses. The time series of $\overline{S}$ and $N$ are shown in Fig. A.3a,b.

To assess the spatial arrangement of cells, we use the index $I_{\mathrm{ORG}}$ (Weger et al., 1992; Tompkins and Semie, 2017). Please note that the naming of $I_{\mathrm{ORG}}$ might be misleading here, as we consider spatial arrangement as only one attribute of spatial organisation. $I_{\mathrm{ORG}}$ is a metric of spatial arrangement based on nearest-neighbour distances and compares the observed distances between the cells to the distances of a random distribution with the same number of cells. If nearest-neighbour distances are on
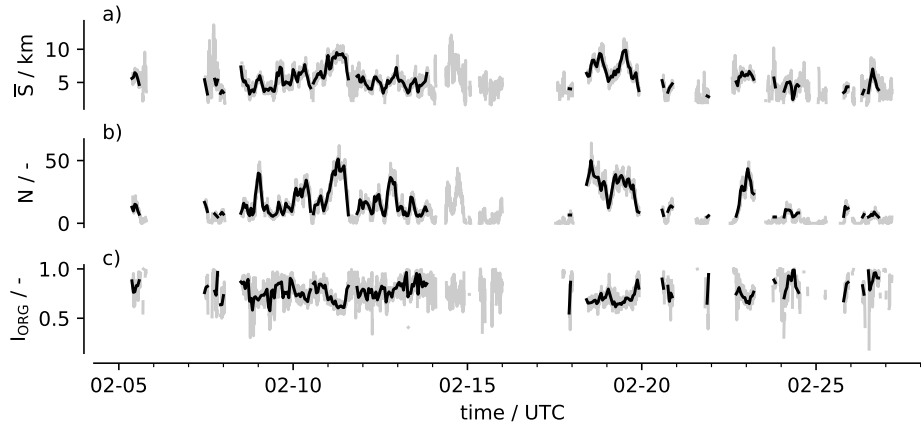
Figure A.3: Time series of a) mean cell size $\overline{S}$, b) number of cells $N$ and c) the spatial arrangement of cells quantified by $I_{\mathrm{ORG}}$ (thick lines display hourly means of the dataset used in the analysis, shading full dataset).

average smaller than expected from a random distribution, the cells are considered clustered, otherwise regularly distributed. The time series of $I_{\mathrm{ORG}}$ is shown in Fig. A.3c. Formally, $I_{\mathrm{ORG}}$ is defined as the integral below the curve of the cumulative density function of the actual observed nearest-neighbour distances (NNCDF) plotted against the NNCDF for a random distribution of the cells. A value of 0.5 corresponds to a random distribution, values larger than 0.5 indicate clustering, whereas values smaller than 0.5 indicate regularly distributed cells. To obtain the random distribution of distances for our domain size, we follow Brueck et al. (2020) and randomly distribute disks with the same areas and same number as the cells present in the scene domain. The random distribution results from taking the mean over hundred realizations of this procedure. As a consistency check, we investigated a second metric of spatial arrangement based on the distances between all possible pairs of cells (Tobin et al., 2012), which compares the observed mean all-neighbour distance to the random mean all-neighbour distance. Both metrics show the same relationships, so that we only show $I_{\mathrm{ORG}}$ in the remainder of this manuscript. Please also note that the dominant relationships between precipitation characteristics and spatial arrangement remain similar when using a different threshold on the number of cells, e.g. considering only scenes with at least 15 or 20 cells.

The time series in Fig. A.3 indicate that $\overline{S}$, $N$, and $I_{\mathrm{ORG}}$ do not vary independently from each other. $\overline{S}$ and $N$ often tend to increase and decrease together and decreases in $I_{\mathrm{ORG}}$ (towards a more regular distribution of rain cells) tend to go along with increases in $N$, e.g. on 11 or 19 February. Figure A.4 provides an overview of the correlations between $\overline{S}$, $N$, $I_{\mathrm{ORG}}$, $P$ and $I$ across the whole dataset. As indicated by the time series, $\overline{S}$ and $N$ are positively correlated. The $I_{\mathrm{ORG}}$ and $N$ are negatively correlated and $I_{\mathrm{ORG}}$ and $\overline{S}$ are weakly negatively correlated. In the following, we will work our way from top to bottom in Fig. A.4. We will first look more closely at $\overline{S}$, $N$, and $I_{\mathrm{ORG}}$ and investigate and interpret how and why they covary (Sect. A.3). To do so, we will span a phase space of $\overline{S}$ and $N$, following analyses in deep convection studies (Louf et al.,

2019; Brueck et al., 2020). We will use this phase space in our subsequent analyses to interpret the correlations shown in Fig. A.4 in more detail. Analysing organisation and precipitation in the phase space will help us to identify two moisture regimes (Sect. A.3.2), show that competing effects lead to the weak correlation of $P$ and $I$ with $I_{ORG}$ (Sect. A.4) and that $I$ predominantly increases with $\overline{S}$, but that this increase differs with the moisture regime.
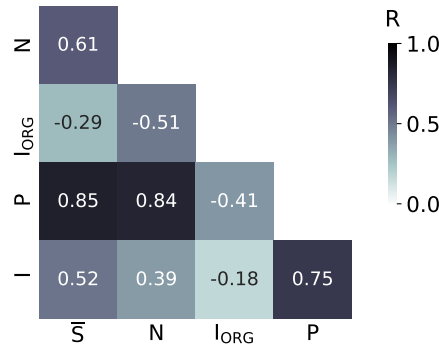


Figure A.4: Spearman correlation coefficient $R$ between cell number $N$, mean cell size $\overline{S}$, the cells' spatial arrangement quantified by the $I_{ORG}$, precipitation amount $P$ and precipitation intensity $I$, coloured according to the absolute correlation between a variable pair.

## A.3 HOW ARE TRADE-WIND PRECIPITATION FIELDS SPATIALLY ORGANISED?

### A.3.1 *Number, size and spatial arrangement*

Figure A.2 shows a scene with a mean cell size $\overline{S}$ of about 9 km and cell sizes ranging between 2.8 and 20.7 km. Therewith, the scene is exemplary for a large mean rain cell size during EUREC$^4$A (Fig. A.3a) and represents well the range of observed cell sizes (Fig. A.5a). Figure A.5a shows that a cell size larger than 20 km was rarely observed. The slope of the distribution of cell sizes falls off towards high cell sizes. This was similarly noted by Trivej and Stevens (2010) for precipitation cells in the RICO campaign. About 50 % of the cells have a size smaller than 5 km, 10 % of the cells have a size larger than 10 km. We investigate how the mean cell size relates to the individual cell sizes in a scene. Fig. A.5b shows that the maximum cell size and spread in cell sizes, quantified as the interquartile range of cell sizes, increase with the mean cell size. Both are strongly correlated with the mean cell size with correlation coefficients of 0.89 and 0.83, respectively. This suggests that a few cells drive the growth in mean cell size. Processes that trigger this growth for a few cells thus probably have a dominant role, e.g the merging of cells or colliding cold pools that trigger large rain cells.

The joint frequency of occurrence of mean cell size $\overline{S}$ and cell number $N$ is shown in Fig. A.6. The example scene contains 24 cells (Fig. A.2), which is exemplary for a
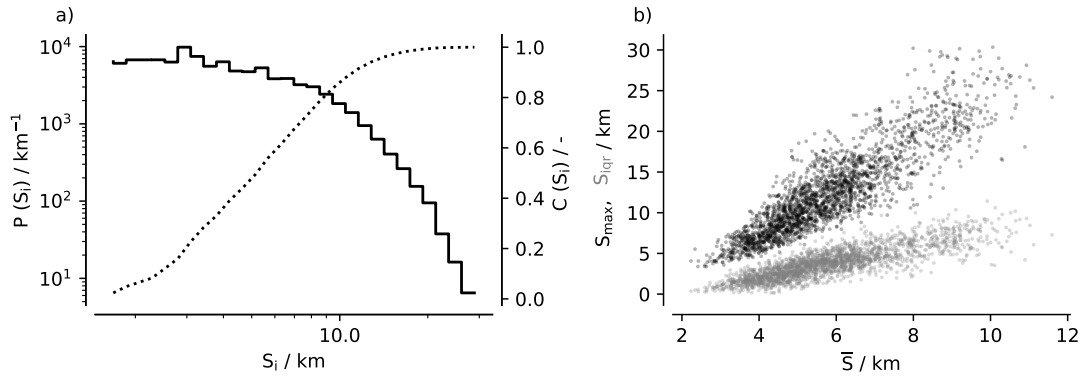
Figure A.5: a) Distribution of cell sizes $P(S_i)$ (solid line) and cumulative distribution of cell sizes $C(S_i)$ (dashed line). b) Maximum cell size $S_{max}$ (dark color) and cell size spread, quantified as the interquartile range of cell sizes $S_{iqr}$ (light color), as a function of mean cell size $\overline{S}$ per scene.

moderate rain cell number $N$ during EUREC⁴A. About 60 % of scenes contained less than 20 cells and most frequently, scenes contained a small cell number between 5 and 15, and a mean cell size of around 5 km. Fig. A.6 shows that $N$ and $\overline{S}$ are positively correlated with a correlation coefficient of 0.61 (Fig. A.4). In radar scans measuring the number and size of rain cells in deep tropical convection no positive correlation was found (Darwin radar observations; Louf et al., 2019). In these observations, the largest cell sizes occur for small cell numbers, while in our analyses the largest cell sizes occur for large cell numbers (Fig. A.6). The difference between Darwin and EUREC⁴A possibly reflects a difference between shallow and deep convection. In deep convection, large cells likely induce local circulations that suppress the growth of other cells around them. Our analyses suggest that this may not always happen in shallow convection. Given their positive correlation, the phase space of $\overline{S}$ and $N$ spanned here, which we will use in our subsequent analysis, allows us to examine the relationship of a variable with cell number separately from the relationship of the same variable with cell size.

In the example scene (Fig. A.2), the cells are distributed at an average distance of 70 km ($L_A$) or 15 km if only the distance to the nearest neighbour is taken into account ($L_{NN}$). Fig. A.7a-b shows how these two properties, $L_A$ and $L_{NN}$, varied during EUREC⁴A and that $L_A$ and $L_{NN}$ in the example scene are typical observed distances. Most frequently a $L_A$ around 65 km and $L_{NN}$ around 14 km were observed. The distribution of $L_{NN}$ is unimodal and skewed towards higher $L_{NN}$ (Fig. A.7b). $L_{NN}$ varies only in a narrow range, that is, rain cells have a typical distance to their neighbouring cell. The distribution of $L_A$ shows a less marked peak and is skewed towards small $L_A$ (Fig. A.7a). Possibly, cold pools (e.g. visible in Fig. A.2 with the typical arc-shaped pattern) smooth and widen the distribution of $L_A$ by their varying strength and extent.

If the rain cells in the example scene were randomly distributed, $L_A$ would be around 90 km and $L_{NN}$ around 19.5 km. That is, the observed distances are shorter than the
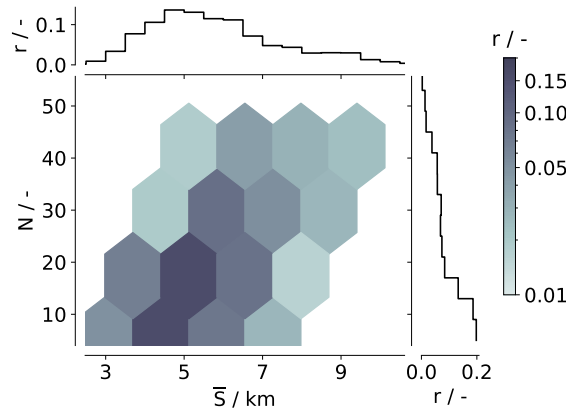
Figure A.6: Joint relative frequency of occurrence of mean cell size $\overline{S}$ and number of cells N with individual histograms.

random distances and the scene in Fig. A.2 shows a clustered state, which is classified by an $I_{ORG}$ of 0.67 (Fig. A.2). As indicated in Fig. A.7a-b and shown in Fig. A.7c, the rain cells arrangement is clustered in almost all scenes ($I_{ORG} > 0.5$). This was similarly found in studies of deep convection (e.g. Brueck et al., 2020; Pscheidt et al., 2019). That precipitation fields are usually clustered fits with the idea that precipitation processes develop in cloud complexes with several clustered updrafts and representing inhomogeneities. Precipitation does not occur randomly but due to inhomogeneities in a field and therewith clustered.
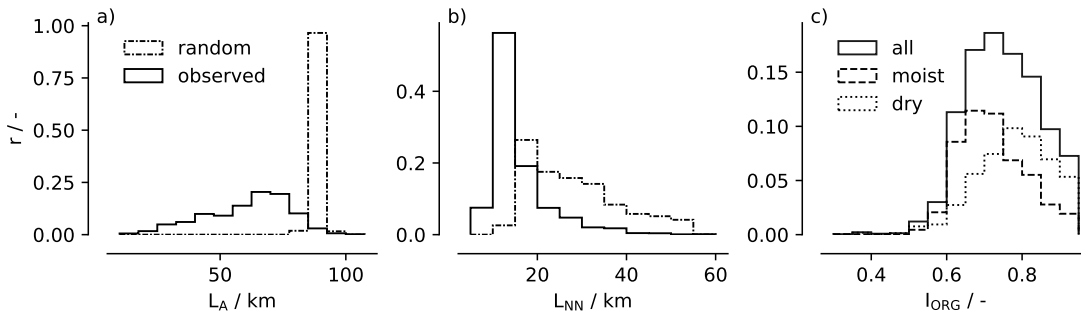


Figure A.7: Relative frequency of a) mean distance between all possible pairs of cells $L_A$, b) mean distance between nearest-neighbour cells $L_{NN}$ and c) the $I_{ORG}$ for all, dry ($W < \text{median}(W)$) and wet scenes ($W > \text{median}(W)$) with median($W$) = $36\,\text{kg}\,\text{m}^{-2}$ .

We now analyse how the cells' spatial arrangement, cell number and size covary by analysing the $I_{ORG}$ in the $\overline{S}$-$N$ phase space spanned before (Fig. A.8a). The analysis reveals three main findings. First, few cells (small $N$) are more clustered (higher $I_{ORG}$) than many cells (high $N$). For a given $\overline{S}$, $I_{ORG}$ decreases with $N$. That is, clustering and cell number are negatively correlated (R = -0.51, Fig. A.4). Brueck et al. (2020), noting the same relationship, point to thermodynamic considerations that can help explain this behaviour. When conducting idealized simulations, it can be seen that in a scene

starting from homogeneous thermodynamic conditions, many randomly distributed cells appear, whereas in the presence of inhomogeneities, the number of cells in a scene can be limited. By subsampling the scenes into four composites representing the four corners of the $\overline{S}$-$N$ phase space (Fig. A.9) to show the variability in each composite, we further note that scenes with few cells have a wider range of possible spatial arrangements than scenes with many cells (Fig. A.9c). Especially few and small cells, indicative of little precipitation, occur in a variety of spatial arrangements, which fits the subjective analysis of radar and satellite imagery during the RICO campaign (Rauber et al., 2007).
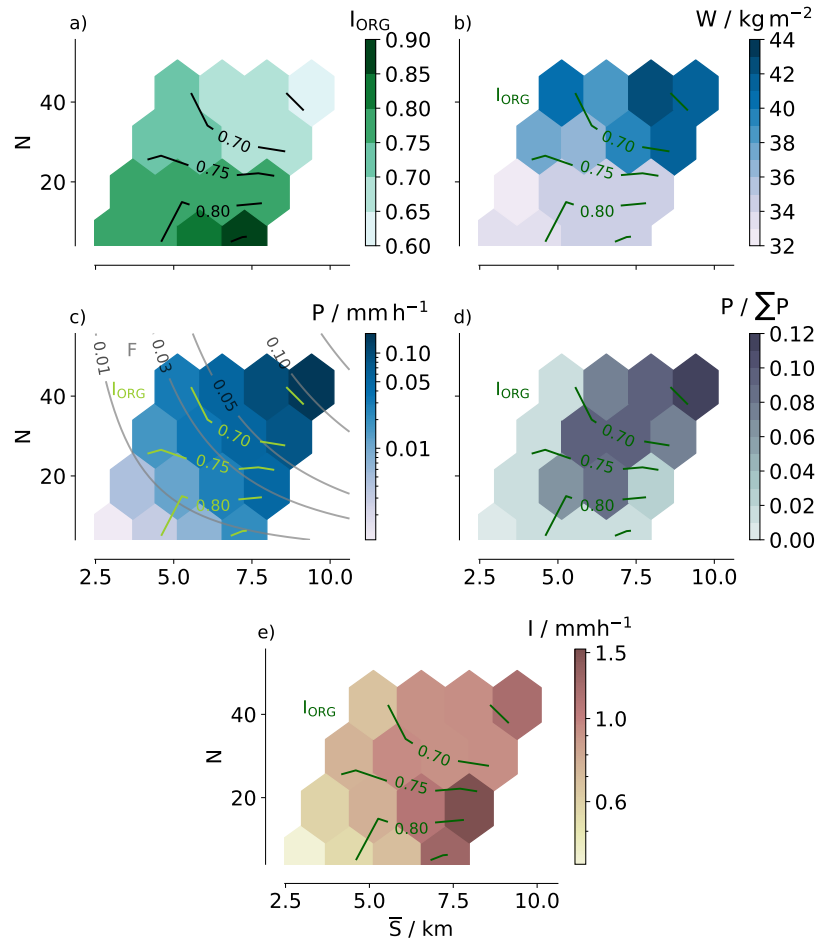


Figure A.8: a) $I_{ORG}$, b) integrated water vapour $W$, c) precipitation amount $P$, d) contribution to total precipitation $P / \sum P$, e) precipitation intensity $I$ as a function of mean cell size $\overline{S}$ and cell number $N$.

Second, the co-variability of clustering with cell size is more complex than with cell number. While $I_{ORG}$ increases with $\overline{S}$ in scenes with a small $N$, in scenes with a large $N$, $I_{ORG}$ decreases with $\overline{S}$ (Fig. A.8a). Thus, overall, the correlation between $\overline{S}$ and $I_{ORG}$ is weak (R = -0.29, Fig. A.4). Third, $I_{ORG}$ consequently maximizes in the lower right corner of the $\overline{S}$-$N$ phase space (Fig. A.8a), that is, clustering is typically highest where cells are few and on average large (see also Fig. A.9c). This was similarly found

for deep tropical convection (Brueck et al., 2020; Retsch et al., 2020). In Brueck et al. (2020) the degree of clustering increases with mean cell size at all cell numbers. The difference between shallow and deep convection might be explained by the idea that deep convective precipitation often originates from large precipitating systems, where large cells are part of a large convective object and hence clustered, whereas trade-wind showers can also be associated with less organised precipitation systems, as suggested by the gravel cloud pattern (Stevens et al., 2020). Nevertheless, our analysis suggests that the organisation of precipitation in trade-wind shallow convection shares similarities to deep convection in that clustering and cell number are negatively correlated and the degree of clustering is typically highest in scenes containing few and, on average, large cells. Next, we will show how the different scaling of $I_{\mathrm{ORG}}$ with $\overline{S}$ in regimes of small and large $N$ is related to different moisture regimes.
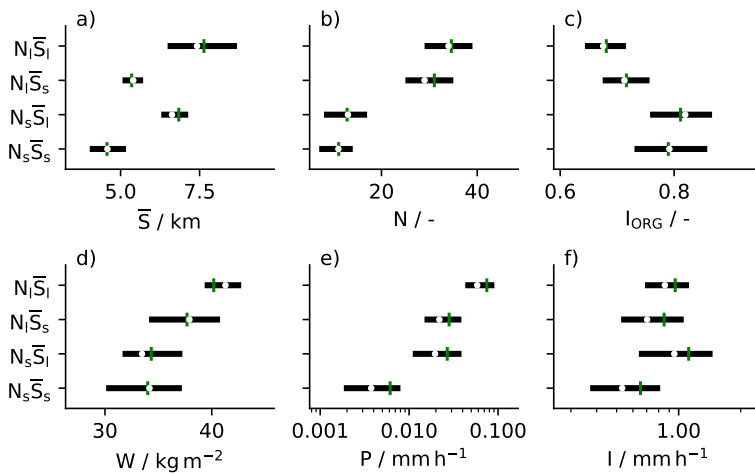


Figure A.9: Interquartile range (black box), median (white dot) and mean (green line) of mean cell size $\overline{S}$, cell number $N$, and $I_{\mathrm{ORG}}$ for four composites representing the four corners in the $\overline{S}$-$N$ phase space with $N_{\mathrm{s}} < 20$, $N_{\mathrm{l}} > 20$, $\overline{S}_{\mathrm{s}} < 6\,\mathrm{km}$, $\overline{S}_{\mathrm{l}} > 6\,\mathrm{km}$. The number of scenes is equal in each composite.

A.3.2 *Moisture environment*

Past studies have shown that water vapour path is related to precipitation (e.g. Bretherton et al., 2004; Nuijens et al., 2009) as well as organisation (e.g. Bretherton et al., 2005; Tobin et al., 2012). Investigating $W$ in the $\overline{S}$-$N$ phase space (Fig. A.8b), we find that the scenes are on average driest (low $W$) at small $N$ and $\overline{S}$ and moistest (high $W$) at large $N$ and $\overline{S}$. With a moistening of the environment, cells tend to be larger and more numerous. However, while $W$ increases markedly with $N$ for a given $\overline{S}$, for a given $N$, the increase of $W$ with $\overline{S}$ is weak. For a large cell number, $W$ tends to increase with $\overline{S}$, but for a small cell number, $W$ varies weakly with $\overline{S}$. Differences in the water vapour path thus mainly appear in the number of rain cells and only slightly in the mean size of the cells. Therefore, the $\overline{S}$-$N$ phase space shows predominantly two regimes: a moist regime (high $W$) at high cell number and a dry regime (low $W$) at low cell number. That dry and moist scenes differ predominantly in the number of cells they

contain, whereas the mean area of the cells only varies weakly with $W$, was also found in radar observations (Louf et al., 2019) and simulations (Brueck et al., 2020) of deep convection. In a moist environment, clouds may be less affected by entrainment, which allows them to reach deeper and eventually start to precipitate (Smalley and Rapp, 2020). Also, clouds and hence precipitating cells may live longer in moister environments. Both could explain the enhanced cell numbers in moist compared to dry environments. That large cells also exist in dry environments, could be related to clustering.

We investigate how the moisture environment and the degree of clustering are related. A comparison of $W$ and the $I_{\mathrm{ORG}}$ in the $\overline{S}$-$N$ phase space (Fig. A.8b) shows that scenes with a small cell number are typically dryer and show a higher degree of clustering than scenes with a large cell number (see also Fig. A.9d). Fig. A.7c displays the histogram of $I_{\mathrm{ORG}}$ in moist versus dry scenes ($W \lessgtr$ median $(W)$ with median $(W)$ = $36\,\mathrm{kg\,m^{-2}}$). In dry scenes, the distribution shifts towards a higher degree of clustering. This agrees with idealised studies of radiative convective equilibrium (Bretherton et al., 2005; Muller and Held, 2012) and observations (e.g. Tobin et al., 2012), which show that aggregated or clustered states of deep convection are typically drier. Our analyses show the same for shallow convection. Possibly, isolated rain cells, that is with a low degree of clustering, can hardly exist in dry environments as they are strongly affected by entrainment. Clustering might reduce the updraft buoyancy reduction through entrainment, allowing cells to develop in hostile, dry environments (Becker et al., 2018).

## A.4  HOW DOES SPATIAL ORGANISATION MATTER FOR PRECIPITATION CHARAC-
TERISTICS?

### A.4.1  *Precipitation amount*

First, we analyse how precipitation amount varies as a function of cell size and number. Figure A.8c shows that for a given $\overline{S}$, $P$ increases with $N$, and vice versa, for a given $N$, $P$ increases with $\overline{S}$. Taken together, contours of $P$ follow well the contour lines of rain fraction $F$. For the amount of precipitation, the intensity of rain showers is hence of secondary importance, which is in agreement with previous studies, e.g. Nuijens et al. (2009). Because precipitation amount scales very well with precipitating fraction, $P$ is strongly correlated with $\overline{S}$ and $N$ (R $\approx$ 0.85, Fig. A.4). Consequently, precipitation amounts can be similar for scenes with few and on average large cells or scenes with many and on average small cells, given a similar rain fraction, and scenes with numerous and on average large cells exhibit usually the highest precipitation amount (Fig. A.9e).

We note two implications from the relationship of $P$ with $N$ and $\overline{S}$. First, although scenes with a mean cell size of $\sim 5\,\mathrm{km}$ and small cell number occur most frequently, they do not contribute the most to the total precipitation during EUREC⁴A (Fig. A.8d). Figure A.8d shows that the precipitation contribution is shifted to larger and more

numerous cells compared to the frequency distribution (Fig. A.6). Although they occur rarely, scenes with the largest and most numerous cells do contribute the most to the total precipitation, because of their high rain amount. Additionally, a moderate cell size and number contribute substantially to the total precipitation through a combination of a moderate rain rate and moderate frequency of occurrence.

Second, as $\overline{S}$ is strongly correlated to the maximum rain cell size and cell size spread (see Sect. A.3), with an increase in $P$, the cell size spread and maximum cell size increases. This fits observations by Trivej and Stevens (2010) from the RICO campaign, who highlight that especially large cells at the tail of the size distribution vary with precipitation area, which, we confirm, determines to a first order the precipitation amount. We find that on average the 20 % largest cells in a scene have a mean cell size 2.5 times larger than the mean scene cell size, contribute half to the precipitating area and 60 % to the precipitation amount. This contribution increases up to 70 % in the 10 % of rainiest scenes (not shown). That is, as the amount of precipitation in a scene increases, the precipitation is distributed more unevenly across the cells.

Recalling our previous analyses, we notice that $P$ varies differently as a function of $\overline{S}$ and $N$ than $I_{\mathrm{ORG}}$. This is clear when comparing $P$ and $I_{\mathrm{ORG}}$ in the $\overline{S}$-$N$ phase space (Fig. A.8c) and is shown in a more condensed form in Fig. A.10, which aggregates the dominant relationships between precipitation amount and cell size, number and arrangement. Figure A.10 shows that $P$ increases with $\overline{S}$ or $N$, $I_{\mathrm{ORG}}$ not. At large $N$, $I_{\mathrm{ORG}}$ is systemically lower than at small $N$ and decreases with $\overline{S}$. While precipitation amount maximizes at large $N$ and $\overline{S}$, the degree of clustering minimizes here, suggesting both are negatively correlated with each other. This is also indicated by contours of $P$ and $I_{\mathrm{ORG}}$ in the upper part of the $\overline{S}$-$N$ phase space (Fig. A.8c), that tend to be roughly parallel. At small $N$, however, $I_{\mathrm{ORG}}$ increases with $\overline{S}$ (Fig. A.10), so that in the lower part of the $\overline{S}$-$N$ phase space (Fig. A.8c), contours of $P$ and $I_{\mathrm{ORG}}$ are perpendicular to each other, i.e. suggesting they vary independently. Across the whole datasets, the relationship between precipitation amount and clustering is therefore negative but foremost weak (R = -0.41, Fig. A.4). Consequently, precipitation amounts can be similar for scenes with a quite different spatial structure (Fig A.10) - with rather many, small and weakly clustered cells or few, large and more strongly clustered cells (see also Fig. A.8c).

These analyses hence suggest that hypothesized mechanisms, such as that clustering increases precipitation through cell interaction, play overall no or a subordinate role for the precipitation amount in a scene because precipitation amount increases with rain fraction and maximizes when cells are large and numerous, while the degree of clustering maximizes when cells are large but few. We find that scenes with small $N$ and large $\overline{S}$, that show on average a high degree of clustering, also contribute little to the total observed precipitation amount (Fig. A.8d). This suggests that scenes with a high degree of clustering neither precipitate the most nor occur frequently enough to contribute much to the precipitation amount and, hence, that the spatial arrangement of rain cells is of second order importance for precipitation amount in the trades.

Similar conclusions were drawn for deep convection (e.g Brueck et al., 2020; Pscheidt et al., 2019).

Only when considering the moisture environment a positive effect of clustering on precipitation amounts may be seen. Combining the results of Fig A.8b and c, at small $N$ in the dry regime, precipitation amount is higher for scenes with larger $\overline{S}$ and a higher degree of clustering. Further, keeping precipitation amount constant while moving in the $\overline{S}$-$N$ phase space into scenes with small $N$, which tend to be dry, an increase in the mean cell size and an increase in the degree of clustering takes place (see also Fig. A.10). In this sense, clustering may be considered important for maintaining precipitation amounts in dry environments as similarly found by Brueck et al. (2020) for deep convection.
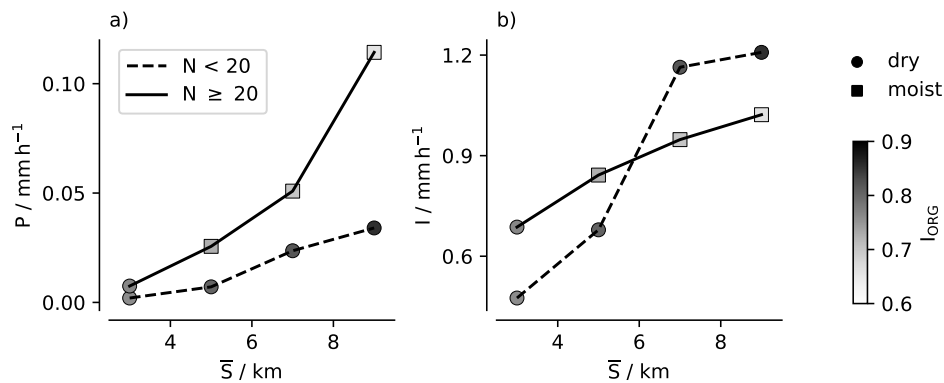


Figure A.10: Overview of relationships between precipitation characteristics and cell number, size and arrangement: a) Precipitation amount $P$ and b) precipitation intensity $I$ for bins of mean cell size $\overline{S}$ conditioned on different cell numbers $N$. The marker shading denotes the cells' degree of clustering as quantified by the $I_{ORG}$, the marker style the moisture environment as quantified by $W \lessgtr 36\,\mathrm{kg\,m^{-2}}$.

A.4.2  *Precipitation intensity*

First, we analyse the relationship between precipitation intensity, cell number and mean cell size using the $\overline{S}$-$N$ phase space. Figure A.8e shows that for a given $N$, $I$ increases with $\overline{S}$. For a given $\overline{S}$, $I$ does not systematically increase or decrease with $N$ (see also Fig. A.10). Consequently, the positive correlation between $I$ and $N$ across the whole dataset ($R = 0.39$, Fig. A.4) is due to an increase of $I$ with $\overline{S}$ ($R = 0.52$, Fig. A.4) and the covariation of $N$ with $S$ ($R = 0.61$, Fig. A.4). While both cell number and size are important for the precipitation amount in the trades, it seems predominantly the latter for precipitation intensity. This was similarly found in regimes of deep tropical convection (Louf et al., 2019; Semie and Bony, 2020) and is e.g. important for cumulus parametrizations, where the convective area is a key ingredient. Whereas the convective or precipitating area well describes the precipitation amount, its composition into cell size and number is decisive for precipitation intensity.

Possible explanations for why precipitation intensity increases with mean cell size are that large cells protect their updrafts better from dilution by entrainment, which allows them to sustain stronger updrafts and grow deeper (e.g. Kirshbaum and Grant, 2012; Schlemmer and Hohenegger, 2014). Additionally, enhanced moisture aggregation through shallow circulations that accompany large clusters (Bretherton and Blossey, 2017), could increase the liquid and rain water content. Also, large cells may dissipate more slowly, i.e. they live longer, and therefore develop a moister (sub)cloud layer that leads to less evaporation of the falling raindrops. Here, we can only provide a quantification of this effect. To do so, we investigate how the rain intensity of an individual cell scales with its size, shown in Fig. A.11 for the mean and maximum rain intensity of a cell. Both, maximum and mean rain intensity, increase with cell size for cell sizes above 3 km. Cells with a size around 10 km have a mean intensity around $1 \, \mathrm{mm \, h^{-1}}$. A maximum intensity above $1 \, \mathrm{mm \, h^{-1}}$ occurs in cells larger than roughly 5 km. As roughly 50 % of cells are larger than 5 km (see Sect. A.3.1), roughly 50 % of the cells exhibit maximum intensities above $1 \, \mathrm{mm \, h^{-1}}$, a threshold associated with the formation of cold pools in past studies (e.g. Barnes and Garstang, 1982; Drager and van den Heever, 2017).
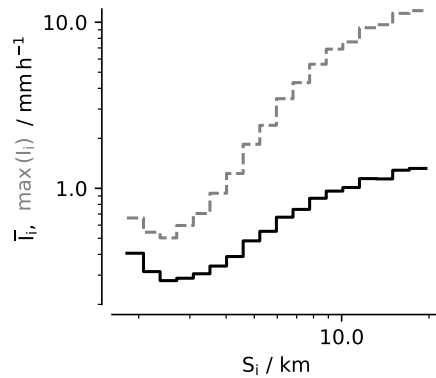


Figure A.11: Mean Intensity $\overline{I_i}$ (solid) and maximum intensity $\max(I_i)$ (dashed) of a cell binned as a function of cell size.

The analysis of $I$ in the $\overline{S}$-$N$ phase space further shows that the increase of $I$ with $\overline{S}$ differs between small and large $N$ (Fig. A.8e), more explicitly shown in Fig. A.10. In scenes with small $N$, the increase of $I$ with $\overline{S}$ is stronger than in scenes with large $N$. This could indicate that cells are competing for moisture and heat - when there are many cells, they can grow larger, but not as intense as if there are few cells, because they have to compete with many cells. We identified a moist regime at large $N$ and a dry regime at small $N$ (Sect. A.3.2), suggesting that $I$ increases more strongly with $\overline{S}$ in dry compared to moist scenes and that precipitation intensities are thus highest in dry scenes. Figure A.12a,b confirms this. The distribution of precipitation intensities in dry scenes shows a higher variability and extends to larger values than in moist scenes. Precipitation intensity is highest in dry environments, which was similarly observed by Louf et al. (2019) for deep convection. Vogel et al. (2020) also find that in dry environments simulated shallow clouds are deeper. Because $I$ increases with $\overline{S}$

and maximizes in dry environments, precipitation amount increases for the same rain fraction when moving from a moist environment with more numerous cells to a dry environment with larger cells (Fig. A.12c).
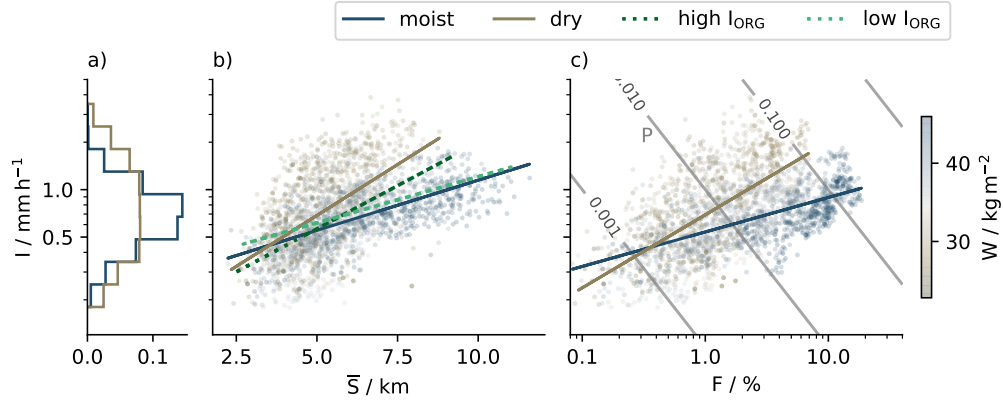


Figure A.12: a) Relative frequency of precipitation intensity $I$ for dry ($W > \mathrm{median}\,(W)$) and wet scenes ($W < \mathrm{median}\,(W)$). $I$ as a function of b) mean cell size $\overline{S}$ and c) rain fraction $F$. The shading in b) and c) denotes the water vapour path $W$. The lines in b) and c) denotes the fit for dry and wet scenes or scenes with high $I_{\mathrm{ORG}}$ ($I_{\mathrm{ORG}} > \mathrm{p75}\,(I_{\mathrm{ORG}})$) and low $I_{\mathrm{ORG}}$ ($I_{\mathrm{ORG}} < \mathrm{p25}\,(I_{\mathrm{ORG}})$). The slanted grey lines labeled $P$ denote the precipitation amount in $\mathrm{mm\,h^{-1}}$.

Our previous analyses show that dry and moist scenes also typically exhibit differences in the degree of clustering. We found that dry scenes are typically more clustered than moist scenes and more clustered convection may help to let the clouds grow deeper and rain more intense, possibly adding to the enhanced increase of precipitation intensity with cell size in dry scenes. Figure A.12 shows that the increase of $I$ with $\overline{S}$ is stronger in scenes with a high degree of clustering than in scenes with a low degree of clustering. This suggests that high precipitation intensities are related to scenes with a high degree of clustering. Comparing the variations of precipitation intensity and clustering in the $\overline{S}$-$N$ phase space (Fig. A.8e) or Fig. A.10, this is confirmed. At large $N$ or moist environments, $I$ increases with $\overline{S}$, whereas $I_{\mathrm{ORG}}$ decreases with $\overline{S}$. At small $N$ or in dry environments, both $I$ and $I_{\mathrm{ORG}}$ increase with $\overline{S}$. Thus both $I$ and $I_{\mathrm{ORG}}$ maximize where $\overline{S}$ is large and $N$ is small (see also Fig. A.9c,f) and scenes are dry. The analyses hence suggest that clustering is important for high precipitation intensities occurring typically in dry environments. For a given mean cell size around $7\,\mathrm{km}$, $I$ and the degree of clustering increase as one moves from scenes with large $N$ in the moist regime to scenes with a small $N$ in the dry regime (Fig. A.10). Overall, however, $I$ and $I_{\mathrm{ORG}}$ vary mostly perpendicular to each other in the $\overline{S}$-$N$ phase space (Fig. A.8e), so that across all regimes the correlation between clustering and precipitation intensity is weak (R = -0.18, Fig. A.4).

Our analysis so far takes a snapshot view of precipitation. To probe the evolution of the rain cells' spatial organisation, we lastly look at the diurnal cycle, a prominent mode of variability in the tropics, revisited recently by Vial et al. (2019). This also allows us to add some context to our results by discussing our analyses of precipitation patterns in light of the analyses of cloud patterns in the diurnal cycle (Vial et al., 2021; Vogel et al., 2021). Measurements from the RICO field experiment show that trade-wind convection exhibits a nighttime to early morning peak and an afternoon minimum in precipitation (Nuijens et al., 2009; Snodgrass et al., 2009), confirmed by the analyses of Vial et al. (2019). Fig. A.13 shows this daily cycle captured in our dataset with precipitation amount peaking in the early morning and having its minimum in the late afternoon before sunset (Fig. A.13a). Please note that the diurnal cycle is not complete on all days due to gaps in the measurements. Considering only the days with no gaps in the measurements, the diurnal cycle is similar.
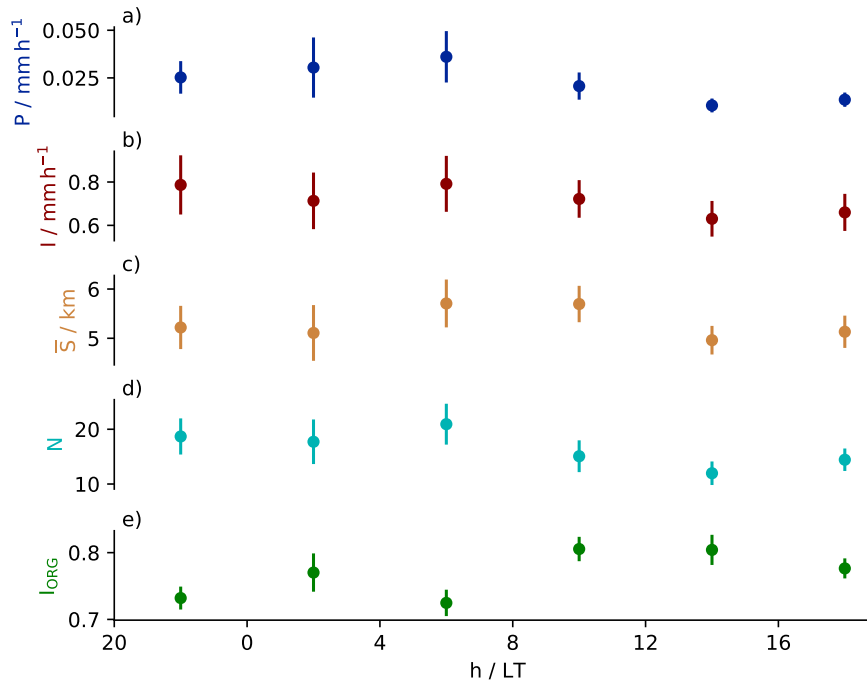


Figure A.13: Mean diurnal cycle of a) precipitation amount $P$, b) precipitation intensity $I$, c) cell number $N$, d) mean cell size $\overline{S}$, and e) the cells' spatial arrangement quantified by the $I_{\mathrm{ORG}}$. Error bars denote the uncertainty in the mean (standard error).

The diurnal cycle of cell number and size roughly follow the diurnal cycle of precipitation amount (Fig. A.13c,d), which matches our previous analyses (Sect. A.4). Thereby, $N$ tends to peaks before $\overline{S}$, suggesting that the increase in precipitation in the night is initially driven by more cells, then increasingly by larger cells. As $N$ peaks, rain cells exhibit a low degree of clustering (Fig. A.13e). $\overline{S}$ stays high as $N$ already decreases. This indicates that small cells might dissipate earlier whereas large cells live

longer and/or that merging of cells is enhanced. Cells are now spaced closed to each other indicated by a large $I_{ORG}$. The early daytime between 8 and 12, where $\overline{S}$ slowly decreases and $I_{ORG}$ is high, is also characterized by a relatively high precipitation intensity (Fig. A.13b). Precipitation intensity does not show a clear diurnal cycle. Vogel et al. (2021) find that cold pools prolong the peak in the diurnal cycle of precipitation into the early afternoon, possibly shaping this behaviour seen here.

Vial et al. (2021) show how the subjectively defined cloud patterns Gravel, Flowers and Fish (Stevens et al., 2020) vary in the diurnal cycle. Please note that these cloud patterns extend in part over a larger scale than the ones analysed here. We may capture the gravel pattern, but only the individual rain cells of a single flower and a part of the fish pattern. Vial et al. (2021) show that the gravel cloud pattern has a peak occurrence around midnight, where we find rain cells to be rather small, numerous and weakly clustered. Flowers, which appearance is mainly dominated through a large mean cloud size (Bony et al., 2020), have a peak occurrence before sunrise, where we also find rain cells to be rather larger, and fish has a peak occurrence around noon, where we find rain cells cells to be rather large and strongly clustered. This might indicate that precipitation patterns and cloud patterns scale with each other. Figure A.13 shows that the relationships revealed by our previous analyses, are evident on the diurnal time scale and indicates how the number, size, and spatial arrangement of rain cells might relate to cloud patterns and the cells' life cycle.

## A.6    SUMMARY AND CONCLUSION

This study investigates the spatial behaviour of precipitating trade-wind convection and its implications for precipitation characteristics in the trades as observed during the EUREC$^4$A field campaign. To do so, scenes of trade-wind convection scanned by the C-band radar Poldirad are examined. We investigate the spatial structure in these scenes by analysing the size, number and spatial arrangement of rain cells and examine how these relate to the scene's precipitation amount and intensity, as well as the water vapour path. A synopsis of the dominant relationships is given in Fig. A.10 and is summarized below.

During EUREC$^4$A, a mean rain cell size of 5 km and a mean distance to the nearest neighbour of about 14 km were most common. Up to 60 cells in one scene and a mean cell size of 12 km were observed. In nearly all scenes, cells were spaced closer than in a random distribution. That is, the spatial arrangement in scenes of precipitation is almost always clustered, which is in line with the expectation that precipitation is related to inhomogeneities. In the diurnal cycle, cell number tends to peak shortly before mean cell size in the early morning, and before the degree of clustering, which peaks around noon. Whereas cell number and mean size are positively correlated and cell number and clustering are negatively correlated, the relationship between mean cell size and clustering is more ambiguous and differs between scenes with a large and small cell number. Scenes with few and, on average, large cells exhibit typically the highest degree of clustering, which was similarly found for deep convection (Senf

et al., 2019; Brueck et al., 2020; Retsch et al., 2020). This suggests similarities between the spatial organisation of shallow and deep precipitating convection. Based on the diurnal cycle we find indications that trade-wind precipitation patterns may scale with cloud patterns, providing a first observational baseline to study the relationship between the spatial organisation of precipitation and clouds.

We identify two regimes: a moist regime which is characterized by a large cell number, and a dry regime, which generally has a small cell number. In the dry regime cells are typically more clustered than in the moist regime, which agrees with deep convective studies (Bretherton et al., 2005; Muller and Held, 2012; Tobin et al., 2012). Clustering might reduce the updraft buoyancy reduction through entrainment, allowing cells to develop in hostile, dry environments (Becker et al., 2018). While we find a systematic relationship between water vapor path, cell number and the degree of clustering, the relationship between water vapour path and cell size is less clear. Regarding the close relationship between water vapour availability and precipitation in the trades highlighted in Nuijens et al. (2009), our analyses suggest that precipitation increases with water vapour path predominantly because of more numerous cells that are more scattered rather than larger cells.

We conclude that the amount and intensity of precipitation behave differently to the spatial patterning in trade-wind precipitation fields:

- The amount of precipitation varies closely with cell number and mean cell size because it scales well with rain fraction. High precipitation amounts typically occur in scenes that contain many, on average large, and weakly clustered cells. Precipitation amounts can be similar for scenes that differ markedly in their spatial structure.

- The intensity of precipitation increases predominantly with mean cell size. In dry scenes with few cells, this increase is stronger than in moist scenes with many cells. High precipitation intensities typically occur in dry scenes that contain on average large, few, and strongly clustered cells.

From the three spatial attributes investigated, cell size and number are equally strongly related to precipitation amount, and cell size is best related to precipitation intensity, thus highlighting the importance of cell size for precipitation characteristics. No causality can be derived from these relationships, though. Clustering and precipitation characteristics are, across all regimes, negatively and predominantly weakly correlated and hence the spatial arrangement of cells is of second order importance for precipitation in the trades. This was similarly noted for deep convection (e.g. Pscheidt et al., 2019; Brueck et al., 2020). We do find indications, however, that clustering may be important for high precipitation intensities and to maintain precipitation amounts in dry environments. Our study shows that precipitation characteristics are related to spatial precipitation patterns and suggests that a better understanding of how spatial patterns are conditioned on the environment, e.g. ambient moisture, will contribute to our understanding of precipitation in the trades.

# B

## SPATIAL ORGANISATION AFFECTS THE PATHWAY TO PRECIPITATION IN SIMULATED TRADE-WIND CONVECTION

The work in this appendix is in preparation for publication as:

**Radtke, J.**, R. Vogel, F. Ament, and A. K. Naumann (2023). "Spatial Organisation Affects the Pathway to Precipitation in Simulated Trade-Wind Convection." In: *preparation*

### AUTHOR CONTRIBUTIONS

I conceptualised the study with advice by R. Vogel, A. K. Naumann and F. Ament. All co-authors supervised the study. I conducted the analysis and prepared the manuscript. All co-authors contributed to the discussion of the results and reviewed the manuscript.

# SPATIAL ORGANISATION AFFECTS THE PATHWAY TO PRECIPITATION IN SIMULATED TRADE-WIND CONVECTION

Jule Radtke[1,2], Raphaela Vogel[1], Felix Ament[1], Ann Kristin Naumann[3,1]

[1]*Meteorological Institute, Center for Earth System Research and Sustainability, Universität Hamburg, Hamburg, Germany*
[2]*International Max Planck Research School on Earth System Modelling, Max Planck Institute for Meteorology, Hamburg, Germany*
[3]*Max Planck Institute for Meteorology, Hamburg, Germany*

## KEYPOINTS

- The formation of surface precipitation is decomposed into a production and sedimentation phase

- As organisation strengthens, cloud condensate is less efficiently converted to rain, but rain sediments more efficiently

- Organisation affects the pathway to precipitation by modulating the local moisture environment, cloud vertical motion and the dominant mechanism producing rain

## ABSTRACT

We investigate whether and how spatial organisation affects the pathway to precipitation in simulated trade-wind convection. We decompose the formation of surface precipitation ($P$) into a production phase, where cloud condensate is converted into rain, and a sedimentation phase, where rain falls towards the ground while some of it evaporates. By modulating the local moisture environment, cloud vertical motion, and the dominant mechanism that produces rain and its properties, organisation affects how these two phases contribute to $P$. In less organised scenes, $P$ is predominantly driven by efficient conversion of cloud condensate to rain. As organisation strengthens, the conversion efficiency decreases but sedimentation efficiency increases, that is more of the rain sediments to the ground instead of evaporating, and this increasingly contributes to $P$. Organisation does not affect how efficiently it precipitates in total, but buffers rain development, we propose. We conclude that the pathway to precipitation differs with spatial organisation.

## PLAIN LANGUAGE SUMMARY

Clouds in the trade-wind region organise into a variety of spatial patterns. We investigate how this spatial organisation may influence rain development in simulations

of trade-wind convection. We divide the formation of surface precipitation into two phases. In the first phase, rain is produced from colliding or collected cloud droplets. In the second phase, rain falls towards the ground while some of the rain evaporates. Our study shows that as organisation strengthens, rain is produced less efficiently, but a larger fraction of that rain reaches the ground instead of evaporating. Thus, organisation in the simulations affects the way surface rain is generated. It does so by modulating the cloud vertical motion in which rain forms, the local moisture environment through which rain falls and the microphysical conversion processes.

## B.1 INTRODUCTION

What makes it rain? Precipitation was often neglected in studies of trade-wind convection because it was assumed that the convection is too shallow and short-lived to form precipitation (Siebesma, 1998; Stevens, 2005). Although there was already ample evidence of precipitation in the trade winds shown by Byers and Hall (1955) or Short and Nakamura (2000), it was not until attention to the trade-wind region and its clouds increased due to their large contribution to uncertainty in cloud feedbacks and climate sensitivity (Bony and Dufresne, 2005; Vial et al., 2013) that a more nuanced picture of trade-wind convection settled. The Rain In Cumulus over the Ocean (RICO) campaign (Rauber et al., 2007) was key in substantiating that precipitation is frequent in the trades (Nuijens et al., 2009), and highlighted that precipitation was often observed with arc-like cloud structures reminiscent of cold pool outflows (Snodgrass et al., 2009). Subsequent studies confirmed that trade-wind convection organises into a variety of spatial structures - and that this often occurs in conjunction with precipitation development (Stevens et al., 2020; Denby, 2020; Bony et al., 2020; Schulz et al., 2021; Radtke et al., 2022). How does spatial organisation influence the development of precipitation - referring here to surface precipitation - in the trades? In this study, we exploit realistic large-domain LES of trade-wind convection to investigate whether and how spatial organisation affects the pathway to trade-cumulus precipitation.

Precipitation formation depends on dynamic, thermodynamic and microphysical interactions on different spatial and temporal scales. Due to the broad range of scales and processes involved, an understanding of rain formation and contributing processes remains, even for warm, shallow cumulus clouds, challenging. The representation of trade-cumulus precipitation in LES differs largely (van Zanten et al., 2011). As spatial organisation and precipitation seem so closely associated in the trades (Stevens et al., 2020; Vogel et al., 2021), an understanding of how spatial organisation relates to warm rain development could help interpret and reduce these differences. Organisation may affect how efficient rain is produced and how much evaporates through modulating circulations and the local moisture environment (Seifert and Heus, 2013; Narenpitak et al., 2021). In turn, understanding the relationship between spatial organisation and precipitation may also be key to disentangle the mechanisms of organisation and explain its influence on the total cloud cover in the trades, a prerequisite to further constrain the climate feedback of the trades (Nuijens and Siebesma, 2019; Bony et al., 2020).

Analysing rain radar measurements upstream of Barbados taken during the EUREC⁴A field campaign (Hagen et al., 2021; Stevens et al., 2021), Radtke et al. (2022) show that while the occurrence of precipitation is related to clustering, the mean rain rate varies largely independently of the cells' degree of clustering. In scenes with similar precipitation but different spatial organisation, also the moisture environment differs. Similarly, Yamaguchi et al. (2019) find that in idealized LES, shallow cumulus precipitation varies little, but cloud sizes and spatial distributions differ in response to large changes in the aerosol environment. Could spatial organisation be a process to maintain precipitation in different environments, enabling or creating different pathways to precipitation?

To answer this question, we make use of large-domain LES of the North Atlantic trades that were run for the period January to February 2020 during the EUREC⁴A campaign (Stevens et al., 2021) and were designed to explore spatial organisation on the mesoscale (20-200km) (**Schulz2023**). We follow Langhans et al. (2015) and decompose the formation of surface precipitation into two phases, (i) a production phase, in which cloud condensate is converted to rain water, and (ii) a sedimentation phase, in which the produced rain water falls towards the ground while part of it re-evaporates. Sect. B.2 describes the setup and microphysical schemes of the simulations and our analysis method. Sect. B.3.1 shows that spatial organisation in scenes of $\mathcal{O}(100\,\text{km})$ influences how these two phases contribute to the formation of precipitation, but not how efficiently it precipitates in total. Sect. B.3.2 explains that organisation influences these two phases by modulating the local moisture environment, cloud vertical motion and the dominant mechanism producing rain and interprets the behaviour as a form of buffering, before we conclude in Sect. B.4.

## B.2    METHODS

### B.2.1    *EUREC⁴A large-domain ICON LES simulations*

The simulations are conducted with the LES version of the ICOsahedral Non-hydrostatic (ICON) model (Dipankar et al., 2015). ICON solves the compressible Navier–Stokes equations on an unstructured grid as detailed in Zängl et al. (2015) and Dipankar et al. (2015). For a more detailed description of the LES setup and an evaluation of the LES, please refer to Schulz (2021). Here, we analyse a simulation with 625 m gridspacing that covers the western tropical Atlantic from about 60.2 to 45 °W and 7.5 to 17 °N and simulates an extended campaign period from 9 January to 19 February 2022. Schulz (2021) show that this simulation reproduces the canonical forms of trade cumulus organisation of Stevens et al. (2020), as well as variability in precipitation, which makes them a good starting point to investigate how the process of precipitation may vary with spatial organisation. The initial and boundary data for the LES are taken from a storm resolving simulation at 1.25-km grid spacing, which is initialised and nudged at its lateral boundaries to the atmospheric analysis of the European Centre for Medium-Range Weather Forecasts (similar to Klocke et al., 2017).

For microphysics, the simulations apply the two-moment mixed-phase microphysics scheme of Seifert and Beheng (2006). In this scheme, warm rain is produced following Seifert and Beheng (2001) by autoconversion and accretion, defined as $\frac{\partial L_r}{\partial t}\big|_{au} \sim L_c^2 \bar{x}_c^2$ and $\frac{\partial L_r}{\partial t}\big|_{acc} \sim L_c L_r$ where $L_r$ rain water content, $L_c$ cloud water content and $\bar{x}_c = \frac{L_c}{N_c}$ mean mass of cloud droplets with cloud droplet number concentration $N_c$. To investigate the production of rain, we recalculate the autoconversion and accretion rates from the instantaneous 3D model output available every 3 h of cloud water, rain water and cloud effective radius $r_{eff}$, from which the volume radius $r_v$ is derived by $(r_v/r_{eff})^3 = 0.8$ (Freud and Rosenfeld, 2012) to calculate the cloud droplets' mean mass.

### B.2.2  *Investigating spatial organisation and the pathway to precipitation*

We assess the degree of spatial organisation by the spread in mesoscale coarse grained total water path, $\mathcal{O}_{rga}(\Delta W_{T_m})$, following Narenpitak et al. (2021). In scenes of $4 \times 4°$ (about $450 \times 450$ km), similar to the area extent of previous studies (Radtke et al., 2022; George et al., 2022), we coarse grain total water path into tile sizes of 20 km and calculate the interquartile range. The metric classifies three example scenes shown in Fig. B.1a from weakly organised (low $\mathcal{O}_{rga}(\Delta W_{T_m})$) on the left, to more strongly organised (high $\mathcal{O}_{rga}(\Delta W_{T_m})$) on the right. This is consistent with a visual subjective classification of the cloud field and the cloud pattern classification of Stevens et al. (2020). According to it, the left scene depicts a gravel pattern, characterised by scattered convection, and the right scene a fish pattern, characterised by very clustered convection. We also detect how cold pools populate each scene, here following the calculation and criterion of Touzé-Peiffer et al. (2022) of a mixed layer height smaller than 400 m. We exclude scenes with outgoing longwave radiation $< 275$ W m$^{-2}$ to mask high clouds, and scenes with little precipitation $P < 0.01$ mm h$^{-1}$. In total about 2000 scenes (about 7 scenes across the domain every 3 hours) are used in the analyses and if not mentioned otherwise, we refer to domain mean values.

To investigate the pathway to precipitation, we decompose the formation of surface precipitation into (i) a production phase and (ii) a sedimentation phase. In phase (i), rain is initially formed by the merging of small cloud droplets, parameterised with the autoconversion rate ($C_{Auto}$). Additionally, rain is produced as falling raindrops collect cloud droplets, parameterised with the accretion rate ($C_{Acc}$). Autoconversion dominates the production of rain especially for young or short-lived clouds while accretion contributes more to the production of rain as clouds live longer and there is more time available for the collision-coalesence process to take place (Feingold et al., 2013). To quantify how efficient the production of rain water is, we define a conversion efficiency

$$\epsilon_{conv} = \frac{C_A}{W_L}, \tag{B.1}$$

where $C_A = C_{Auto} + C_{Acc}$ and $W_L$ the cloud liquid water path. In phase (ii), the rain water produced by autoconversion and accretion sediments towards the ground. During this process, some rain evaporates ($E$), which we refer to as evaporation efficiency
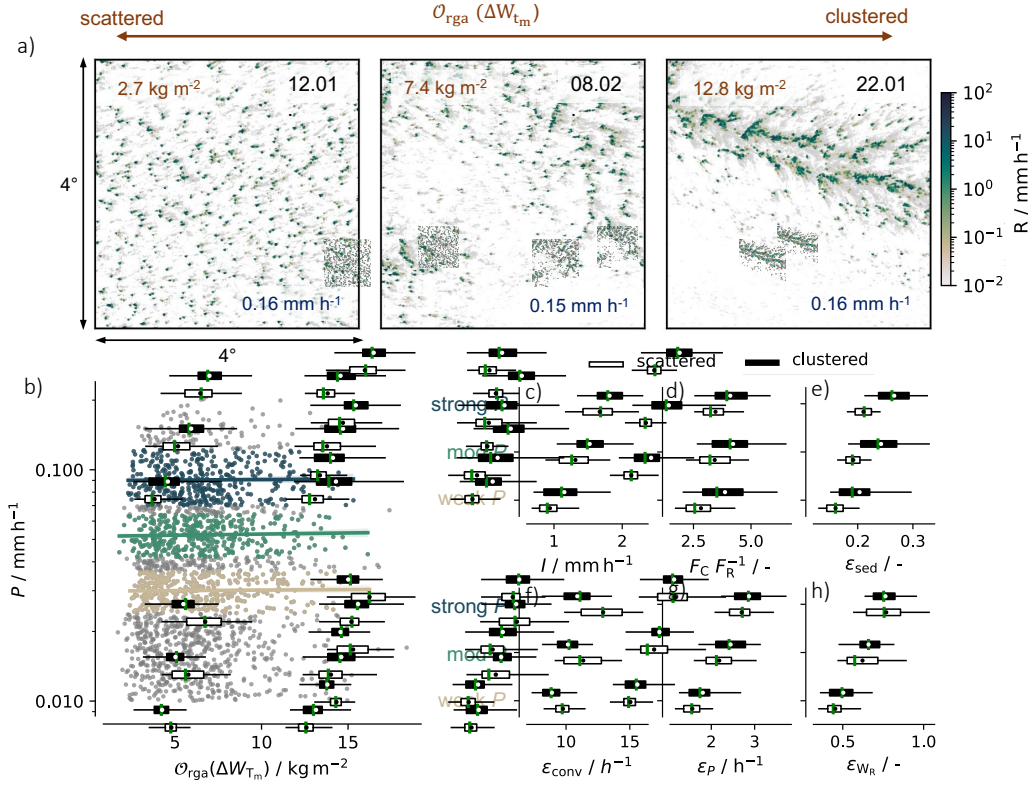
Figure B.1: a) Three example scenes with similar scene-averaged precipitation $P$ (i.e. rain amount, blue) but different degrees of organisation $\mathcal{O}_{\mathrm{rga}}(\Delta W_{\mathrm{T_m}})$ (orange). Colour shading denotes rain rate $R$. Grey shading denotes cloud albedo calculated from simulated cloud liquid water path. b) $P$ as a function of $\mathcal{O}_{\mathrm{rga}}(\Delta W_{\mathrm{T_m}})$. Three different rain regimes with weak P =(0.024, 0.037], mod P = (0.042, 0.064] and high P = (0.07, 0.12] are visualized. c) Rain intensity $I$, d) cold pool fraction $F_{\mathrm{C}}$ per rain fraction $F_{\mathrm{R}}$, e) sedimentation efficiency $\epsilon_{\mathrm{sed}}$, f) conversion efficiency $\epsilon_{\mathrm{conv}}$, g) precipitation efficiency $\epsilon_{\mathrm{P}}$ and h) water loading efficiency $\epsilon_{\mathrm{W_R}} = \frac{W_{\mathrm{R}}}{W_{\mathrm{L}}}$ where $W_{\mathrm{R}}$ rain water path for the three precipitation regimes separated into a clustered ($>70^{\mathrm{th}}$ percentile) and scattered sample ($<30^{\mathrm{th}}$ percentile). The green line denotes the median, the dot the mean, the box the interquartile range and the whiskers denote the $5^{\mathrm{th}}$ and $95^{\mathrm{th}}$ percentile.

$\epsilon_{\mathrm{evap}} = \frac{E}{C_{\mathrm{A}}}$. The rain that does not evaporate reaches the ground as precipitation, $P$, so that we call

$$\epsilon_{\mathrm{sed}} = \frac{P}{C_{\mathrm{A}}} = 1 - \frac{E}{C_{\mathrm{A}}} = 1 - \epsilon_{\mathrm{evap}} \tag{B.2}$$

the sedimentation efficiency. $\epsilon_{\mathrm{sed}}$ describes how much of the produced rain water reaches the ground as precipitation versus how much evaporates on the way.

The product of the conversion and sedimentation efficiency describes how much cloud water precipitates, in other words a precipitation efficiency $\epsilon_{\mathrm{P}}$ following Lang-

hans et al. (2015), defined as the ratio of precipitation to cloud liquid water path:

$$\underbrace{\frac{P}{W_L}}_{\epsilon_P} = \underbrace{\frac{C_A}{W_L}}_{\epsilon_{conv}} \cdot \underbrace{\frac{P}{C_A}}_{\epsilon_{sed}} . \tag{B.3}$$

The precipitation efficiency describes how much cloud water per hour is returned to the surface as precipitation versus how much can detrain and moisten the atmosphere. It is to note that precipitation efficiency itself has no unique definition (e.g. Sui et al., 2020). Different results may emerge for different definitions and depend on local versus domain mean views. However, using an approximation of the condensation rate following Muller and Takayabu (2020) instead of liquid water path in (B.3) results in the same qualitative behaviour. Here, we mainly exploit precipitation efficiency and its decomposition into conversion and sedimentation efficiency as a proxy for the pathway precipitation development takes.

## B.3 RESULTS

### B.3.1 *The pathway to precipitation varies with organisation*

The LES reproduce EUREC[4]A observations that scene precipitation in the trades varies mainly independently of organisation (Radtke et al., 2022). This is shown in Fig. B.1b and more visually depicted in the example scenes in Fig. B.1a, which display a similar rain rate but vastly different degrees of organisation. In the LES, scene rain rates vary up to $0.2\,\mathrm{mm\,h^{-1}}$ as shown in Fig. B.1b, which compares well to rain rates observed in the RICO (Nuijens et al., 2009) and EUREC[4]A campaign (Radtke et al., 2022). In the following, we will show whether also the pathway to these rain rates is similar or in how far organisation affects how these rain rates are generated, and could thus be a process to maintain precipitation in different environments. To investigate this, we group our sample of scenes into three precipitation regimes, a weak, a moderate, and a strong precipitation regime, as visualised in Fig. B.1b. In each regime, we divide the scenes into a more organised (>70th percentile) and a less organised (<30th percentile) sample, which we refer to as clustered and scattered, and show aggregated statistics for theses samples to condense the results (Fig. B.1c-h). Although precipitation varies independently of the degree of organisation, Fig. B.1c shows that organisation tends to increase the rain intensity. This is also suggested by observational studies of trade-wind (Radtke et al., 2022) and deep convection (Louf et al., 2019). That is, clustered convection produces the same amount of scene precipitation than scattered convection with more intense rain covering a smaller area. Possibly associated with this, clustered scenes are also populated by more cold pools than scattered scenes as shown in Fig. B.1d. In clustered scenes, the cold pool fraction is around four times greater than the rain fraction, whereas in scattered scenes it is around three times greater. These findings may already hint to an altered precipitation process in more organised compared to less organised scenes. We now investigate this using (B.3).

How organisation varies as a function of conversion and sedimentation efficiency is shown in Fig. B.2a. Organisation maximises towards the lower right of the phase space, at low conversion and high sedimentation efficiency. An increase in the degree of organisation is thus related to a decrease in how efficient cloud water is converted to rain and an increase in how efficient rain sediments, meaning a greater contribution of rain reaches the ground instead of evaporating. Sedimentation efficiency varies between 0.1 and 0.3, emphasising that much rain re-evaporates, as reported by Naumann and Seifert (2016) and Sarkar et al. (2022). Precipitation maximises towards the upper right of the same phase space, that is at high sedimentation and conversion efficiency (Fig. B.2b). Within a precipitation regime as shown in Fig. B.1e, f, rain thus sediments more efficiently in clustered scenes, but is produced less efficiently than in scattered scenes. This behaviour is slightly enhanced with stronger precipitation.
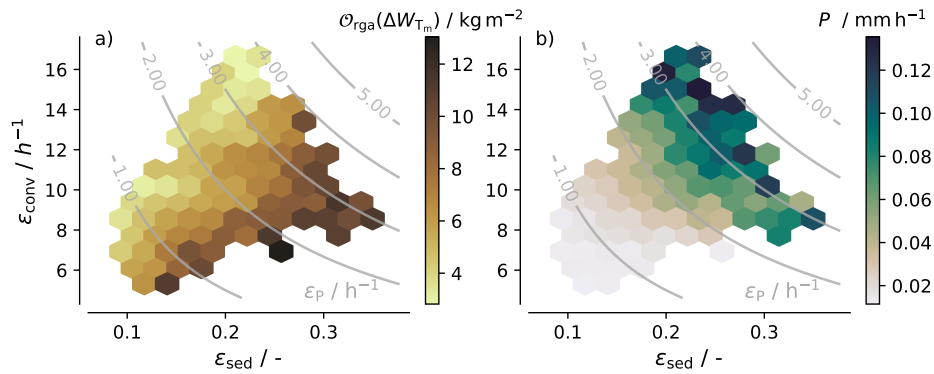


Figure B.2: a) Degree of mesoscale organisation $\mathcal{O}_{\mathrm{rga}}(\Delta W_{\mathrm{T_m}})$ and b) precipitation $P$ (shading) as a function of conversion efficiency $\epsilon_{\mathrm{conv}}$ and sedimentation efficiency $\epsilon_{\mathrm{sed}}$. Contour lines denote precipitation efficiency $\epsilon_{\mathrm{P}} = \epsilon_{\mathrm{conv}} \cdot \epsilon_{\mathrm{sed}}$.

The product of the conversion and sedimentation efficiency gives the precipitation efficiency, denoted in the contour lines in Fig. B.2. Precipitation efficiency varies mostly between $1\,\mathrm{h^{-1}}$ and $3\,\mathrm{h^{-1}}$ and closely with precipitation. One to three times the cloud liquid water path precipitates per hour, emphasising the rapid turnover and rain formation in trade-wind clouds, which with tops greater than $2500\,\mathrm{m}$ "usually rain within half an hour" (Squires 1958). Because conversion efficiency decreases but sedimentation efficiency increases with organisation, contours of precipitation efficiency and organisation lie perpendicular to each other in the phase space. This means that organisation and precipitation efficiency, like precipitation, vary mainly independently of each other. Composited on three different precipitation regimes, Fig. B.1g shows that precipitation efficiency varies only marginally with organisation. Whereas in a moderate precipitation regime, precipitation efficiency tends to increase slightly, this behaviour diminishes in the high precipitation regime. Analysing the ratio of rain water path to cloud water path instead of the ratio between precipitation and cloud liquid water path gives the same result (Fig. B.1h). Thus, organisation weakly affects precipitation efficiency in terms of how much cloud water precipitates, but changes the pathway to precipitation in terms of how much the production versus

sedimentation phase contributes to the formation of surface precipitation. Next, we investigate physical mechanisms behind this behaviour.

### B.3.2  *Why does organisation affect the pathway to precipitation?*

#### B.3.2.1  *Sedimentation efficiency*

The sedimentation efficiency describes how much rain reaches the ground instead of evaporating. We suggest that it should scale to a first approximation with the moisture environment through which rain falls, or more explicitly with the saturation deficit, and the time rain falls, following Lutsko and Cronin (2018):

$$\underbrace{\epsilon_{\text{evap}}}_{1-\epsilon_{\text{sed}}} \sim (1 - \mathcal{R}_{\text{rain}}) \cdot t_{\text{fall}} = (1 - \mathcal{R}_{\text{rain}}) \cdot \frac{h}{v}, \qquad (\text{B.4})$$

where $\mathcal{R}_{\text{rain}}$ is the averaged relative humidity through which rain falls, i.e. conditioned on pixels with rain water $q_{\text{r}} > 0.001\,\text{g\,kg}^{-1}$ (van Zanten et al., 2011), and $t_{\text{fall}}$ the average fall time, which depends on the average fall height $h$ and velocity $v$. The higher the saturation deficit or the longer rain falls and thus has time to evaporate, the higher evaporation and the lower the amount of rain reaching the ground.
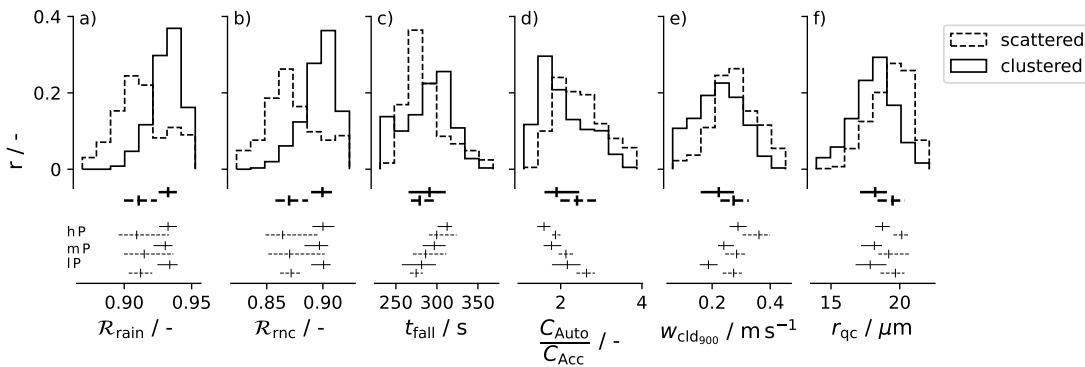


Figure B.3: Relative frequency of a) rain-conditioned relative humidity $\mathcal{R}_{\text{rain}}$, b) rain-and-no-cloud-conditioned relative humidity $\mathcal{R}_{\text{rnc}}$, c) fall time $t_{\text{fall}}$, d) ratio of autoconversion $C_{\text{Auto}}$ to accretion $C_{\text{Acc}}$, e) cloud-conditioned vertical velocity at 900 hPa $w_{\text{cld}_{900}}$, f) mean cloud droplet radius $r_{\text{qc}}$ for the scattered and clustered sample (as in Fig. B.1) for all scenes and divided into three precipitation regimes (hP denoting the high P regime, mP the mod P regime and lP the low P regime defined above). Horizontal lines denote the interquartile range, vertical lines the median.

We hypothesise that organisation influences the moisture environment through which rain falls, since it manifests itself in an uneven (horizontal) distribution of moisture, as also used in our metric of organisation. Figure B.3a shows that in the simulations, rain in clustered scenes indeed typically falls through a more humid environment with a lower saturation deficit than in scattered scenes. This is true for all precipitation regimes, with little variations in $\mathcal{R}_{\text{rain}}$ between precipitation regimes. We find that rain falls through a moister environment because the environment outside of or beneath

clouds is closer to saturation (about 3%,Fig. B.3b), not just because more rain may falls within than outside of clouds, e.g. due to different wind shears and cloud tilts. This is in line with the idea that clouds in more organised scenes develop preferentially in the parts of the domain with moister, more favourable thermodynamic conditions, e.g. preconditioned by former clouds, leading to the formation of clusters and protecting clouds from dilution and rain from evaporation, the so called mutual protection hypothesis (Seifert and Heus, 2013).

Besides the moisture environment, organisation could also influence the time in which rain falls by modulating the fall height or fall velocity. We define the average height where rain is produced by autoconversion and accretion $h_A$ (which is similar to the average top height of all raining but non-cloudy pixels) as fall height. With this definition, rain in clustered convection falls on average from slightly higher heights than in scattered convection, related to a tendency of cloud growing deeper and inversion heights increasing with organisation (not shown). Using $h = h_A$ and approximating the fall velocity as $v \sim (\rho q_r)^{\frac{1}{8}}$ where $\rho$ density (Doms et al., 2021), the fall time increases with organisation, but only marginally (Fig. B.3c). This would suggest that organisation has little effect on the time it takes for rain to fall to the ground. However, the fall time approximation used so far applies a simplified fall velocity that does not directly capture variations in the raindrop size. The raindrop size was not included in the model output but the way rain is produced, i.e. in how far autoconversion or accretion dominates the production of rain, may serve as a proxy for the raindrops' size. Because autoconversion produces initial "embryo" raindrops as small cloud droplets merge whereas accretion describes the growth of raindrops by collecting cloud droplets, an increased contribution of accretion to rain production indicates that raindrops have grown larger. Fig. B.3d shows that in more organised scenes this is the case. Figure B.4a shows that in how far autoconversion versus accretion contributes to rain production explains 79 % of the variations in sedimentation efficiency, increasing to 85 % when including $\mathcal{R}_{\mathrm{rain}}$ as additional predictor. When including additionally $h_A$ no further variations can be explained.

Our analysis thus suggest that organisation reduces evaporation and increases the sedimentation efficiency because rain in more organised scenes is increasingly produced by accretion so that raindrops are larger and they additionally fall through a moister environment. Variations in the height from which rain falls are of minor importance.

B.3.2.2 *Rain production efficiency*

Rain starts to form when sufficient cloud water has been produced and cloud droplets have grown to precipitation size. To initiate and grow cloud particles the air's saturation is important and influenced by vertical motions as well as the thermodynamic condition. In the simulations, organisation influences the clouds' vertical motion. Figure B.3e shows that the mean vertical motion at cloud base $w_{\mathrm{cld}_{900}}$ (cloud-conditioned, i.e where cloud water $q_c > 0.01\,\mathrm{g\,kg^{-1}}$, and at 900 hPa) is in clustered scenes slightly weaker than in more scattered scenes. This is related in part to stronger downdrafts (e.g. the 25th percentile of $w_{\mathrm{cld}_{900}}$ is lower), but also to weaker updrafts: the mean cloud
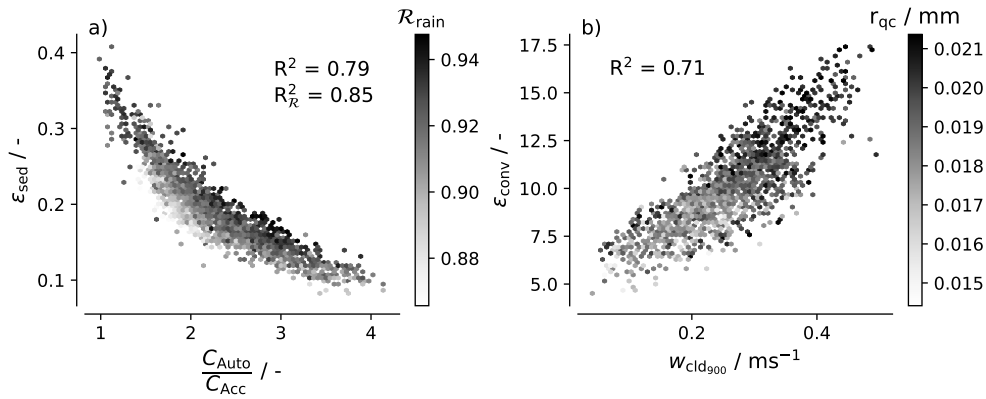
Figure B.4: a) Sedimentation efficiency $\epsilon_\text{sed}$ as a function of the relative importance of autoconversion $C_\text{Auto}$ and accretion $C_\text{Acc}$. Shading denotes the rain-conditioned relative humidity $\mathcal{R}_\text{rain}$. b) Conversion efficiency $\epsilon_\text{conv}$ as a function of cloud-conditioned vertical velocity at 900 hPa $w_{\text{cld}_{900}}$. Shading denotes the mean cloud droplet radius $r_\text{qc}$.

upward motion, but not maximum vertical velocities differ between clustered and scattered scenes, suggesting that weaker updrafts are more common in clustered scenes (not shown). Analysing deep convection, Bao and Windmiller (2021) also found that vertical motions decrease with organisation. As organisation creates more favourable thermodynamic conditions for cloud and rain formation as shown above (rain forms in more humid environments), clouds might be able to develop in weaker dynamic conditions.

More organised scenes also differ from less organised scenes in the mean cloud droplet radius. Fig. B.3f shows that in clustered scenes, the mean cloud droplet size is smaller by about 1.3 μm than in scattered scenes. From moderate to high precipitation, this difference increases, which is in line with the strong decrease in conversion efficiency at high precipitation. The smaller cloud size in more organised scenes accords with the weaker vertical motions. Besides, organisation might also influences the cloud droplets' size by changing the mixing characteristic of clouds. Cooper et al. (2013) showed that mixing and entrainment enhances cloud droplet growth and can result in a fast onset of precipitation. Organisation is thought to reduce the dilution of clouds by entrainment, which might contribute to the smaller cloud droplet size.

Because rain forms in weaker updrafts and from smaller cloud droplets, clouds may need to grow deeper before they produce rain and so cloud water is less efficiently converted to rain. Figure B.4b shows that 70 % of the variations in conversion efficiency are explained by the mean vertical motion at cloud base, to which the mean cloud droplet size is correlated. To conclude, our analyses suggest that organisation reduces the efficiency with which cloud water is converted to rain water because in clustered scenes rain forms in weaker updrafts from on average smaller cloud droplets. We hypothesise this is because clouds develop in more favourable thermodynamic

environments due to organisation, and organisation changes the mixing characteristics of clouds.

### B.3.2.3   *Buffering*

Organisation increases the sedimentation efficiency, but decreases the conversion efficiency, that is influences them in a compensating way. Why? One explanation may be that organisation establishes more favourable thermodynamic conditions - rain forms in more humid environments. This may result from enhanced moisture transport to the already moist patches by local circulations (Narenpitak et al., 2021; George et al., 2022) and larger cloud clusters that are less prone to dilution (Tian and Kuang, 2016) as well as clouds pre-conditioning the environment for subsequent convection (Kuang and Bretherton, 2006). The more favourable thermodynamic conditions could allow clouds to develop under less favourable dynamic conditions, leading to a less efficient rain production. At the same time they act to reduce evaporation, leading to a more efficient sedimentation of rain. An alternative explanation is that (life)time effcts might simply balance the production and sedimentation efficiency. As clouds grow more slowly due to weaker vertical motions producing rain inefficiently, the lifetime of clouds may increase. Time then is available for the rain production process to evolve, for accretion to increasingly contribute to rain production. The increased contribution of accretion to rain production in more organised scenes ultimately indicates that clouds are older and supports the idea that organisation increases the lifetime of clouds. As accretion increasingly contributes to rain production, raindrops grow larger, resulting in rain falling out more efficiently.

The compensation is in line with the concept of buffering (Feingold et al., 2017). It states that if there are different paths leading to the same state, they buffer the system against disruptions to any particular path. Our analyses suggest that organisation is one form of buffering. While in less organised scenes rain development is predominantly driven by an efficient conversion of cloud water to rain water, in more organised scenes, increased sedimentation efficiency, that is more rain reaching the ground instead of evaporating, increasingly contributes to precipitation. This may contribute to explain why rain development is so common in the trades, unlike previously thought. Organisation enables different pathways to precipitation.

### B.4   SUMMARY AND CONCLUSIONS

We exploit realistic large-domain LES of the trades during EUREC[4]A to investigate whether and how organisation affects the pathway to precipitation. We decompose the formation of surface precipitation following Langhans et al. (2015) into a production phase, where cloud condensate is converted to rain, and a sedimentation phase, where the produced raindrops fall to the ground while some evaporate.

In the simulations, organisation affects how these two phases contribute to precipitation formation. With organisation, rain forms and falls through a locally more

humid environment. Additionally, rain is increasingly produced by accretion rather than autoconversion which indicates that clouds are older and raindrops grow larger. Larger raindrops, that fall through a more humid environment experience less evaporation, leading to an increase in the sedimentation efficiency. The relative importance of accretion and autoconversion explains 79% of the variations in sedimentation efficiency, increasing to 85% when including the rain-conditioned relative humidity as additional predictor. A more humid environment is in line with the idea that clustering leads to more humid patches in which clouds develop and which protect clouds from dilution and raindrops from evaporation. It may suggest that organisation also increases the efficiency with which cloud condensate is converted to rain. However, in more organised scenes rain forms in weaker updrafts, as in Bao and Windmiller (2021), and from smaller cloud droplets. This leads to cloud water being less efficiently converted to rain, similarly found in radiative-convective equilibrium simulations by Lutsko and Cronin (2018). 71% of the variations in conversion efficiency are explained by the vertical motion at cloud base, to which the cloud droplet size is correlated. Possibly because the thermodynamic environment is more favourable with organisation, weaker dynamic conditions do not prevent rain formation, or lifetime effects may play a role here. Both effects, the increase in sedimentation efficiency and the decrease in conversion efficiency, mainly compensate, so that organisation does not substantially affect how efficiently it precipitates.

We interpret the influence of organisation on the conversion and sedimentation of rain as a form of buffering (Feingold et al., 2017). While in less organised scenes rain development is predominantly driven by efficient conversion of cloud condensate to rain, in more organised scenes increased efficient sedimentation, that is more of the rain reaching the ground instead of evaporating, increasingly contributes to surface rain formation. What makes it rain? There is not only one way to rain, and this study shows that and how organisation can be one mechanism through which a different pathway to precipitation is possible.

# BIBLIOGRAPHY

Aristophanes, translated by Hickie, W. J. (417 BC). *The Clouds*. Perseus Digital Library.

Bach, R. (1981). *Illusions : the adventures of a reluctant Messiah*. New York: Dell/E. Friede.

Bao, J. and Windmiller, J. M. (2021). "Impact of Microphysics on Tropical Precipitation Extremes in a Global Storm-Resolving Model." In: *Geophysical Research Letters* 48.13, e2021GL094206. ISSN: 1944-8007. DOI: `10.1029/2021GL094206`.

Barnes, G. M. and Garstang, M. (1982). "Subcloud Layer Energetics of Precipitating Convection." In: *Monthly Weather Review* 110.2, pp. 102–117. ISSN: 1520-0493, 0027-0644. DOI: `10.1175/1520-0493(1982)110<0102:SLEOPC>2.0.CO;2`.

Becker, T., Bretherton, C. S., Hohenegger, C., and Stevens, B. (2018). "Estimating Bulk Entrainment With Unaggregated and Aggregated Convection." In: *Geophysical Research Letters* 45.1, pp. 455–462. ISSN: 1944-8007. DOI: `10.1002/2017GL076640`.

Betts, A. K. (1997). "Trade Cumulus: Observations and Modelling." In: *The Physics and Parameterization of Moist Atmospheric Convection*. Ed. by R. K. Smith. Dordrecht: Springer Netherlands, pp. 99–126. ISBN: 978-94-015-8828-7. DOI: `10.1007/978-94-015-8828-7_4`.

Bock, O., Bosser, P., Flamant, C., Doerflinger, E., Jansen, F., Fages, R., Bony, S., and Schnitt, S. (2021). "Integrated Water Vapour Observations in the Caribbean Arc from a Network of Ground-Based GNSS Receivers during EUREC⁴A." In: *Earth System Science Data* 13.5, pp. 2407–2436. ISSN: 1866-3508. DOI: `10.5194/essd-13-2407-2021`.

Bony, S. and Dufresne, J.-L. (2005). "Marine Boundary Layer Clouds at the Heart of Tropical Cloud Feedback Uncertainties in Climate Models." In: *Geophysical Research Letters* 32.20. ISSN: 1944-8007. DOI: `10.1029/2005GL023851`.

Bony, S., Schulz, H., Vial, J., and Stevens, B. (2020). "Sugar, Gravel, Fish, and Flowers: Dependence of Mesoscale Patterns of Trade-Wind Clouds on Environmental Conditions." In: *Geophysical Research Letters* 47.7, e2019GL085988. ISSN: 1944-8007. DOI: `10.1029/2019GL085988`.

Bony, S., Stevens, B., Ament, F., et al. (2017). "EUREC4A: A Field Campaign to Elucidate the Couplings Between Clouds, Convection and Circulation." In: *Surveys in Geophysics* 38.6, pp. 1529–1568. ISSN: 15730956. DOI: `10.1007/s10712-017-9428-0`.

Boucher, O., Randall, D., Artaxo, P., et al. (2013). "Clouds and aerosols." In: *Climate Change 2013: The Physical Science Basis. Contribution of Working Group I to the Fifth Assessment Report of the Intergovernmental Panel on Climate Change*. Ed. by T. F. Stocker, D. Qin, G.-K. Plattner, M. Tignor, S. K. Allen, J. Doschung, A. Nauels, Y. Xia, V. Bex, and P. M. Midgley. Cambridge, UK: Cambridge University Press, pp. 571–657. DOI: `10.1017/CBO9781107415324.016`.

Bretherton, C. S. and Blossey, P. N. (2017). "Understanding Mesoscale Aggregation of Shallow Cumulus Convection Using Large-Eddy Simulation." In: *Journal of Advances in Modeling Earth Systems* 9.8, pp. 2798–2821. ISSN: 19422466. DOI: `10.1002/2017MS000981`.

Bretherton, C. S., Blossey, P. N., and Jones, C. R. (2013). "Mechanisms of Marine Low Cloud Sensitivity to Idealized Climate Perturbations: A Single-LES Exploration Extending the CGILS Cases." In: *Journal of Advances in Modeling Earth Systems* 5.2, pp. 316–337. ISSN: 19422466. DOI: 10.1002/jame.20019.

Bretherton, C. S., Blossey, P. N., and Khairoutdinov, M. (2005). "An Energy-Balance Analysis of Deep Convective Self-Aggregation above Uniform SST." In: *Journal of the Atmospheric Sciences* 62.12, pp. 4273–4292. ISSN: 0022-4928, 1520-0469. DOI: 10.1175/JAS3614.1.

Bretherton, C. S., Peters, M. E., and Back, L. E. (2004). "Relationships between Water Vapor Path and Precipitation over the Tropical Oceans." In: *Journal of Climate* 17.7, pp. 1517–1528. ISSN: 0894-8755, 1520-0442. DOI: 10.1175/1520-0442(2004)017<1517:RBWVPA>2.0.CO;2.

Brueck, M., Hohenegger, C., and Stevens, B. (2020). "Mesoscale Marine Tropical Precipitation Varies Independently from the Spatial Arrangement of Its Convective Cells." In: *Quarterly Journal of the Royal Meteorological Society* 146.728, pp. 1391–1402. ISSN: 0035-9009. DOI: 10.1002/qj.3742.

Byers, H. R. and Hall, R. K. (1955). "A CENSUS OF CUMULUS-CLOUD HEIGHT VERSUS PRECIPITATION IN THE VICINITY OF PUERTO RICO DURING THE WINTER AND SPRING OF 1953-1954." In: *Journal of the Atmospheric Sciences* 12.2, pp. 176–178. ISSN: 1520-0469. DOI: 10.1175/1520-0469(1955)012<0176:ACOCCH>2.0.CO;2.

Cesana, G. V. and Del Genio, A. D. (2021). "Observational Constraint on Cloud Feedbacks Suggests Moderate Climate Sensitivity." In: *Nature Climate Change*. ISSN: 1758-678X. DOI: 10.1038/s41558-020-00970-y.

Cooper, W. A., Lasher-Trapp, S. G., and Blyth, A. M. (2013). "The Influence of Entrainment and Mixing on the Initial Formation of Rain in a Warm Cumulus Cloud." In: *Journal of the Atmospheric Sciences* 70.6, pp. 1727–1743. ISSN: 0022-4928, 1520-0469. DOI: 10.1175/JAS-D-12-0128.1.

Denby, L. (2020). "Discovering the Importance of Mesoscale Cloud Organization Through Unsupervised Classification." In: *Geophysical Research Letters* 47.1, pp. 1–10. ISSN: 19448007. DOI: 10.1029/2019GL085190.

Dipankar, A., Stevens, B., Heinze, R., Moseley, C., Zängl, G., Giorgetta, M., and Brdar, S. (2015). "Large Eddy Simulation Using the General Circulation Model ICON." In: *Journal of Advances in Modeling Earth Systems* 7.3, pp. 963–986. ISSN: 1942-2466. DOI: 10.1002/2015MS000431.

Doms, G., Förstner, J., Heise, E., Reinhardt, T., Ritter, B., and Schrodin, R. (2021). *A Description of the Nonhydrostatic Regional COSMO-Model Part II Physical Parameterizations*. Tech. rep. Consortium for Small-Scale Modelling.

Drager, A. J. and van den Heever, S. C. (2017). "Characterizing Convective Cold Pools." In: *Journal of Advances in Modeling Earth Systems* 9.2, pp. 1091–1115. ISSN: 1942-2466. DOI: 10.1002/2016MS000788.

Feingold, G., Balsells, J., Glassmeier, F., Yamaguchi, T., Kazil, J., and McComiskey, A. (2017). "Analysis of Albedo versus Cloud Fraction Relationships in Liquid Water Clouds Using Heuristicmodels and Large Eddy Simulation." In: *Journal of Geophysical Research* 122.13, pp. 7086–7102. ISSN: 21562202. DOI: 10.1002/2017JD026467.

Feingold, G., McComiskey, A., Rosenfeld, D., and Sorooshian, A. (2013). "On the Relationship between Cloud Contact Time and Precipitation Susceptibility to Aerosol." In: *Journal of Geophysical Research: Atmospheres* 118.18, pp. 10, 544–10, 554. ISSN: 2169-8996. DOI: 10.1002/jgrd.50819.

Fiedler, S., Crueger, T., D'Agostino, R., et al. (2020). "Simulated Tropical Precipitation Assessed across Three Major Phases of the Coupled Model Intercomparison Project (CMIP)." In: *Monthly Weather Review* 148.9, pp. 3653–3680. ISSN: 1520-0493, 0027-0644. DOI: 10.1175/MWR-D-19-0404.1.

Fleming, J. R. (2020). *First Woman: Joanne Simpson and the Tropical Atmosphere*. Oxford: Oxford University Press. ISBN: 978-0-19-886273-4.

Freud, E. and Rosenfeld, D. (2012). "Linear Relation between Convective Cloud Drop Number Concentration and Depth for Rain Initiation." In: *Journal of Geophysical Research: Atmospheres* 117.D2. ISSN: 2156-2202. DOI: 10.1029/2011JD016457.

George, G., Stevens, B., Bony, S., Klingebiel, M., and Vogel, R. (2021). "Observed Impact of Meso-Scale Vertical Motion on Cloudiness." In: *Journal of the Atmospheric Sciences*, pp. 2413–2427. ISSN: 0022-4928. DOI: 10.1175/jas-d-20-0335.1.

George, G., Stevens, B., Bony, S., Vogel, R., and Naumann, A. K. (2022). *Ubiquity of Shallow Mesoscale Circulations in the Trades and Their Influence on Moisture Variance*. DOI: 10.1002/essoar.10512427.1.

Hadley, G. (1735). "Concerning the Cause of the General Trade-Winds." In: *Philosophical Transactions of the Royal Society of London* 39.437, pp. 58–62. DOI: 10.1098/rstl.1735.0014.

Hagen, M., Ewald, F., Groß, S., et al. (2021). "Deployment of the C-band Radar Poldirad on Barbados during EUREC⁴A." In: *Earth System Science Data* 13.12, pp. 5899–5914. ISSN: 1866-3508. DOI: 10.5194/essd-13-5899-2021.

Halley, E. (1686). "An Historical Account of the Trade Winds, and Monsoons, Observable in the Seas between and near the Tropicks, with an Attempt to Assign the Physical Cause of the Said Winds." In: *Philosophical Transactions of the Royal Society of London* 16.183, pp. 153–168. DOI: 10.1098/rstl.1686.0026.

Hartmann, D. L. and Short, D. A. (1980). "On the Use of Earth Radiation Budget Statistics for Studies of Clouds and Climate." In: *Journal of the Atmospheric Sciences* 37.6, pp. 1233–1250. ISSN: 0022-4928, 1520-0469. DOI: 10.1175/1520-0469(1980)037<1233:OTUOER>2.0.CO;2.

Heinze, R., Dipankar, A., Henken, C. C., et al. (2017). "Large-Eddy Simulations over Germany Using ICON: A Comprehensive Evaluation." In: *Quarterly Journal of the Royal Meteorological Society* 143.702, pp. 69–100. ISSN: 1477-870X. DOI: 10.1002/qj.2947.

Houze Jr., R. A. and Betts, A. K. (1981). "Convection in GATE." In: *Reviews of Geophysics* 19.4, pp. 541–576. ISSN: 1944-9208. DOI: 10.1029/RG019i004p00541.

Illingworth, A. J., Barker, H. W., Beljaars, A., et al. (2015). "The EarthCARE Satellite: The Next Step Forward in Global Measurements of Clouds, Aerosols, Precipitation, and Radiation." In: *Bulletin of the American Meteorological Society* 96.8, pp. 1311–1332. ISSN: 0003-0007, 1520-0477. DOI: 10.1175/BAMS-D-12-00227.1.

Janssens, M., Arellano, J., van Heerwaarden, C., Roode, S., Siebesma, A., and Glass-meier, F. (2022). "Non-Precipitating Shallow Cumulus Convection Is Intrinsically Unstable to Length-Scale Growth." In.

Janssens, M., Vilà-Guerau de Arellano, J., Scheffer, M., Antonissen, C., Siebesma, A. P., and Glassmeier, F. (2021). "Cloud Patterns in the Trades Have Four Interpretable Dimensions." In: *Geophysical Research Letters* 48.5, e2020GL091001. ISSN: 1944-8007. DOI: 10.1029/2020GL091001.

Kirshbaum, D. J. and Grant, A. L. M. (2012). "Invigoration of Cumulus Cloud Fields by Mesoscale Ascent." In: *Quarterly Journal of the Royal Meteorological Society* 138.669, pp. 2136–2150. ISSN: 1477-870X. DOI: 10.1002/qj.1954.

Klocke, D., Brueck, M., Hohenegger, C., and Stevens, B. (2017). "Rediscovery of the Doldrums in Storm-Resolving Simulations over the Tropical Atlantic /704/106 /704/106/35 /704/106/35/823 Perspective." In: *Nature Geoscience* 10.12, pp. 891–896. ISSN: 17520908. DOI: 10.1038/s41561-017-0005-4.

Konow, H., Ewald, F., George, G., et al. (2021). "EUREC⁴A's *HALO*." In: *Earth System Science Data* 13.12, pp. 5545–5563. ISSN: 1866-3508. DOI: 10.5194/essd-13-5545-2021.

Kuang, Z. and Bretherton, C. S. (2006). "A Mass-Flux Scheme View of a High-Resolution Simulation of a Transition from Shallow to Deep Cumulus Convection." In: *Journal of the Atmospheric Sciences* 63.7, pp. 1895–1909. ISSN: 0022-4928, 1520-0469. DOI: 10.1175/JAS3723.1.

Langhans, W., Yeo, K., and Romps, D. M. (2015). "Lagrangian Investigation of the Precipitation Efficiency of Convective Clouds." In: *Journal of the Atmospheric Sciences* 72.3, pp. 1045–1062. ISSN: 0022-4928, 1520-0469. DOI: 10.1175/JAS-D-14-0159.1.

Lau, K. M. and Wu, H. T. (2003). "Warm Rain Processes over Tropical Oceans and Climate Implications." In: *Geophysical Research Letters* 30.24, pp. 2–6. ISSN: 00948276. DOI: 10.1029/2003GL018567.

Loeb, N. G., Doelling, D. R., Wang, H., Su, W., Nguyen, C., Corbett, J. G., Liang, L., Mitrescu, C., Rose, F. G., and Kato, S. (2018). "Clouds and the Earth's Radiant Energy System (CERES) Energy Balanced and Filled (EBAF) Top-of-Atmosphere (TOA) Edition-4.0 Data Product." In: *Journal of Climate* 31.2, pp. 895–918. ISSN: 0894-8755, 1520-0442. DOI: 10.1175/JCLI-D-17-0208.1.

López, R. E. (1978). "Internal Structure and Development Processes of C-Scale Aggregates of Cumulus Clouds." In: *Monthly Weather Review* 106.10, pp. 1488–1494. ISSN: 1520-0493, 0027-0644. DOI: 10.1175/1520-0493(1978)106<1488:ISADPO>2.0.CO;2.

Lorenz, E. N. (1967). *The nature and theory of the general circulation of the atmosphere*. Vol. 218. World Meteorological Organisation Geneva.

Louf, V., Jakob, C., Protat, A., Bergemann, M., and Narsey, S. (2019). "The Relationship of Cloud Number and Size With Their Large-Scale Environment in Deep Tropical Convection." In: *Geophysical Research Letters* 46.15, pp. 9203–9212. ISSN: 19448007. DOI: 10.1029/2019GL083964.

Lutsko, N. J. and Cronin, T. W. (2018). "Increase in Precipitation Efficiency With Surface Warming in Radiative-Convective Equilibrium." In: *Journal of Advances in Modeling Earth Systems* 10.11, pp. 2992–3010. ISSN: 1942-2466. DOI: 10.1029/2018MS001482.

Malkus, J. S. (1954). "Some Results Of a Trade-Cumulus Cloud Investigation." In: *Journal of the Atmospheric Sciences* 11.3, pp. 220–237. ISSN: 1520-0469. DOI: 10.1175/1520-0469(1954)011<0220:SROATC>2.0.CO;2.

– (1956). "On the Maintenance of the Trade Winds." In: *Tellus* 8.3, pp. 335–350. ISSN: 2153-3490. DOI: 10.1111/j.2153-3490.1956.tb01231.x.

– (1958). "On the Structure of the Trade Wind Moist Layer." In: 13.2, pp. 1–47. DOI: 10.1575/1912/1065.

Marshall, J. S., Hitschfeld, W., and Gunn, K. L. S. (1955). "Advances in Radar Weather." In: *Advances in Geophysics*. Ed. by H. E. Landsberg. Vol. 2. Elsevier, pp. 1–56. DOI: 10.1016/S0065-2687(08)60310-6.

Medeiros, B. and Nuijens, L. (2016). "Clouds at Barbados Are Representative of Clouds across the Trade Wind Regions in Observations and Climate Models." In: *Proceedings of the National Academy of Sciences of the United States of America* 113.22, E3062–E3070. ISSN: 10916490. DOI: 10.1073/pnas.1521494113.

Meehl, G. A., Senior, C. A., Eyring, V., Flato, G., Lamarque, J.-F., Stouffer, R. J., Taylor, K. E., and Schlund, M. (2020). "Context for Interpreting Equilibrium Climate Sensitivity and Transient Climate Response from the CMIP6 Earth System Models." In: *Science Advances* 6.26, eaba1981. DOI: 10.1126/sciadv.aba1981.

Mieslinger, T. (2021). "Small and Optically Thin Clouds in the Trades." PhD thesis. Hamburg: Universität Hamburg.

Muller, C. and Held, I. M. (2012). "Detailed Investigation of the Self-Aggregation of Convection in Cloud-Resolving Simulations." In: *Journal of the Atmospheric Sciences* 69.8, pp. 2551–2565. ISSN: 0022-4928, 1520-0469. DOI: 10.1175/JAS-D-11-0257.1.

Muller, C. and Takayabu, Y. (2020). "Response of Precipitation Extremes to Warming: What Have We Learned from Theory and Idealized Cloud-Resolving Simulations, and What Remains to Be Learned?" In: *Environmental Research Letters* 15.3, p. 035001. ISSN: 1748-9326. DOI: 10.1088/1748-9326/ab7130.

Myers, T. A., Scott, R. C., Zelinka, M. D., Klein, S. A., Norris, J. R., and Caldwell, P. M. (2021). "Observational Constraints on Low Cloud Feedback Reduce Uncertainty of Climate Sensitivity." In: *Nature Climate Change* 11.6, pp. 501–507. ISSN: 1758-6798. DOI: 10.1038/s41558-021-01039-0.

Narenpitak, P., Kazil, J., Yamaguchi, T., Quinn, P., and Feingold, G. (2021). "From Sugar to Flowers: A Transition of Shallow Cumulus Organization During ATOMIC." In: *Journal of Advances in Modeling Earth Systems* 13.10, e2021MS002619. ISSN: 1942-2466. DOI: 10.1029/2021MS002619.

Narenpitak, P., Kazil, J., Yamaguchi, T., Quinn, P. K., and Feingold, G. (2022). "The Sugar-to-Flower Shallow Cumulus Transition Under the Influences of Diel Cycle and Free-Tropospheric Mineral Dust." In: *Journal of Advances in Modeling Earth Systems* n/a.n/a, e2022MS003228. ISSN: 1942-2466. DOI: 10.1029/2022MS003228.

Naumann, A. K. and Seifert, A. (2016). "Recirculation and Growth of Raindrops in Simulated Shallow Cumulus." In: *Journal of Advances in Modeling Earth Systems* 8.2, pp. 520–537. ISSN: 1942-2466. DOI: 10.1002/2016MS000631.

Nitta, T. and Esbensen, S. (1974). "Heat and Moisture Budget Analyses Using BOMEX Data." In: *Monthly Weather Review* 102.1, pp. 17–28. ISSN: 1520-0493, 0027-0644. DOI: 10.1175/1520-0493(1974)102<0017:HAMBAU>2.0.CO;2.

Nuijens, L., Emanuel, K., Masunaga, H., and L'Ecuyer, T. (2017). "Implications of Warm Rain in Shallow Cumulus and Congestus Clouds for Large-Scale Circulations." In: *Surveys in Geophysics* 38.6, pp. 1257–1282. ISSN: 15730956. DOI: 10.1007/s10712-017-9429-z.

Nuijens, L. and Siebesma, A. P. (2019). "Boundary Layer Clouds and Convection over Subtropical Oceans in Our Current and in a Warmer Climate." In: *Current Climate Change Reports* 5.2, pp. 80–94. ISSN: 21986061. DOI: 10.1007/s40641-019-00126-x.

Nuijens, L., Stevens, B., and Siebesma, A. P. (2009). "The Environment of Precipitating Shallow Cumulus Convection." In: *Journal of the Atmospheric Sciences* 66.7, pp. 1962–1979. ISSN: 00224928. DOI: 10.1175/2008JAS2841.1.

Planck, M. (1949). "The Meaning and Limits of Exact Science." In: *Science* 110.2857, pp. 319–327. DOI: 10.1126/science.110.2857.319.

Pscheidt, I., Senf, F., Heinze, R., Deneke, H., Trömel, S., and Hohenegger, C. (2019). "How Organized Is Deep Convection over Germany?" In: *Quarterly Journal of the Royal Meteorological Society* 145.723, pp. 2366–2384. ISSN: 1477870X. DOI: 10.1002/qj.3552.

Radtke, J., Mauritsen, T., and Hohenegger, C. (2021). "Shallow Cumulus Cloud Feedback in Large Eddy Simulations – Bridging the Gap to Storm-Resolving Models." In: *Atmospheric Chemistry and Physics* 21.5, pp. 3275–3288. ISSN: 1680-7316. DOI: 10.5194/acp-21-3275-2021.

Radtke, J., Naumann, A. K., Hagen, M., and Ament, F. (2022). "The Relationship between Precipitation and Its Spatial Pattern in the Trades Observed during EUREC$^4$A." In: *Quarterly Journal of the Royal Meteorological Society*, qj.4284. ISSN: 0035-9009, 1477-870X. DOI: 10.1002/qj.4284.

Rasp, S., Schulz, H., Bony, S., and Stevens, B. (2019). "Combining Crowd-Sourcing and Deep Learning to Explore the Meso-Scale Organization of Shallow Convection." In: *arXiv*, pp. 1980–1995. ISSN: 23318422.

Rauber, R. M., Stevens, B., Ochs, H. T., Knight, C., Albrecht, B. a., Blyth, a. M., Fairall, C. W., and Jensen, J. B. (2007). "Over the Ocean: The RICO Campaign." In: *Bulletin of the American Meteorological Society* December 2007, pp. 1912–1928. ISSN: 0003-0007. DOI: 10.1175/BAMS-88-12-1912.

Retsch, M. H., Jakob, C., and Singh, M. S. (2020). "Assessing Convective Organization in Tropical Radar Observations." In: *Journal of Geophysical Research: Atmospheres* 125.7. ISSN: 2169-897X. DOI: 10.1029/2019JD031801.

Rieck, M., Nuijens, L., and Stevens, B. (2012). "Marine Boundary Layer Cloud Feedbacks in a Constant Relative Humidity Atmosphere." In: *Journal of the Atmospheric Sciences* 69.8, pp. 2538–2550. ISSN: 00224928. DOI: 10.1175/JAS-D-11-0203.1.

Riehl, H., Yeh, T. C., Malkus, J. S., and la Seur, N. E. (1951). "The North-East Trade of the Pacific Ocean." In: *Quarterly Journal of the Royal Meteorological Society* 77.334, pp. 598–626. ISSN: 1477-870X. DOI: 10.1002/qj.49707733405.

Sarkar, M., Bailey, A., Blossey, P., de Szoeke, S. P., Noone, D., Quinones Melendez, E., Leandro, M., and Chuang, P. (2022). "Sub-Cloud Rain Evaporation in the North Atlantic Ocean." In: *EGUsphere*, pp. 1–37. DOI: 10.5194/egusphere-2022-1143.

Schlemmer, L. and Hohenegger, C. (2014). "The Formation of Wider and Deeper Clouds as a Result of Cold-Pool Dynamics." In: *Journal of the Atmospheric Sciences* 71.8, pp. 2842–2858. ISSN: 0022-4928, 1520-0469. DOI: 10.1175/JAS-D-13-0170.1.

Schroth, A. C., Chandra, M. S., and Meischner, P. F. (1988). "A C -Band Coherent Polarimetric Radar for Propagation and Cloud Physics Research." In: *Journal of Atmospheric and Oceanic Technology* 5.6, pp. 803–822. ISSN: 0739-0572. DOI: 10.1175/1520-0426(1988)005<0803:ABCPRF>2.0.CO;2.

Schulz, H. (2021). "Meso-Scale Patterns of Shallow Convection in the Trades." PhD thesis. Universität Hamburg.

Schulz, H., Eastman, R., and Stevens, B. (2021). "Characterization and Evolution of Organized Shallow Convection in the Downstream North Atlantic Trades." In: *Journal of Geophysical Research: Atmospheres* 126.17, e2021JD034575. ISSN: 2169-8996. DOI: 10.1029/2021JD034575.

Seifert, A. and Beheng, K. D. (2006). "A Two-Moment Cloud Microphysics Parameterization for Mixed-Phase Clouds. Part 1: Model Description." In: *Meteorology and Atmospheric Physics* 92.1-2, pp. 45–66. ISSN: 0177-7971, 1436-5065. DOI: 10.1007/s00703-005-0112-4.

Seifert, A. and Heus, T. (2013). "Large-Eddy Simulation of Organized Precipitating Trade Wind Cumulus Clouds." In: *Atmospheric Chemistry and Physics* 13.11, pp. 5631–5645. ISSN: 16807316. DOI: 10.5194/acp-13-5631-2013.

Seifert, A. and Beheng, K. D. (2001). "A Double-Moment Parameterization for Simulating Autoconversion, Accretion and Selfcollection." In: *Atmospheric Research* 59–60, pp. 265–281. ISSN: 01698095. DOI: 10.1016/S0169-8095(01)00126-0.

Semie, A. G. and Bony, S. (2020). "Relationship Between Precipitation Extremes and Convective Organization Inferred From Satellite Observations." In: *Geophysical Research Letters* 47.9. ISSN: 0094-8276. DOI: 10.1029/2019GL086927.

Senf, F., Brueck, M., and Klocke, D. (2019). "Pair Correlations and Spatial Statistics of Deep Convection over the Tropical Atlantic." In: *Journal of the Atmospheric Sciences* 76.10, pp. 3211–3228. ISSN: 15200469. DOI: 10.1175/JAS-D-18-0326.1.

Sherwood, S. C., Webb, M. J., Annan, J. D., et al. (2020). "An Assessment of Earth's Climate Sensitivity Using Multiple Lines of Evidence." In: *Reviews of Geophysics* 58.4, pp. 0–2. ISSN: 8755-1209. DOI: 10.1029/2019RG000678.

Short, D. A. and Nakamura, K. (2000). "TRMM Radar Observations of Shallow Precipitation over the Tropical Oceans." In: *Journal of Climate* 13.23, pp. 4107–4124. ISSN: 08948755. DOI: 10.1175/1520-0442(2000)013<4107:TROOSP>2.0.CO;2.

Siebesma, A. P. (1998). "Shallow Cumulus Convection." In: *Buoyant Convection in Geophysical Flows*. Ed. by E. J. Plate, E. E. Fedorovich, D. X. Viegas, and J. C. Wyngaard. Dordrecht: Springer Netherlands, pp. 441–486. ISBN: 978-94-011-5058-3. DOI: 10.1007/978-94-011-5058-3_19.

Siebesma, A. P., Bony, S., Jakob, C., and Stevens, B., eds. (2020). *Clouds and Climate: Climate Science's Greatest Challenge*. Cambridge: Cambridge University Press. ISBN: 978-1-107-06107-1. DOI: 10.1017/9781107447738.

Siebesma, A. P., Bretherton, C. S., Brown, A., et al. (2003). "A Large Eddy Simulation Intercomparison Study of Shallow Cumulus Convection." In: *Journal of the Atmo-*

*spheric Sciences* 60.10, pp. 1201–1219. ISSN: 0022-4928, 1520-0469. DOI: 10.1175/1520-0469(2003)60<1201:ALESIS>2.0.CO;2.

Smalley, K. M. and Rapp, A. D. (2020). "The Role of Cloud Size and Environmental Moisture in Shallow Cumulus Precipitation." In: *Journal of Applied Meteorology and Climatology* 59.3, pp. 535–550. ISSN: 15588432. DOI: 10.1175/JAMC-D-19-0145.1.

Snodgrass, E. R., Di Girolamo, L., and Rauber, R. M. (2009). "Precipitation Characteristics of Trade Wind Clouds during RICO Derived from Radar, Satellite, and Aircraft Measurements." In: *Journal of Applied Meteorology and Climatology* 48.3, pp. 464–483. ISSN: 15588424. DOI: 10.1175/2008JAMC1946.1.

Squires, P. (1958). "The Microstructure and Colloidal Stability of Warm Clouds." In: *Tellus* 10.2, pp. 256–261. ISSN: 2153-3490. DOI: 10.1111/j.2153-3490.1958.tb02011.x.

Stevens, B. (2005). "Atmospheric Moist Convection." In: *Annual Review of Earth and Planetary Sciences* 33.1, pp. 605–643. ISSN: 0084-6597. DOI: 10.1146/annurev.earth.33.092203.122658.

Stevens, B., Ament, F., Bony, S., et al. (2019a). "A High-Altitude Long-Range Aircraft Configured as a Cloud Observatory: The NARVAL Expeditions." In: *Bulletin of the American Meteorological Society* 100.6, pp. 1061–1077. ISSN: 0003-0007. DOI: 10.1175/bams-d-18-0198.1.

Stevens, B., Bony, S., Brogniez, H., et al. (2020). "Sugar, Gravel, Fish and Flowers: Mesoscale Cloud Patterns in the Trade Winds." In: *Quarterly Journal of the Royal Meteorological Society* 146.726, pp. 141–152. ISSN: 0035-9009, 1477-870X. DOI: 10.1002/qj.3662.

Stevens, B., Bony, S., Farrell, D., et al. (2021). "EUREC⁴A." In: *Earth System Science Data* 13.8, pp. 4067–4119. ISSN: 1866-3508. DOI: 10.5194/essd-13-4067-2021.

Stevens, B., Farrell, D., Hirsch, L., et al. (2016). "The Barbados Cloud Observatory: Anchoring Investigations of Clouds and Circulation on the Edge of the Itcz." In: *Bulletin of the American Meteorological Society* 97.5, pp. 735–754. ISSN: 00030007. DOI: 10.1175/BAMS-D-14-00247.1.

Stevens, B., Satoh, M., Auger, L., et al. (2019b). "DYAMOND: The DYnamics of the Atmospheric General Circulation Modeled On Non-hydrostatic Domains." In: *Progress in Earth and Planetary Science* 6.1, p. 61. ISSN: 2197-4284. DOI: 10.1186/s40645-019-0304-z.

Sui, C.-H., Satoh, M., and Suzuki, K. (2020). "Precipitation Efficiency and Its Role in Cloud-Radiative Feedbacks to Climate Variability." In: *Journal of the Meteorological Society of Japan. Ser. II* 98.2, pp. 261–282. DOI: 10.2151/jmsj.2020-024.

Tan, Z., Zhuang, Q., Walter Anthony, K., Wang, M., Larson, V. E., and Ghan, S. J. (2015). "Mechanisms of Convective Cloud Organization by Cold Pools over Tropical Warm Ocean during the AMIE/DYNAMO Field Campaign." In: *Journal of Advances in Modeling Earth Systems* 6, pp. 513–526. ISSN: 19422466. DOI: 10.1002/2014MS000384.Received.

Tian, Y. and Kuang, Z. (2016). "Dependence of Entrainment in Shallow Cumulus Convection on Vertical Velocity and Distance to Cloud Edge." In: *Geophysical Research Letters* 43.8, pp. 4056–4065. ISSN: 1944-8007. DOI: 10.1002/2016GL069005.

Tiedtke, M., Heckley, W. A., and Slingo, J. (1988). "Tropical Forecasting at ECMWF: The Influence of Physical Parametrization on the Mean Structure of Forecasts and Analyses." In: *Quarterly Journal of the Royal Meteorological Society* 114.481, pp. 639–664. ISSN: 1477-870X. DOI: 10.1002/qj.49711448106.

Tobin, I., Bony, S., and Roca, R. (2012). "Observational Evidence for Relationships between the Degree of Aggregation of Deep Convection, Water Vapor, Surface Fluxes, and Radiation." In: *Journal of Climate* 25.20, pp. 6885–6904. ISSN: 08948755. DOI: 10.1175/JCLI-D-11-00258.1.

Tompkins, A. M. and Semie, A. G. (2017). "Organization of Tropical Convection in Low Vertical Wind Shears: Role of Updraft Entrainment." In: *Journal of Advances in Modeling Earth Systems* 9.2, pp. 1046–1068. DOI: 10.1002/2016MS000802.

Tompkins, A. M. (2001). "Organization of Tropical Convection in Low Vertical Wind Shears: The Role of Cold Pools Journal of the Atmospheric Sciences 2001 58: 1650-1672." In: *Journal of the Atmospheric Sciences* 58.13, pp. 1650–1672. ISSN: 0022-4928. DOI: 10.1175/1520-0469(2001)058<1650.

Touzé-Peiffer, L., Vogel, R., and Rochetin, N. (2022). "Cold Pools Observed during EUREC4A: Detection and Characterization from Atmospheric Soundings." In: *Journal of Applied Meteorology and Climatology* 61.5, pp. 593–610. ISSN: 1558-8424, 1558-8432. DOI: 10.1175/JAMC-D-21-0048.1.

Trivej, P. and Stevens, B. (2010). "The Echo Size Distribution of Precipitating Shallow Cumuli." In: *Journal of the Atmospheric Sciences* 67.3, pp. 788–804. ISSN: 00224928. DOI: 10.1175/2009JAS3178.1.

van Zanten, M. C., Stevens, B., Nuijens, L., et al. (2011). "Controls on Precipitation and Cloudiness in Simulations of Trade-Wind Cumulus as Observed during RICO." In: *Journal of Advances in Modeling Earth Systems* 3.2, n/a–n/a. ISSN: 19422466. DOI: 10.1029/2011MS000056.

Vial, J., Bony, S., Dufresne, J.-L., and Roehrig, R. (2016). "Coupling between Lower-tropospheric Convective Mixing and Low-level Clouds: Physical Mechanisms and Dependence on Convection Scheme." In: *Journal of Advances in Modeling Earth Systems* 8.4, pp. 1892–1911. ISSN: 1942-2466. DOI: 10.1002/2016MS000740.

Vial, J., Dufresne, J. L., and Bony, S. (2013). "On the Interpretation of Inter-Model Spread in CMIP5 Climate Sensitivity Estimates." In: *Climate Dynamics* 41.11-12, pp. 3339–3362. ISSN: 09307575. DOI: 10.1007/s00382-013-1725-9.

Vial, J., Vogel, R., Bony, S., Stevens, B., Winker, D. M., Cai, X., Hohenegger, C., Naumann, A. K., and Brogniez, H. (2019). "A New Look at the Daily Cycle of Trade Wind Cumuli." In: *Journal of Advances in Modeling Earth Systems*, pp. 3148–3166. ISSN: 19422466. DOI: 10.1029/2019MS001746.

Vial, J., Vogel, R., and Schulz, H. (2021). "On the Daily Cycle of Mesoscale Cloud Organization in the Winter Trades." In: *Quarterly Journal of the Royal Meteorological Society* June, pp. 2850–2873. ISSN: 1477870X. DOI: 10.1002/qj.4103.

Villiger, L., Wernli, H., Boettcher, M., Hagen, M., and Aemisegger, F. (2022). "Lagrangian Formation Pathways of Moist Anomalies in the Trade-Wind Region during the Dry Season: Two Case Studies from EUREC4A." In: *Weather and Climate Dynamics* 3.1, pp. 59–88. DOI: 10.5194/wcd-3-59-2022.

Vogel, R., Albright, A. L., Vial, J., George, G., Stevens, B., and Bony, S. (2022). "Strong Cloud–Circulation Coupling Explains Weak Trade Cumulus Feedback." In: *Nature*, pp. 1–5. ISSN: 1476-4687. DOI: 10.1038/s41586-022-05364-y.

Vogel, R., Konow, H., Schulz, H., and Zuidema, P. (2021). "A Climatology of Trade-Wind Cumulus Cold Pools and Their Link to Mesoscale Cloud Organization." In: *Atmospheric Chemistry and Physics* 21.21, pp. 16609–16630. ISSN: 1680-7316. DOI: 10.5194/acp-21-16609-2021.

Vogel, R., Nuijens, L., and Stevens, B. (2016). "The Role of Precipitation and Spatial Organization in the Response of Trade-Wind Clouds to Warming." In: *Journal of Advances in Modeling Earth Systems* 8.2, pp. 843–862. ISSN: 19422466. DOI: 10.1002/2015MS000568.

– (2020). "Influence of Deepening and Mesoscale Organization of Shallow Convection on Stratiform Cloudiness in the Downstream Trades." In: *Quarterly Journal of the Royal Meteorological Society* 146.726, pp. 174–185. ISSN: 0035-9009. DOI: 10.1002/qj.3664.

Weger, R. C., Lee, J., Tianri Zhu, and Welch, R. M. (1992). "Clustering, Randomness and Regularity in Cloud Fields: 1. Theoretical Considerations." In: *Journal of Geophysical Research* 97.D18. ISSN: 01480227. DOI: 10.1029/92jd02038.

White, B. A., Buchanan, A. M., Birch, C. E., Stier, P., and Pearson, K. J. (2018). "Quantifying the Effects of Horizontal Grid Length and Parameterized Convection on the Degree of Convective Organization Using a Metric of the Potential for Convective Interaction." In: *Journal of the Atmospheric Sciences* 75.2, pp. 425–450. ISSN: 15200469. DOI: 10.1175/JAS-D-16-0307.1.

Yamaguchi, T., Feingold, G., and Kazil, J. (2019). "Aerosol-Cloud Interactions in Trade Wind Cumulus Clouds and the Role of Vertical Wind Shear." In: *Journal of Geophysical Research: Atmospheres* 124.22, pp. 12244–12261. ISSN: 21698996. DOI: 10.1029/2019JD031073.

Zängl, G., Reinert, D., Rípodas, P., and Baldauf, M. (2015). "The ICON (ICOsahedral Non-hydrostatic) Modelling Framework of DWD and MPI-M: Description of the Non-Hydrostatic Dynamical Core." In: *Quarterly Journal of the Royal Meteorological Society* 141.687, pp. 563–579. ISSN: 1477870X. DOI: 10.1002/qj.2378.

Zuidema, P., Li, Z., Hill, R. J., Bariteau, L., Rilling, B., Fairall, C., Brewer, W. A., Albrecht, B., and Hare, J. (2012). "On Trade Wind Cumulus Cold Pools." In: *Journal of the Atmospheric Sciences* 69.1, pp. 258–280. ISSN: 00224928. DOI: 10.1175/JAS-D-11-0143.1.

## EIDESSTATTLICHE VERSICHERUNG
### *DECLARATION ON OATH*

Hiermit erkläre ich an Eides statt, dass ich die vorliegende Dissertationsschrift selbst verfasst und keine anderen als die angegebenen Quellen und Hilfsmittel benutzt habe.

*I hereby declare upon oath that I have written the present dissertation independently and have not used further resources and aids than those stated.*

Hamburg, den 20.01.2023

JULE RADTKE

# Hinweis / Reference

Die gesamten Veröffentlichungen in der Publikationsreihe des MPI-M
„Berichte zur Erdsystemforschung / Reports on Earth System Science",
ISSN 1614-1199

sind über die Internetseiten des Max-Planck-Instituts für Meteorologie erhältlich:
**https://mpimet.mpg.de/forschung/publikationen**

*All the publications in the series of the MPI -M*
*„Berichte zur Erdsystemforschung / Reports on Earth System Science",*
*ISSN 1614-1199*

*are available on the website of the Max Planck Institute for Meteorology:*
***https://mpimet.mpg.de/en/research/publications***